MACHINE LEARNING BASED INTELLIGENT SENSING USING NON-CONTACT ULTRASONIC SENSOR

A thesis submitted during 2022 to the University of Hyderabad in partial fulfillment of the award of a Ph.D. degree in Computer Science

by

AJIT KUMAR SAHOO



School of Computer and Information Sciences
University of Hyderabad
(P.O.) Central University Campus
Hyderabad-500 046, India
December, 2022



CERTIFICATE

This is to certify that the thesis entitled "Machine learning based intelligent sensing using non-contact ultrasonic sensor" submitted by Ajit Kumar Sahoo bearing Reg. No. 16MCPC03 in partial fulfilment of the requirements for award of Doctor of Philosophy in Computer Science is a bonafide work carried out by him under my supervision and guidance.

This thesis is free from plagiarism and has not been submitted previously in part or in full to this or any other university or institution for award of any degree or diploma. The student has the following publications before submission of the thesis for adjudication and has produced evidence for the same.

- A. K. Sahoo and S. K. Udgata, "A Novel ANN-Based Adaptive Ultrasonic Measurement System for Accurate Water Level Monitoring," in *IEEE Transactions on Instrumentation and Measurement*, vol. 69, no. 6, pp. 3359-3369, June 2020.
- 2. A. K. Sahoo and S. K. Udgata, "Machine Learning-Based Ambient Temperature Estimation Using Ultrasonic Sensor," in Next Generation of Internet of Things. *Lecture Notes in Networks and Systems*, vol 201. Springer, Singapore, 2021.
- 3. A. K. Sahoo and S. K. Udgata, "A novel fuzzy inspired machine learning framework for relative humidity estimation using time-of-flight of ultrasonic sensor," *Measurement*, Volume 195, 111035,ISSN 0263-2241, 2022.

- 4. A. K. Sahoo, Akhil K. and S.K. Udgata, "Wi-Fi Signal-Based Through-Wall Sensing for Human Presence and Fall Detection Using ESP32 Module," *Intelligent Systems: Proceedings of ICMIB 2021*, p.459.
- A. K. Sahoo, Vaishnavi K. and S.K. Udgata, "Wi-Fi Sensing based Real-Time Activity Detection in Smart Home Environment," *IEEE Applied Sensing Conference (IEEE APSCON)* 2023. (Accepted for publication)

Further, the student has passed the following courses towards fulfilment of coursework requirement for Ph.D.

Course Code	Name	Credits	Pass/Fail
CS801	Data Structure and Algorithms	4	PASS
CS802	Operating Systems and Programming	4	PASS
AI851	Trends in Softcomputing	4	PASS
AI853	Datamining	4	PASS

Prof. Siba K. Udgata Prof. Chakravarthy Bhagvati
Supervisor, Dean,

School of Computer and School of Computer and

Information Sciences, Information Sciences,

University of Hyderabad University of Hyderabad

DECLARATION

I, Ajit Kumar Sahoo, hereby declare that this thesis entitled "Machine learning based

intelligent sensing using non-contact ultrasonic sensor" submitted by me under the

guidance and supervision of Prof. Siba K. Udgata, School of Computer and Information

Sciences, University of Hyderabad, is a bonafide research work. I also declare that it has

not been submitted previously in part or in full to this University or any other University or

Institution for the award of any degree or diploma. A report on plagiarism statistics from the

University Librarian is enclosed.

Date:

Ajit Kumar Sahoo

Regd.No. 16MCPC03

i

ACKNOWLEDGMENTS

It is my pleasure to acknowledge every individual who helped me during my PhD journey. At first, I would like to express my deepest gratitude and appreciation to my supervisor Professor Siba K. Udgata for his support and guidance throughout this journey. I am thankful for his constant motivation and encouragement, and also for his invaluable efforts to bring the best out of me during my doctoral studies. I express my sincere regards to Mrs. Mamata Mishra for her encouragement, and support during my doctoral journey.

I would like to extend my thanks to all the members of my research advisory committee, Prof. C. Raghavendra Rao, Prof. Arun Agarwal, and Prof. Alok Singh for their valuable suggestions and feedback. I would like to thank the Dean, Prof. Chakravarthy Bhagvati for providing much-needed administrative support and inspiration to complete my research. Besides, I would like to acknowledge University of Hyderabad and School of Computer and Information Sciences for providing the necessary administrative, financial and academic support to pursue my doctoral studies. I am thankful to my PhD classmates and friends, who have helped me throughout my doctoral journey. I would like acknowledge the UGC, GoI, for finance assistance in form UGC NET JRF/SRF.

My greatest gratitude to my family members for always pushing me forward. Especially, I am indebted and owe to my parents for their patience, encouragement, support and sacrifices. I would like to extend my special gratitude to my wife for her support, motivation and encouragement in all difficult times throughout this PhD work. Finally, I would like to thank Almighty God, for letting me through all the difficulties and complete this doctoral journey.

This thesis is dedicated to less support, encouragement	my family members for their limit- t and to you as a reader

ABSTRACT

This thesis presents the study and development of a non-contact intelligent ultrasonic measurement for various environmental conditions. The idea of intelligent sensing is to deploy machine learning models on the resource-constrained micro-controller unit of a sensing module to make it self-contained and carry out intelligent tasks. Non-contact airborne ultrasonic sensors use ultrasonic sound waves to detect or sense the object without any physical contact. The principle of ultrasonic sensor measurement is based on the determination of the time of flight. In addition to time of flight based range measurements, features of ultrasonic echo signals can be used to recognize and distinguish the target objects and materials. Airborne ultrasonic sensor uses air as the transmission medium. The ultrasonic wave propagates in air medium at the speed of sound. The speed of sound depends on the air medium, which depends on the medium temperature and humidity. Therefore, the accuracy of ultrasonic measurement system waves is very susceptible to variations in temperature, humidity, and other gases present in the environment. This research aims to develop an ultrasonic-based intelligent sensing system to enhance measurement accuracy in presence of environmental variations. In this work, we study both machine learning algorithms and ultrasonic wave characteristics to develop an intelligent framework for different types of applications. This work examines three research topics viz., a) accurate level measurement, b) estimation of ambient temperature and humidity, and c) material classification using echo envelope signal.

The liquid level measurement involves measuring the liquid level in a container or tank

under dynamic conditions. The variation of medium temperature and humidity between the sensor and liquid level influences the sensor measurement accuracy. In this work, we developed an adaptive intelligent ultrasonic measurement system using a modified artificial neural network to accurately measure the water level under a dynamic environment. The proposed model reduces the error to 0.3% and also extends the range of maximum operating range of the ultrasonic measurement system by 25%. Moreover, the model is validated by comparing actual water levels at various depths under different environmental conditions over a period of one year. The speed of sound in air medium primarily depends on the medium temperature. There is an approximately linear relationship between the speed of sound and air temperature. The ultrasonic sensor can be used to measure the temperature of the medium. Unlike conventional sensors such as thermocouples and thermal resistance sensors, which measure temperature at a single point. Whereas, an ultrasonic sensor measures the gradient of temperature in the propagation medium in a non-contact manner. We proposed a machine learning-based method to estimate the ambient temperature using the ultrasonic sensor. The temperature estimation error of the proposed method is bounded by $\pm 0.4^{\circ}C$. Similarly, the speed of sound also depends on the relative humidity of the medium, and the relative humidity is also influenced by the temperature. In presence of both temperature and relative humidity, the speed of sound becomes non-linear. We developed a machine learning framework based on fuzzy logic and modified neural network architecture to accurately predict the relative humidity of the medium. The variation in relative humidity estimation is bounded by $\pm 3\%$ compared to commercially available off-the-shelf relative humidity sensors with an accuracy of $\pm 5\%$. Ultrasonic echo envelope signals can be used to differentiate the materials from which the ultrasonic signal is getting reflected. We proposed a convolutional neural network model to accurately classify different materials like cloth, sponge, glass, steel, and wood with an accuracy of 95% Overall, this work provides a concept and implementation of intelligent sensing using the ultrasonic sensor to enhance the performance under various environmental conditions.

Table of Contents

Declara	ration	• •	 • • • •	i
Acknow	wledgements	• • •	 • • • •	. i
Abstrac	act	• • •	 • • • •	. iv
List of t	tables	• • •	 • • • •	, . У
List of f	figures	• • •	 • • • •	. xi
Abbrev	viations	• • •	 • • • •	. XV
Nomeno	nclature	• • •	 • • • •	. XV i
Chapte	er 1: Introduction	• • •	 • • • •	. 1
1.1	Intelligent sensing		 	2
1.2	Research motivation		 	6
1.3	Research objective		 	7
1.4	Research contributions		 	8
1.5	Organization of thesis		 	. 10
1.6	List of publications		 	12

Chapte	r 2: Ba	ckground	13
2.1	Introd	uction to sensors	13
	2.1.1	Intelligent sensor	15
	2.1.2	Machine learning methods in intelligent sensing	16
	2.1.3	Deep learning algorithms in intelligent sensing	19
	2.1.4	Applications of intelligent sensors	20
2.2	Ultras	onic sensor-based sensing	21
2.3	Princip	oles and characteristics of sound waves	31
	2.3.1	Characteristics of ultrasonic waves	35
Chapte	r 3: Liq	uid level measurement using intelligent ultrasonic sensor	45
3.1	Introd	uction	46
3.2	Relate	d works	48
3.3	Speed	of sound in air medium with temperature and relative humidity	53
3.4	Uncert	tainty in distance measurement	56
3.5	Metho	ds	58
	3.5.1	General scheme of the proposed method	58
	3.5.2	Proposed neural network architecture	61
	3.5.3	Training of the neural network	63
3.6	Experi	mental setup	65
3.7	Result	s	68
	3.7.1	Standard approach analysis	68
	3.7.2	Proposed ANN result analysis	68

	3.7.3 Testing and evaluation of the model with new data sets	74
3.8	Discussions	76
3.9	Conclusions	77
Chapte	r 4: Temperature estimation using non-contact ultrasonic sensor	78
4.1	Introduction	79
4.2	Related works	80
4.3	Basic principle of ultrasonic measurement	82
4.4	Theory behind the model	83
4.5	Proposed method	85
	4.5.1 Multiple Linear Regression (MLR)	85
	4.5.2 Support Vector Machine (SVM)	85
	4.5.3 Performance evaluation metric	87
4.6	System implementation	87
4.7	Results and discussions	88
4.8	Conclusions	93
Chapte	r 5: Relative humidity estimation using non-contact ultrasonic sensor	94
5.1	Introduction	95
5.2	Related works	99
5.3	Methodology	101
	5.3.1 Support Vector Regression (SVR)	101
	5.3.2 K-Nearest Neighbors Regression(KNNR)	103
	5.3.3 Random Forest Regression (RFR)	104

	5.3.4	Proposed method	104
	5.3.5	Fuzzy logic controller	105
	5.3.6	Integrated artificial neural network model	107
	5.3.7	Training of the neural network	108
5.4	Experi	ment design	112
	5.4.1	Experimental setup	112
	5.4.2	Measurement system	113
5.5	Result	s and discussions	114
5.6	Conclu	isions	124
Chapte	r 6: Ma	terial classification using ultrasonic echo envelope signal	126
6.1	Introdu	action	126
6.2	Backg	round	128
	6.2.1	Hilbert transform	130
	6.2.2	Convolutional Neural Network (CNN) model	132
6.3	Metho	d	140
6.4	Experi	mental setup	142
6.5	Results	s and analysis	143
6.6	Conclu	nsions	145
Dafaman	205		1 // 4

List of Tables

3.1	Mean absolute error and standard deviation of all five segments	62
3.2	The parameters and the corresponding values used to train the ANN model .	64
3.3	Specifications of the ultrasonic sensor, temperature and humidity sensor used in the experiment	65
3.4	Training, validation and test datasets of each segment of all five neural sub-networks	70
3.5	The performance results of all five neural sub-networks	70
3.6	R-values of all, training, validation and testing of the five neural subnetworks	71
3.7	Variation in temperature and relative humidity at three different positions for different storage tanks	71
4.1	Components used in this experiment with specifications	89
4.2	Performance metric (RMSE, MSE, MAE and MAPE and \mathbb{R}^2) of MLR	91
4.3	SVM-regression model performance metric (RMSE, MSE, MAE, MAPE, R^2)	91
5.1	The different ranges of temperature and relative humidity considered for experimentation	115
5.2	Training data samples for each range of temperature and relative humidity (Ref. Table. 5.1)	115
5.3	Performance evaluation of the proposed model using unseen dataset	117

5.4	Average performance of 10-fold cross validation of ANN, SVR, KNN and RFR	119
5.5	Performance comparison of proposed hybrid ANN model on unseen dataset for different ranges of temperature and humidity for different distances	124
6.1	Model configuration parameters and the corresponding values	141
6.2	Performance accuracy of training, validation and test	144

List of Figures

1.1	Intelligent sensor architecture	4
1.2	Intelligent sensing hierarchical structure	ϵ
1.3	Overall workflow and applications of intelligent ultrasonic sensor followed in this work	10
2.1	A transducer (sensor) block diagram	13
2.2	Non-contact ultrasonic sensor time-of-flight measurement	23
2.3	HC-SR04 ultrasonic sensor	24
2.4	Ultrasonic sensor timing diagram	24
2.5	Pulse width signal of ultrasonic sensor, where the width of the reflected signal from an object placed 5cm apart from the sensor shown in green color	25
2.6	The echo envelope signal of the ultrasonic sensor from an object placed 5cm apart from the sensor shown in green color	25
2.7	Schematic diagram of ultrasonic measurement system	26
2.8	Ultrasonic transducers	27
2.9	Piezoelectric ultrasonic transducer structure and representation of the transducer	28
2.10	Threshold detection method	29
2.11	Cross-correlation method	30
2.12	Envelope detection method	31

2.13	longitudinal and transverse waves with direction of particle movement	32
2.14	Frequency ranges of sound waves	35
2.15	Sound intensity with distance	36
2.16	Reflection, incident, and transmitted ultrasonic waves	37
2.17	Diffraction in sound wave	38
2.18	Refraction of the sound wave in different medium	38
2.19	Variation of temperature <i>versus</i> speed of sound in dry air	39
2.20	Variation of speed of sound with relative humidity at different temperatures	40
2.21	Attenuation <i>versus</i> relative humidity with different frequencies for the air temperature at 20 °C	41
2.22	Attenuation coefficient of the sound wave as a function relative humidity with different temperatures at frequency 40kHz	42
2.23	Atmospheric attenuation of the speed of sound in air varies with distances for different frequencies at temperature 20 °C and relative humidity 50%	43
3.1	Variation of speed of sound with temperature in air medium	54
3.2	Variation of speed of sound in presence of both temperature and relative humidity	55
3.3	Structure of a simple neural network with single node	59
3.4	Back-propagation neural network with one hidden layer used in this proposed model	61
3.5	Segmentation of measurements errors using k-means clustering method	62
3.6	Proposed modified ANN model with five sub-network for different ranges .	63
3.7	Components used in ultrasonic measurement system	66
3.8	Physical components of the ultrasonic measurement module	67
3.9	Experimental setup module used in liquid level measurement	67

3.10	Deviation of estimated distance from actual distance	69
3.11	The performance plots of all five neural sub-networks	72
3.12	Error histograms of all five neural sub-networks	73
3.13	Distance deviations after applying the proposed method to new dataset	75
4.1	Basic working principle of ultrasonic based measurement system	83
4.2	(a) Variation observed in speed of sound with respect to temperature, (b) Percentage of increase in speed of sound vs. change in temperature and humidity	84
4.3	Experimental setup of ultrasonic module for temperature measurement	89
4.4	Performance plots of MLR, Fig.(a)-(d) histogram plots of residuals and Fig.(e)-(h) actual versus predicted temperature	90
4.5	Performance plots of SVM Regression, Fig.(a)-(d) histogram of residuals and Fig.(e)-(h) actual versus predicted temperature	92
5.1	The schematic diagram of proposed two-phase method to estimate relative humidity	102
5.2	Fuzzy inference system architecture	105
5.3	Membership functions for input variable temperature and speed of sound	106
5.4	Membership functions for output variable relative humidity	107
5.5	Architecture of neural network proposed in this work	108
5.6	Flowchart of the procedure of the proposed method to estimate relative humidity	111
5.7	The hardware module developed for non-contact humidity measurement	113
5.8	Experimental setup for data collection	114
5.9	The residual scatter plots for unseen dataset and using proposed model. D1-D4 represent distances of 100, 200, 300, and 400 cm respectively. R1 represents the ranges of input and output variables as shown in Table 5.1.	120

5.10	The residual scatter plots for unseen dataset and using proposed model. D1-D4 represent distances of 100, 200, 300, and 400 cm respectively. R2 represents the ranges of input and output variables as shown in Table 5.1 121
5.11	The residual scatter plots for unseen dataset and using proposed model. D1-D4 represent distances of 100, 200, 300, and 400 cm respectively. R3 represents the ranges of input and output variables as shown in Table 5.1 122
5.12	The residual scatter plots for unseen dataset and using the proposed model. D1-D4 represent distances of 100, 200, 300, and 400 cm respectively. R4 represent the ranges of input and output variables as shown in Table 5.1 123
6.1	Ultrasonic signal processing steps
6.2	Hilbert transform block diagram
6.3	Steps involved in calculation of envelope signal using Hilbert transform 130
6.4	The process of extraction of envelope from raw signal using Hilbert transform 131
6.5	Envelope signals for five different class of materials
6.6	System flow of material classification using proposed approach 141
6.7	Architecture of CNN model
6.8	Experimental setup
6.9	(a) Training loss and validation loss of the convolutional neural network versus the number of epochs, (b) Training and validation accuracy of CNN versus number of epochs
6.10	Confusion matrix for CNN based material classification using ultrasonic echo envelope signal

Abbreviations

ML	Machine Learning	ADC	Analog-to-Digital Converter
AI	Artificial Intelligence	UAV	Unmanned Aerial Vehicles
ANN	Artificial Neural Network	KNN	k-Nearest Neighbors
MLP	Multi-Layer Perceptron	RFR	Random Forest Regression
SVM	Support Vector Machine	FLC	Fuzzy Logic Control
SVR	Support Vector Regression	UMS	Ultrasonic Measurement System
MLR	Multi-Layer Regression	MCU	Micro Controller Unit
ToF	Time-of-Flight	RBF	Radial Basis Function
LMBP-ANN Levenberg-Marquardt-Back-		HT	Hilbert Transform
	Propagation Artificial Neural Network	CNN	Convolution Neural Network
MEMS	Micro-Electromechanical Systems	DNN	Deep Neural Network

Nomenclature

List of symbols		Μ	molecular weight of the air
С	speed of sound	M_h	molecular weight of humid air
t	temperature in degrees Celsius	M_0	molecular weight of dry air
h	relative humidity as a fraction	C_p	specific heat at constant pressure
RH	relative humidity in percentage	C_{ν}	specific heat at constant volume
γ	ratio of specific heats in air, di- mensionless	x_c	mole fraction of CO_2 in air
		x_w	water vapor mole fraction in air
<i>C</i> ₀	speed of sound in dry air	Χa	mole fraction for dry air
Ch	speed of sound in humid air	В, С	second and third virial coeffi-
р	atmospheric pressure	_, _	cients
V	molar volume	°С	degree celsius
R	universal gas constant	STP	standard temperature and pressure
T	absolute temperature in kelvin	PPM	parts per million

CHAPTER 1

Introduction

Recent advances in sensing technology and machine learning algorithms enable more capable sensing devices. A sensor is a device that senses the physical phenomenon and converts it into an electrical signal suitable for processing. The term *intelligence sensing* was coined in the 1990s. The transformation in intelligence technology is due to the advancement in Artificial Intelligence (AI) - concentrated in Machine Learning (ML). Sensors with AI capabilities are known as intelligent sensing. The ability of intelligent sensors not only to extract insights from the data but also designed to understand the environment, make decisions, and draw conclusions [1]. ML techniques assist sensors in examining the sensor data or signal to make more robust predictions and classifications. The basic concept of intelligent sensing is to deploy machine learning models on the resource-constrained microcontroller unit of a smart sensor. Intelligent sensors are self-contained module that employs on-device machine learning algorithms to obtain useful information from a complex set of sensing data.

Ultrasonic sensors are used for range measurement, presence detection, position changes, and level measurement. Non-contact airborne ultrasonic sensors use ultrasonic sound waves to detect or sense the target object without physical contact [2]. The ultrasonic sensor measurement principle is based on estimating time-of-flight (ToF). The time-of-flight is the measurement of the elapsed time between the start of the emission of a signal from the transmitter of the sensor and the beginning of the echo signal received in the receiver of the sensor [3]. A basic ultrasonic sensor comprises two components: a transmitter and a receiver. The transmitter sends ultrasonic pulses to the target, and the receiver captures the

reflected echoes [4]. Then, the distance between the sensor and the object can be measured based on the time of flight and the speed of the ultrasonic wave (i.e., speed of sound wave). In addition to range measurement, ultrasonic echo signals can extract other important information about the target. Extracting the features from ultrasonic echo signals helps to recognize and distinguish the target objects or materials. Two kinds of information can be extracted from echo signals: the time of flight and the amplitude of the echo's envelope. The envelope contains significant information about the target material [5]. Machine learning models can be trained using these echo signals to improve the performance of the ultrasonic measurement system. Moreover, machine learning models can be employed to analyze extracted features from envelope signals for efficient classification, and prediction tasks [6].

Ultrasonic signals are useful for range measurement, localization, autonomous mobile robot navigation, material detection, communication, level measurement, people detection for counting, food and beverage processing, automotive, manufacturing, healthcare, autonomous vehicles, drone navigation, and a wide variety of industrial automation applications [7].

1.1 Intelligent sensing

The progress in AI, cognitive technology, big data, machine learning, deep learning, and other emerging technologies has significantly contributed to the development of intelligent sensing systems. Intelligent sensors can modify their behavior by utilizing intelligent data fusion techniques, advanced signal processing techniques, and artificial intelligence concepts to have a better understanding of sensor data. The term intelligence means introducing computational power to sensors to make them intelligent. An intelligent sensor's main characteristic combines apriori knowledge and adaptive learning to make decisions. The architecture of the intelligent sensor is shown in Figure 1.1. Conventional sensor architecture is the part of the intelligent sensor shown in the figure that contains a sensing unit and signal

conditioning to produce an analog signal for further processing. The sensing unit may include one or more sensors, and the signal conditioning circuit amplifies and tunes the signal received from the sensing units. The measurement instrument or device is used to visualize or capture the analog signal. Conventional sensors are not adaptive to changes in conditions and drift over time. These sensors do not possess advanced signal processing and communication unit. The function of the signal conditioning circuit is to amplify, isolate, remove DC-offset or DC-bias, and filter the signal. After signal conditioning, the continuous analog signal is fed into Analog to Digital Converter (ADC) to convert it into a discrete-time digital signal for the subsequent processing stage. The intelligent algorithm inside the microcontroller unit uses the sensing data to train the machine learning model, and then the trained model makes a prediction based on new sensing data. Generally, the term smart and intelligent are used interchangeably in sensing tasks. But there is a difference between smart and intelligent sensor definitions. A smart sensor comprises a sensing unit, signal conditioning, ADC, micro-controller unit, and communication unit and has some onboard diagnostics. An intelligent sensor is a smart sensor with intelligent functions. The term" smart" is closely associated with the technological aspect, and" intelligent" is more related to functional aspects. Intelligent logic and control functions of the intelligent sensor can independently trigger events. The most important part of an intelligent sensor is intelligent algorithms, which help the sensors to extract features from sensing data and make decisions.

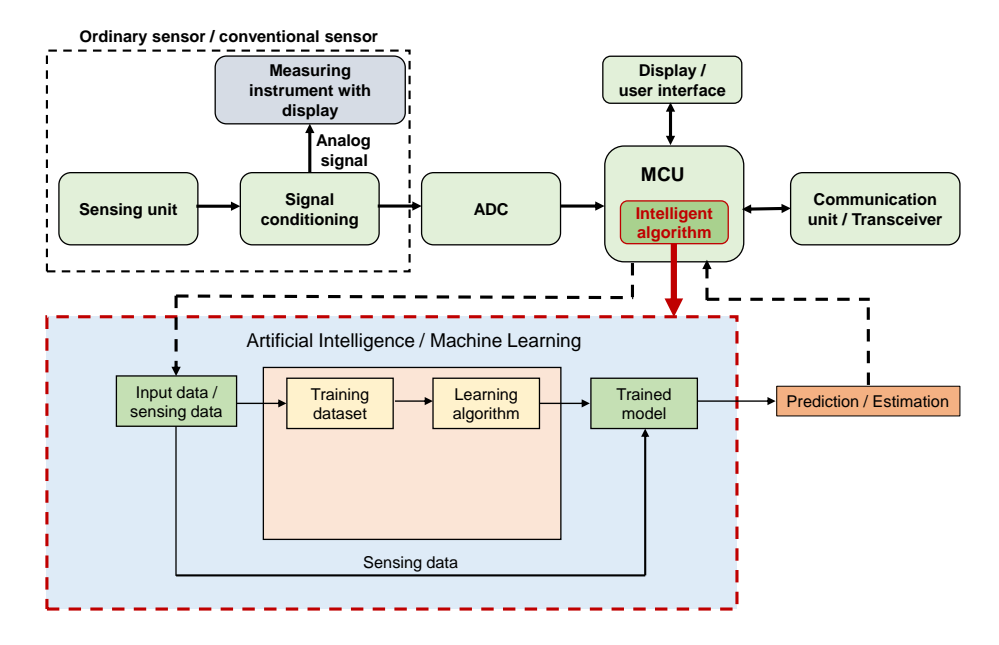


Figure 1.1: Intelligent sensor architecture

This work aims to investigate and develop intelligent sensing using machine learning techniques. We propose and develop an intelligent ultrasonic measurement system using intelligent algorithms in combination with an ultrasonic sensor to enhance the performance of the ultrasonic sensing system. This work investigates three research topics viz., 1) accurate level measurement, 2) estimation of temperature and humidity, and 3) material classification using echo envelope signal.

Level measurement is among the most commonly found processes in many industrial processes. The liquid level measurement system ideally involves measuring liquid level and volume in a container or tank under a dynamic or static condition. Many measurement techniques are available for liquid level measurement [8]. Ultrasonic sensors are most widely used for non-contact liquid level measurement. Since ultrasonic sensors use ultrasonic sound waves for measurement, the speed of the ultrasonic wave depends on the properties of the medium. In an air medium, the speed of sound depends on the medium temperature, relative humidity, and other gases present in the environment [9]. The environmental parameter variation influences the sensor's measurement accuracy, leading to inaccurate level or

distance measurement. In this thesis, we proposed an intelligent ultrasonic measurement system to measure the water level under dynamic conditions.

The speed of ultrasonic sound waves depends on the medium temperature. The speed of sound and temperature in air medium is nearly linear [10]. In many applications, non-contact temperature measurement and medium temperature distribution data are required. Therefore, the medium temperature can be estimated using the time-of-flight signal of the ultrasonic sensor [11]. Conventional sensors such as mercury thermometers, thermocouples, and thermal resistance sensors are single-point sensors that fail to give accurate temperatures in many situations and environments. We proposed a machine learning method to measure the medium temperature using an ultrasonic measurement system accurately. In addition to temperature, ultrasonic sensors depend on the medium relative humidity. In the presence of both temperature and relative humidity speed of sound is non-linear [10]. The medium's temperature and relative humidity can be estimated using an ultrasonic sensor [12]. We proposed a novel two-step machine-learning framework to estimate the relative humidity of the medium. Material type and shape determination are important requirements for mobile robot navigation and autonomous vehicles [13]. The proposed intelligent sensing framework uses the echo envelop signal to distinguish different material types.

The intelligent algorithms and framework require computing resources. Therefore, building an efficient, intelligent sensing system as a multilevel hierarchical structure is necessary. Figure 1.2 depicts the three-layer hierarchical structure of intelligent sensing [14]. This hierarchical framework is developed to reduce computation costs and makes the process faster and memory efficient. The lower layer function includes sensing, filtering, signal conditioning, and converting analog to digital signals. This layer is more closely related to the sensor's hardware and structure. Intermediate signal processing in the middle layer involves the integration of signals from multiple sensors, parameter tuning, signal fusion, feature extraction, and optimization. The role of the upper layer is to make decisions based on the inputs from the middle layer using intelligent algorithms. This layer performs

prediction, classification, clustering, and decision-making.

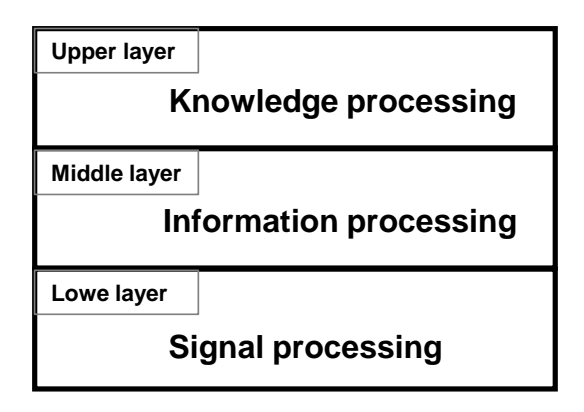


Figure 1.2: Intelligent sensing hierarchical structure

1.2 Research motivation

An ultrasonic transducer is a device that can convert electrical energy into acoustic energy and vice versa. The acoustic wave frequency above 20 kHz is known as ultrasound. Ultrasonic sensor uses ultrasonic sound waves for sensing. Ultrasonic sensors are non-intrusive, cost-effective, small in size, and provide precise and stable measurements. These sensors are not sensitive to electromagnetic interference, ambient light, dust, smoke, gas, and other airborne particles. In robotic applications, target localization using a vision-based sensor can not be precise due to environmental conditions like dark, fog, and low visibility. Therefore, the ultrasonic sensor is an alternative and cost-effective solution.

Ultrasonic sound waves are very sensitive to temperature and humidity fluctuation. The speed of sound in the air medium is affected due to variations in temperature, humidity, and other environmental parameters, which introduces errors in sensor measurement accuracy and resolution. This research aims to develop ultrasonic-based intelligent sensing to improve measurement accuracy in the presence of temperature, humidity, and other environmental

attenuation. In addition, we are using the intelligent algorithm to classify material using an ultrasonic echo envelope signal.

The characteristics of the ultrasonic sensor waves lead to the development of different sensing applications like range measurement, ambient temperature, and humidity estimation, localization, human presence and activity detection, object type and shape determination, and respiration rate estimation, among a few others. The advancements in machine learning algorithms help in enhancing the performance of the ultrasonic measurement system. Hence, in this work, we study machine learning algorithms and ultrasonic wave characteristics to develop an intelligent framework for different sensing systems.

Most existing work on liquid-level sensing focused on compensating the effect of temperature only and assumed that the temperature and humidity remain constant between the sensor and the liquid surface. Since ultrasonic wave propagation depends on the medium temperature and humidity [10], variation of these parameters will affect the measurement accuracy. The temperature and humidity values are different between the sensor and the surface of the liquid, specifically in the case of water. The objective of this work is to make the ultrasonic measurement system adaptive to changes in environmental parameters and improve the accuracy. The speed of sound depends on the medium's temperature, and the medium temperature can be measured using an ultrasonic sensor [11]. Since ultrasonic wave depends upon temperature and humidity, an ultrasonic sensor can also be used to estimate relative humidity [12].

1.3 Research objective

This research aims to investigate the use of machine learning techniques in combination with ultrasonic sensors to enhance the accuracy of the ultrasonic measurement system in dynamic environments. Several experiments are carried out in dynamic environmental conditions to validate the proposed intelligent ultrasonic measurement system. In summary,

the research aims to address the followings:

- To understand the issues of the existing ultrasonic measurement system.
- To use ultrasonic sensor-based intelligent sensing techniques for analyzing and enhancing the performance of the ultrasonic measurement system.
- To improve the measurement accuracy of the proposed intelligent ultrasonic measurement system in the presence of varying temperature, relative humidity, and influence of other parameters.
- To use the ultrasonic echo envelop signal for classifying different types of materials.
- To explore various applications of the ultrasonic-based intelligent sensing system.

1.4 Research contributions

In this thesis, we propose methods for intelligent sensing using a non-contact air-coupled ultrasonic sensor. The overall workflow of intelligent ultrasonic sensor followed in this thesis is shown in Figure 1.3. A brief description of the research contributions of this thesis is given below:

• Intelligent sensing models use intelligent algorithms to improve the performance of ultrasonic measurement systems in the presence of various types of noises and different environmental conditions. Machine learning algorithms are coupled with an ultrasonic sensor to improve the performance of ultrasonic measurement systems under dynamic conditions. We developed an adaptive intelligent ultrasonic sensing model using modified ANN to accurately measure the water level under a dynamic environment where the error is reduced to 0.3%. Water level measurement in water tanks was considered a case study to verify and validate the proposed method. MLP neural networks with a single hidden layer are used for universal function approximation to

enhance the accuracy of the estimation or prediction. Levenberg-Marquardt Back-Propagation Artificial Neural Network (LMBP-ANN) algorithm is used to improve the prediction performance of MLP network. The experimental findings demonstrate the model's effectiveness in making ultrasonic measurement systems adaptive to find accurate ranges under different environmental conditions.

- The speed of sound in an air medium is mainly influenced by temperature and relative humidity. The air temperature is directly proportional to the speed of sound. Speed of sound in air increases with temperature. Therefore, we presented a machine learning-based method to estimate the air temperature using an ultrasonic sensor. This method accurately measures the average temperature of the medium with a reasonable accuracy bounded by a maximum of ± 0.4 °C under different environmental conditions. We conduct experiments in different environmental conditions with temperature ranging from 22 °C to 45 °C and relative humidity ranging from 30% to 85% to validate the proposed system's accuracy, Experimental results indicate that the temperature estimation error in the proposed measurement system is bounded by ± 0.4 °C.
- Temperature and relative humidity highly influence the speed of sound in the air medium. An ultrasonic sensor can achieve a highly accurate air relative humidity measurement with temperature compensation. We proposed a combination of fuzzy logic and an artificial neural network approach for estimating relative humidity using ultrasonic sensors. The framework of the proposed model is to classify the input data into different segments based on the fuzzy controller output, and each data segment is then fed to a specific pre-trained neural network to estimate the relative humidity. Other popular machine learning approaches, like support vector regression, k-nearest neighbor, and random forest regression, are compared with the proposed method's accuracy. The result shows that the proposed fuzzy-artificial neural network model gives better performance. Experimental results indicate that the variation in relative

humidity estimation is bounded by $\pm 3\%$, which is as good as commercially available off-the-shelf relative humidity sensors.

• Ultrasonic echo envelope signal information can be used to identify or recognize the target object [15]. Features of the signal can be used to solve classification tasks. Material information is essential for robot navigation, autonomous vehicles, and unmanned aerial vehicles (UAV) navigation. Ultrasonic sensors are widely used for robotic navigating systems. However, ambient temperature, humidity, and signal attenuation affect the sensor accuracy. A combination of echo amplitude and time-of-flight can distinguish material types. Statistical properties of envelope signals can be useful to characterize the materials. We proposed a method to differentiate various materials in the presence of external noise accurately.

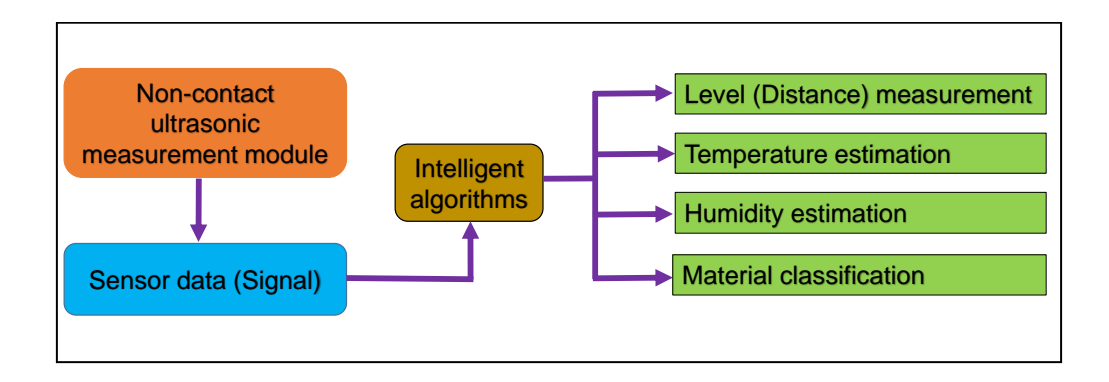


Figure 1.3: Overall workflow and applications of intelligent ultrasonic sensor followed in this work

1.5 Organization of thesis

The thesis comprised six chapters, and the organization of the thesis is as follows:

1. **Chapter 1 - Introduction** provides an introduction to intelligent sensing and ultrasonic sensor. An overview of the problem statement, the objectives of this research, and the contributions are detailed in this chapter.

- 2. Chapter 2 Background and literature survey presents the basics of ultrasonic sensors, intelligent sensing algorithms, theory of sound, characteristics of ultrasonic wave, factors influencing ultrasonic sensing, application of intelligent sensing, application, and limitation of ultrasonic sensor measurement. It also provides a brief literature survey on different water level sensing techniques, temperature and humidity estimation methods using non-contact airborne ultrasonic sensors, and various material identification and classification methods using non-contact ultrasonic sensors.
- 3. Chapter 3 Development of intelligent level sensing using modified artificial neural network architecture proposes a novel concept of ANN to accurately estimate the water level in a dynamic environment. A modified ANN effectively compensates for the environmental influence and noise on the ultrasonic measurement system. A brief overview of various level measurement methods, a description of the sensing module, and an experimentation procedure are discussed in this chapter.
- 4. **Chapter 4 Estimation of ambient temperature** provides a novel concept of having an ultrasonic sensor combined with machine learning methods to estimate or predict the air temperature in the measurement medium.
- 5. **Chapter 5 Estimation of relative humidity** provides the innovative concept of having an ultrasonic sensor together with machine learning methods to estimate or predict the relative humidity in the measurement medium. First, we estimate the temperature; then, with the help of the estimated temperature and using a fuzzy logic controller and modified neural network, we estimate the relative humidity.
- 6. Chapter 6 Material identification and classification presents a method to classify the materials with the help of a reflected ultrasonic echo envelope signal. The method classifies the material using an ultrasonic sensor and machine learning. Material information helps accomplish robot navigation, autonomous vehicles, and unmanned aerial vehicles (UAV) navigation.

7. **Chapter 7 - Conclusions and future scope** summarizes the research investigation, briefly explains the findings of this research, the possible future improvements to the proposed methods, and the future directions in this research area.

1.6 List of publications

- 1. A. K. Sahoo and S. K. Udgata, "A Novel ANN-Based Adaptive Ultrasonic Measurement System for Accurate Water Level Monitoring," in *IEEE Transactions on Instrumentation and Measurement*, vol. 69, no. 6, pp. 3359-3369, June 2020.
- A. K. Sahoo and S. K. Udgata, "Machine Learning-Based Ambient Temperature Estimation Using Ultrasonic Sensor," in Next Generation of Internet of Things. *Lecture Notes in Networks and Systems*, vol 201. Springer, Singapore, 2021.
- 3. A. K. Sahoo and S. K. Udgata, "A novel fuzzy inspired machine learning framework for relative humidity estimation using time-of-flight of ultrasonic sensor," *Measurement*, Volume 195, 111035,ISSN 0263-2241, 2022.
- 4. A. K. Sahoo, Akhil K. and S.K. Udgata, "Wi-Fi Signal-Based Through-Wall Sensing for Human Presence and Fall Detection Using ESP32 Module," *Intelligent Systems: Proceedings of ICMIB 2021*, p.459.
- A. K. Sahoo, Vaishnavi K., and S.K. Udgata, "Wi-Fi Sensing based Real-Time Activity Detection in Smart Home Environment," *IEEE Applied Sensing Conference(IEEE APSCON)* 2023. (Accepted for publication)
- 6. A. K. Sahoo and S. K. Udgata, "Material classification using ultrasonic echo envelope signal and convolutional neural network". (Communicated)

CHAPTER 2

Background

2.1 Introduction to sensors

A sensor is a device that converts physical phenomena (e.g., temperature, humidity, pressure, etc.) to a form (e.g., an electrical signal) that is more convenient to use [16]. Sensors are sometimes called transducers. A transducer is a device that converts one form of signal into another form as depicted in Figure 2.1. Every transducer is a sensor, but every sensor need not be a transducer. An actuator is a device that converts the signal into a physical action or motion.

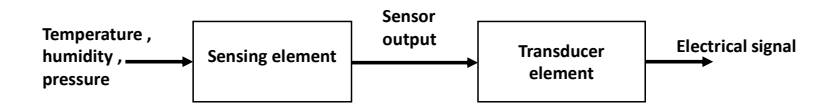


Figure 2.1: A transducer (sensor) block diagram

Classification of sensors

- Active sensor: Require an external source of power for its operation. Active sensors
 emit energy and then measure the reflected energy. Active sensors include LIDAR,
 RADAR, InfraRed, GPS, ultrasonic sensors, etc.
- 2. **Passive sensor :** These sensors need no additional energy source as they do not create a special field of energy but rather generate an electric signal in response to changes

in physical quantities or external stimuli. Passive sensors include a thermocouple, a photodiode, a piezoelectric sensor, thermal sensors, electric field sensing, and metal detecting.

- Contact sensor: Contact sensors require physical contact with the object that is being measured.
- 4. **Non-contact sensor:** Non-contact Sensors require no physical contact with the object. It remotely senses or detects the object.

Characteristics of sensors

- Sensitivity It represents the relationship between the input signal and output signal.
 It is also expressed as the ratio of the change in output of the sensor to a unit change in input value that causes a change in output.
- 2. **Accuracy -** It is the degree of exactness between the measured value and the actual value. Accuracy is related to the bias of a set of measurements and is expressed in absolute and relative errors.

Absolute error = Measured value - True value

Relative error = (Measured value – True value) / True value

- 3. **Precision -**: It is defined as closeness among a set of reading under the same prescribed conditions. Accurate measurements are always precise.
- 4. **Resolution (Discrimination)** It is defined as the smallest measurement a sensor can detect or the degree of fineness with which measurements can be made.
- 5. **Drift -** Defines the gradual change of sensors output as the ambient or operating condition changes over time.

- 6. **Repeatability -** Repeatability is the ability to reproduce the same output under the same circumstances over and over again under environmental conditions
- 7. **Linearity** Linearity indicates the consistency of measurements over the entire range of measurements. It is specified in terms of the percentage of non-linearity. Non-linearity is defined as the maximum deviation of the output curve from the best-fit straight line or the curve of actual measurement.
- 8. **Hysteresis** (backslash) Hysteresis describes the maximum difference between two separate measurements taken at the same point, before and after a physical quantity is increased and decreased.
- 9. Offset Defines as the sensor's output is higher or lower than the ideal output. Calibration is required to correct the offset error. Calibration is correcting or adjusting the sensor measurements to make the sensor perform accurately.

2.1.1 Intelligent sensor

Conventional sensors can only sense and produce an unprocessed signal. An intelligent sensor is designed with multiple functions. Smart sensor integrated with intelligent algorithms and artificial intelligence techniques is known as intelligent sensing [1]. Intelligent sensors need to have the following features.

- Self-diagnostics: Verifies the correct operation of the sensor and detects and identifies
 errors due to faults.
- 2. **Self-calibration**: Also called auto-calibration, it allows for correctly relating the sensor measurement and measurement systems to the physical values of the quantities under measurement without any external support.
- 3. **Self-adaptation :** The ability of the sensor to adjust its response to the perception of the environment.

- 4. **Self-testing**: The mechanism of the sensor permits it to perform automatic tests.
- 5. **Self-validation**: Sensor data validation ensures that the data is valid during the acquisition and processing.
- 6. **Self-compensation :** Automatic compensation function is to improve the accuracy of the sensor.

2.1.2 Machine learning methods in intelligent sensing

The remarkable development in AI and ML generated a wave of applications in the field of sensor technology. As a result, there is a huge opportunity in the area of intelligent sensing. This section briefly describes machine learning and deep learning techniques from an intelligent sensing perspective. ML algorithms are generally divided into supervised, unsupervised, semi-supervised, and reinforcement learning [17, 18].

Supervised learning-based intelligent sensing

Supervised machine learning uses labeled input data to train the models to yield the desired output. The labeled data includes inputs and actual outputs, which allow the model to learn and predict the output for unseen inputs. Supervised learning can be divided into two types: classification and regression. Classification is the method of accurately assigning data into specific categories. Regression is used to understand the relationship between response (dependent) and independent (predictors or explanatory) variables. Supervised learning algorithms are used to discover a mapping function to map the input with the output.

• Neural Networks are artificial networks inspired by the human brain used in ML (AI) to recognize relationships between vast amounts of data [19, 20]. Artificial neural networks (ANNs) comprise an input layer, one or more hidden layers, and an output layer. The nodes or neurons in ANN are connected, and each node is associated with

inputs, weights, a bias (or threshold), and an output. The backpropagation algorithm is used in neural network training to minimize the loss function. Neural networks try to adjust the weights and biases of the neurons to minimize the overall cost or to get more accurate output. Neural network techniques are used to introduce intelligence by enhancing the characteristics of sensors.

- Support Vector Machine (SVM) is basically used for classification and regression [21]. This algorithm finds a hyperplane that maximizes the margin between the two classes of data points.
- K-Nearest Neighbor (KNN) classifies a new data point based on the similarity. K refers to the number of neighbors to consider for classification. It examines the training data and finds the K training examples closest to the new data point. Then, the most common class label is assigned to the new data points based on the majority of votes.
- **Linear regression** is a statistical method that helps us to analyze and identify the relationship between two or more variables of interest. Linear regression attempts to model by fitting a linear equation between a dependent and independent variables. In multiple linear regression the number of independent variables are more than one.
- **Decision trees** are tree-shape models for classification and regression. It is comprised of nodes and branches. Each internal node represents a test on features, each leaf node represents a class label, and each branch represents an alternative course of action or decision.
- Ensemble learning is a standard machine learning technique that combines the insights of multiple classifiers to boost the prediction performance. There are two families of ensemble methods: 1) averaging method, mainly used for regression problems. It builds multiple independent models and averages their predictions for

better model performance. 2) boosting method, used for classification problems, combines weak classifiers to create a strong classifier. It reduces biases and variance to improve the model performance.

• Random forest used for classification and regression purposes [22]. It utilizes ensemble learning techniques to merge the outcomes of decision trees to make more accurate predictions. Random forest algorithm is trained through bagging. Bagging is an ensemble learning method that improves the accuracy of the random forest algorithm.

Unsupervised learning-based intelligent sensing

Unsupervised learning techniques use unlabeled data to identify patterns. These algorithms include principal component analysis, hierarchical clustering, k-means clustering, anomaly detection, and Gaussian mixture models.

Semi-supervised learning-based intelligent sensing

The semi-supervised learning algorithm is a combination of supervised and unsupervised learning. This learning model deals with the combination of labeled and unlabeled data. Semi-supervised learning can be achieved through the combination of clustering and classification algorithms. Clustering algorithms group the most relevant samples based on their similarities. Then labeling can be performed on those and used to train a supervised model for the classification.

Reinforcement learning-based intelligent sensing

Reinforcement learning is focused on training machine learning models to make a sequence of decisions by interacting with their environment without human interference.

An agent learns the sequence of actions by interacting with the environment and observing

the rewards in every state. One of the successful applications of this approach is to design self-driving cars based on automatic decision-making approaches.

2.1.3 Deep learning algorithms in intelligent sensing

Deep learning is one of the latest trends in artificial intelligence research and has been successfully applied in different fields [23]. Traditional machine learning algorithms' potential is limited to processing raw data and requires experts to extract and build features. Deep learning methods automatically discover features from raw input data needed for detection or classification. Popular deep learning algorithms used in intelligent sensing are;

Convolutional Neural Network (CNN) is advantageous compared to other deep learning algorithms because it automatically identifies the relevant features without the help of any experts. A CNN typically consists of three layers: a convolutional layer, a pooling layer, and a fully connected layer.

Recurrent Neural Networks (RNNs) is a deep learning network structure that uses information from the previous step fed as input to the current step to improve the network's performance. This network model contains memory and is best suited for sequential data.

Long Short-Term Memory Networks (LSTMs) is designed to more accurately model temporal sequences and their long-range dependencies than traditional RNNs. LSTM network has a memory cell to retain some information about the sequence; it is allowing to remember the important features at the beginning of the sequence that might affect the later parts of the sequence instead of computing the output based on just the previous time step. The main components of the LSTM are its gates. There are three gates in an LSTM: the input gate, the forget gate, and the output gate.

Generative Adversarial Networks (GANs) is an unsupervised deep-learning-based gen-

erative model. They are composed of two networks, a generator and a discriminator. The generator network is typically a deconvolutional neural network, and the discriminator is a convolutional neural network.

2.1.4 Applications of intelligent sensors

There are many applications based on intelligent sensing and some key areas such as healthcare, agriculture, image segmentation, transportation, automotive industry, environment monitoring, soft sensors, detection of safety hazards, healthcare and medical, etc.

Smart agriculture intelligent sensing helps farmers maximize yields with minimal resources. Intelligent sensors assist farmers in crop disease infestations, weed management, pesticide control, soil, water, crop growth, environmental impact monitoring, etc.

Smart healthcare smart sensors are used in healthcare and medicine for health screening, diagnosis, monitoring, and treatment purposes. Intelligent sensing helps doctors to keep track of patients' early health conditions. Healthcare management uses intelligent sensing to monitor the patient remotely.

Intelligent transportation sensor technology can be integrated with the transportation infrastructure to improve the efficiency of the traffic management system using the traffic information. In addition to traffic data, the in-vehicle sensor information is used for safety, traffic management, and infotainment.

Autonomous vehicle senses its surrounding environment and makes intelligent real-time decisions. Intelligent sensing systems combine information from LiDAR, Radar, camera, and ultrasonic sensors to create a more intelligent perception system.

Smart home The advancement in machine learning and artificial intelligence have enabled the implementation of smart systems and interactive environments. Embedding intelligent sensors in the built environment makes the living space environment interactive smart sensing spaces, affecting residents' perception, cognition, and experience of their spaces.

2.2 Ultrasonic sensor-based sensing

Ultrasonic sensors have been used for many different applications that include distance measurement, robotic sensing, human presence detection, and counting, localization, automotive applications, vehicle parking assistant systems, liquid level measurement, temperature measurement, fermentation process, food processing, and many other industrial, medical and scientific applications [7, 24, 25]. Ultrasonic sensor-based measurement can be categorized into contact and non-contact modes. In contact measurement, the ultrasonic transducer is coupled directly to the surface of the object or material. Transducers are typically embedded in structures using couplant. Couplant (liquid or gel) is applied to the surface of the material and the transducer to ensure that there will be no air gaps between them. The presence of air gaps can scatter the signal propagation to the surrounding environments, which can arrive at low-sensitivity measurements. Application of contact-type ultrasonic sensors includes material testing, non-destructive testing, measurement of materials, medical diagnosis, ultrasonography, and many industrial automation applications.

Ultrasonic measurement using the non-contact method overcomes the problem of acoustic impedance mismatch in the contact-based method. The non-contact method is also known as an air-couple technique since air is the medium between the sensor and the object mainly two non-contact ultrasonic sensors used in various applications. The first type is proximity detection ultrasonic sensors; in this type, the object is detected if it is within the predefined detection range. The detection is irrespective of target size, material, and

reflectivity. The second type is the range measurement ultrasonic sensor, which can give accurate distance measurements of an object moving to and from the sensor. The precise distance is calculated continuously based on the interval between the ultrasonic sensor's transmitted and reflected sound bursts.

There are two different methods used for ultrasonic measurements. The first is a pulse-echo method, and the second is a continuous wave (or phase shift) method. One transducer can act as both transmit—receive modes in the pulse-echo type. The transducer emits a short ultrasonic pulse and waits for the reflected signal (echo) from the target to receive. The sensor consists of two transducers; one transmits the pulse signal, and the other receives the reflected echo signal. The second type, the continuous wave technique, consists of two separate transducers; one operates in transmit mode, and the other operates in receive mode. The transmitting transducer emits a continuous pulse, and the receiver receives the echo. The accuracy of this method depends on continuous measurement of the phase difference (phase shift) between transmitted and received signals. However, this method requires complex hardware and has a limited measurement range.

There is some other sensing technology that is a similar principle to ultrasonic technology. Compared to infrared (IR) sensors, ultrasonic sensors are more reliable. IR sensors can be affected by environmental conditions such as fog, dust, and pollution. The limitation of the IR sensor is interference with sunlight and different absorption characteristics. Optical time of flight sensor sensing uses light waves to measure distance. Ambient light can interfere and make its operation difficult limitation of detecting clear and transparent materials like water and glass as light passes through these materials. Light detection and ranging (LiDAR) and radar sensor use an array of emitter/detector instead of a single time-of-flight measurement. The limitations of LiDAR include a higher cost and harm to the naked eye. Limitations of radar sensors include complex functionality, expensive, and depend dielectric constant of the material.

Ultrasonic measurement principles

Ultrasonic sensors have a transmitter and a receiver component The transmitter converts electrical signals into ultrasonic waves, whereas the receiver does the reverse. The ultrasonic sensor can also be a single transceiver module, where the transmitter and receiver are in the same physical housing. Non-contact airborne ultrasonic sensors are used to measure distance and detect the presence of an object without requiring physical contact. The basic principle of ultrasonic sensing is that the transmitter sends an ultrasonic pulse toward the object, and the receiver receives the reflected echo signal. The propagation time between the sent and the received signal is known as the time-of-fight. The ToF and speed of sound are used to determine the distance from the sensor to the object as shown in the Figure 2.2.

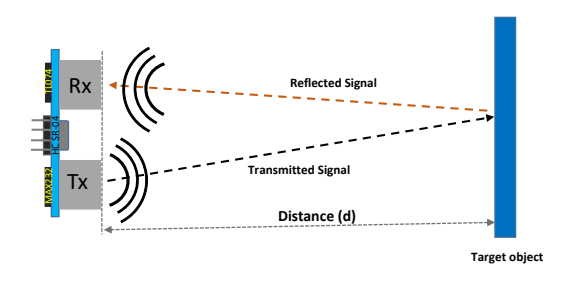


Figure 2.2: Non-contact ultrasonic sensor time-of-flight measurement

Ultrasonic sensors HC-SR04 consists of two components, one transmitter, and one receiver, as shown in Figure 2.3. The working frequency of this ultrasonic sensor is 40 kHz. The HC-SR04 has four pins: VCC and GND pins used to power the HC-SR04 ultrasonic sensor. The Trig pin is used to trigger ultrasonic sound pulses. Setting this pin to HIGH for 10 µs, the sensor transmits a burst of eight pulses at 40 kHz frequency as depicted in Figure 2.4. After sending the burst, the echo pin immediately goes high until the sensor receives an echo signal, after that it immediately goes low. The echo pin goes low if no echo signal is received after a certain time. Thus, by measuring the width (duration or round trip time) of the pulse on the echo pin and knowing the speed of sound, the distance between the sensor

and the object can be calculated using the following formula.

Distance = Speed of sound \times duration (width of the pulse)/2

.



Figure 2.3: HC-SR04 ultrasonic sensor

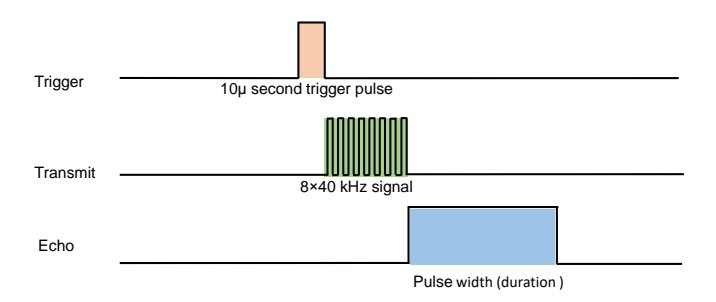


Figure 2.4: Ultrasonic sensor timing diagram

The transmitted and received signal of the ultrasonic sensor can be visually inspected via an oscilloscope. An example of the PWM signal of an ultrasonic sensor is depicted in Figure 2.5. Similarly, an example of each envelope signal is shown in Figure 2.6.

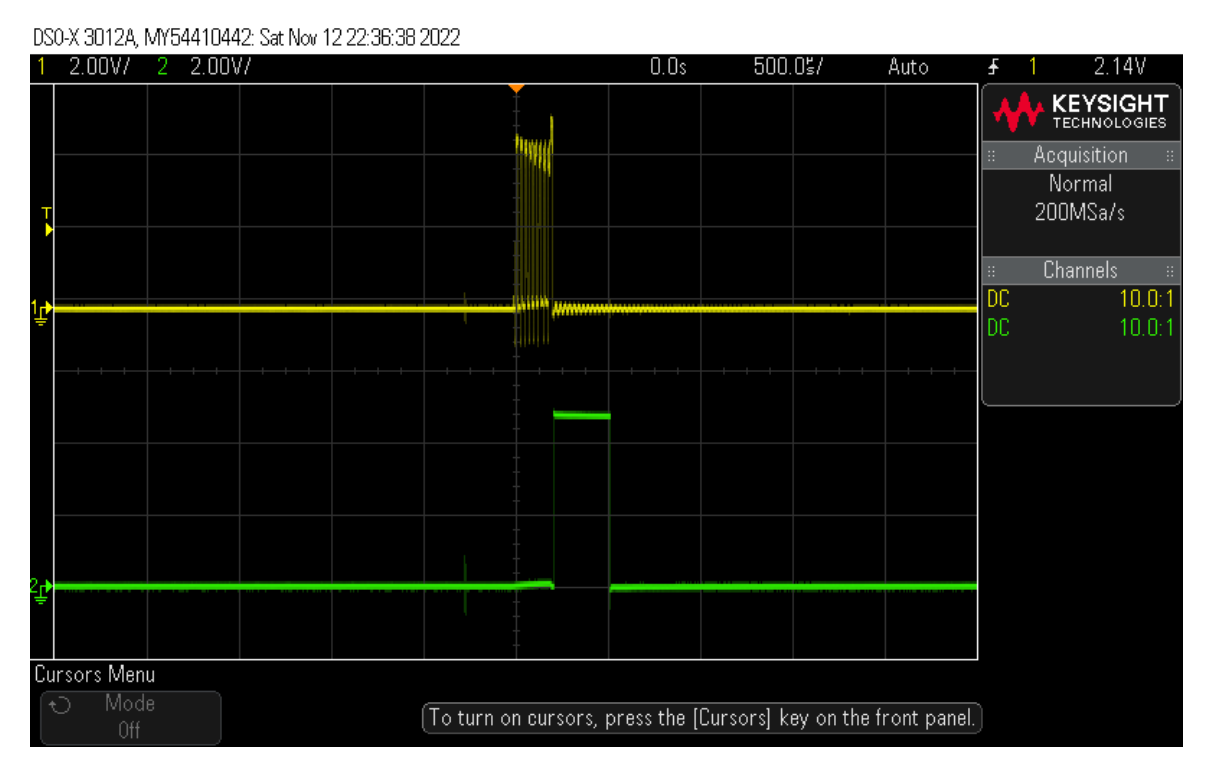


Figure 2.5: Pulse width signal of ultrasonic sensor, where the width of the reflected signal from an object placed 5cm apart from the sensor shown in green color

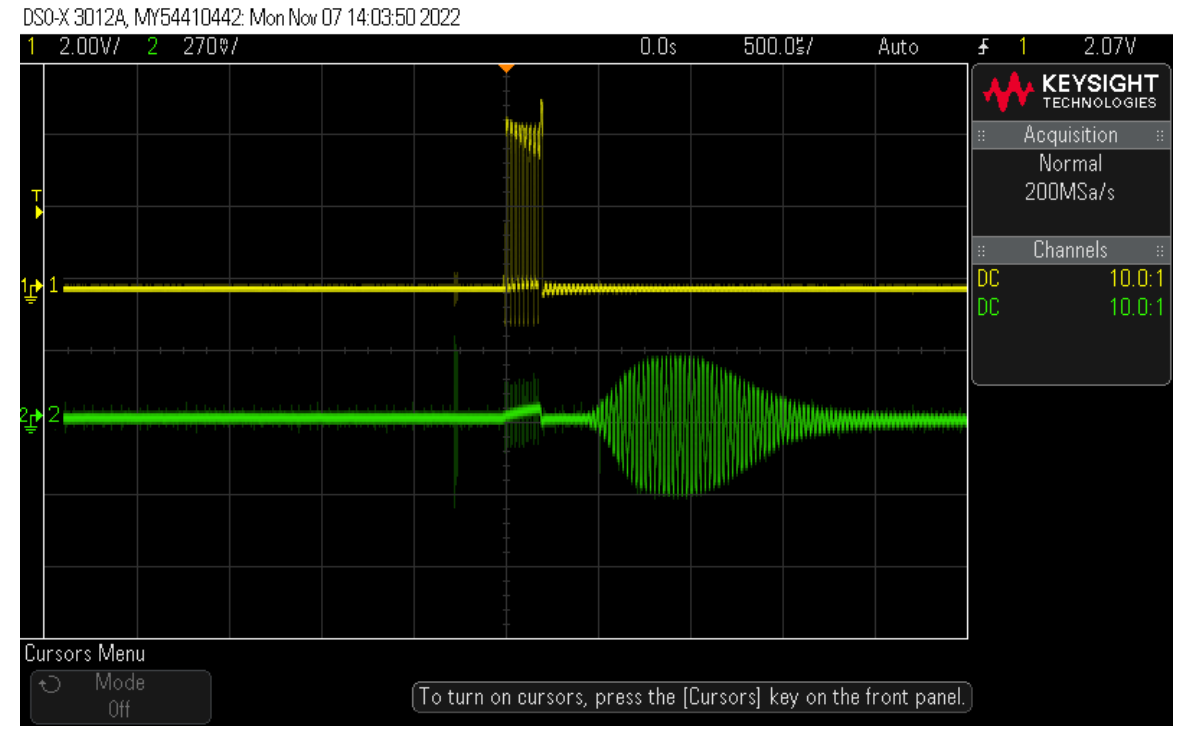


Figure 2.6: The echo envelope signal of the ultrasonic sensor from an object placed 5cm apart from the sensor shown in green color

Ultrasonic measurement system

A typical ultrasonic measurement system shown in the Figure 2.7 consists of an ultrasonic sensor with transmitting and receiving units, a micro-controller unit, a temperature, and humidity sensor to compensate the effect of temperature and humidity in measurement, a Bluetooth module to transmit data to end user or a display module to display.

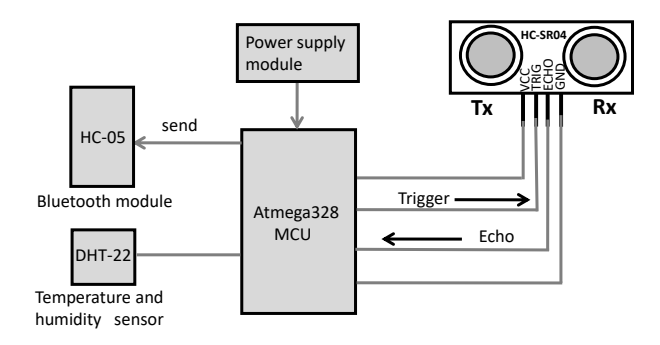


Figure 2.7: Schematic diagram of ultrasonic measurement system

The HC-SR04 ultrasonic sensor circuit board contains an STC11 single-chip microcontroller, MAX232 voltage levels driver, and TL074 operational (op-amp). Voltage levels drive used to supply power to a transmitter unit (T_X). Op-amp compares and amplifies the received signal at R_X . When the trigger pulse is received at the microcontroller, it creates a 40 kHz square wave applied to the voltage shifter and then to the transmitter. After receiving the amplified signal of frequency 40 kHz, the microcontroller pushes the echo pin to low.

Ultrasonic piezoelectric transducer principle

Ultrasonic transducers within sensors consist of two parts, generating part (emitting sound waves) and a receiving (detecting the reflected echo) part. Generally, ultrasonic transducers are divided into piezoelectric, capacitor, and magneto-elastic types. An ultrasonic piezoelectric sensor is most commonly used because of its good frequency response and smaller dimensions. The ultrasonic sensors (transducers) used in this work are piezoelectric. Piezoelectric transducer working is based on the principle of piezoelectricity. The most

commonly used sensing material in piezoelectric sensors is a ceramic material with a high dielectric constant which is capable of producing high piezoelectric voltage corresponding to force pressure, strain, and vibration. The construction of both transmitter and receiver are almost identical, as shown in Figure 2.8.



Figure 2.8: Ultrasonic transducers

The structure of the ultrasonic piezoelectric transducer is shown in the Figure 2.9. The components are a metal case, metallic cone, diaphragm, piezoceramic element, elastic body, and base. The metal case protects the transducer from moisture, dew, and dust. A metallic cone known as the resonator is used to emit ultrasonic waves and concentrate the waves in the case of an ultrasonic receiver. The metal disc and the piezoelectric ceramic plate are electrically connected with the terminal leads through wires. Piezoelectric ceramic material converts electrical signals to ultrasonic waves and vice versa. When an electrical voltage is applied across the piezoceramic causes stretching and contracting of the plate, generating forces on the plate. The metal diaphragm disc, also called the vibrator, generates ultrasonic waves. The forces excite the vibration of the metal diaphragm, and the cone consequently radiates ultrasonic waves. The receiver transducer works on the just reverse concept.

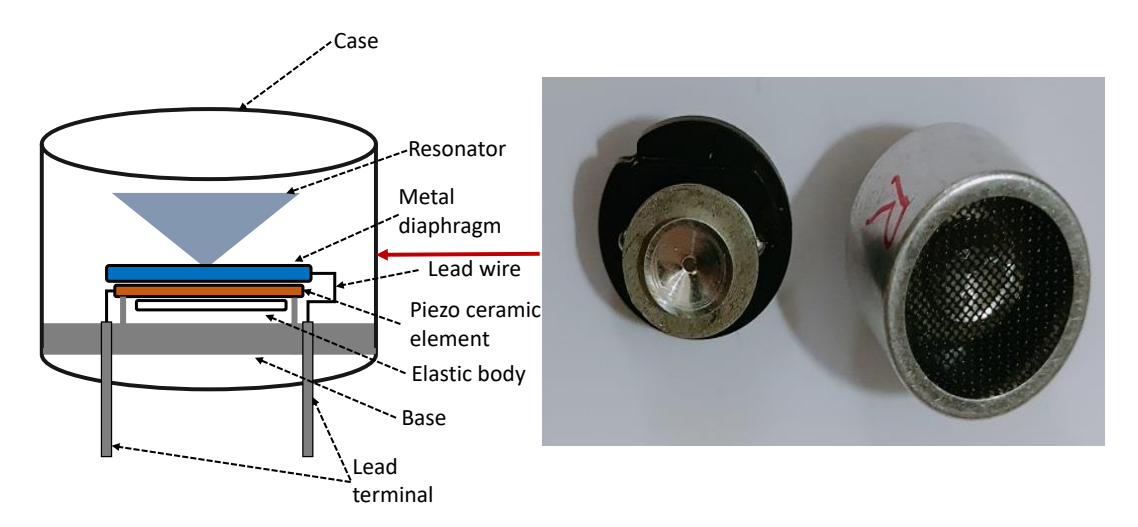


Figure 2.9: Piezoelectric ultrasonic transducer structure and representation of the transducer

Ultrasonic-based range measurement methods

The most popular approach to determine the range is based on the determination of time-of-flight (ToF). Accurate estimation of ToF is essential for ultrasonic measurement systems. There are mainly three most common methods for estimating ToF:

Threshold detection method: This is the simplest and fastest procedure to calculate the ToF. A predefined threshold level is used to compare the ultrasonic received signal. When the amplitude of the received signal reaches or exceeds the threshold value, the signal is considered to have been received at the receiver. A low signal-to-noise ratio (SNR) could result incorrect readings. The second most important factor is that setting a threshold level in the presence of bias can give incorrect measurements.

Algorithm 1 Threshold detection method

- 1: **procedure** Threshold(*Inputsignal*, *threshold*)
- 2: Step-1: Detect ultrasonic transmit time t_0
- 3: Step-2: Detect the echo signal at time t_1 when match with threshold value
- 4: Step-3: Calculate time of flight = $t_1 t_0$
- 5: Step 4: Determine the range or distance

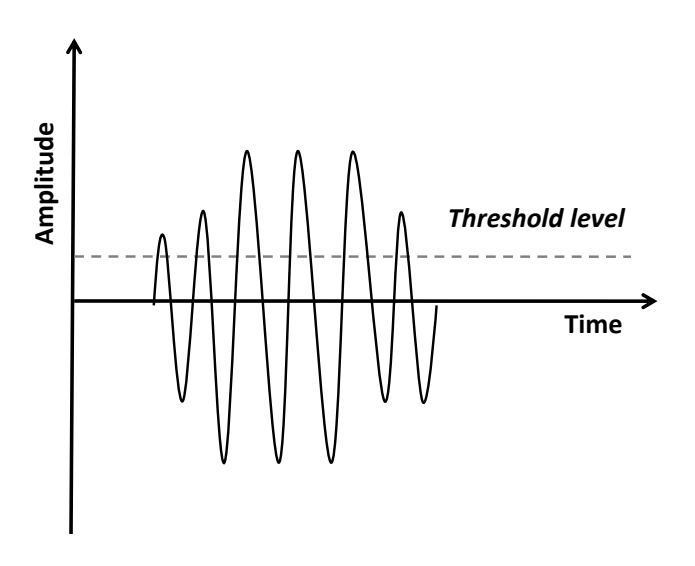


Figure 2.10: Threshold detection method

Cross-correlation method: The cross-correlation between a transmitted and received signal to calculate the time-of-flight of ultrasonic signals. The Accuracy of this method mainly depends on the width of the correlation peak; the narrower the peak, the higher the ToF estimation accuracy. The presence of multiple obstacles can introduce errors into the system. The disadvantage of this method is that it requires high computation time.

Algorithm 2 Cross-correlation method

- 1: **procedure** Threshold determination(*transmittedsignal*, *echosignal*)
- 2: Step-1: Perform cross correlation between transmitted and received signal
- 3: Step-2: Determine the cross-correlation peak value
- 4: Step3: The distance *d* is calculated using peak value information

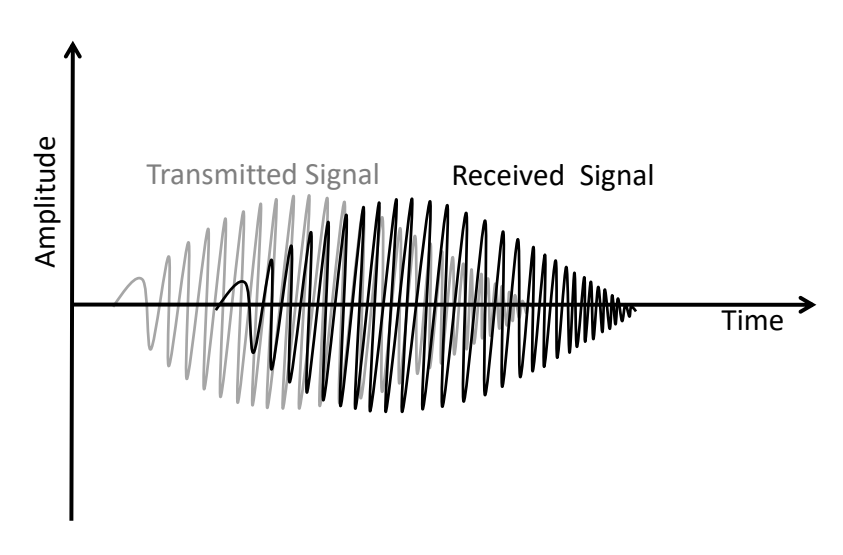


Figure 2.11: Cross-correlation method

Envelope detection method: The envelope of ultrasonic echo signals is used to estimate the ToF and to locate the peaks. Reflected ultrasonic echo envelope signal can also be used to obtain extra information about the target which helps in the classification of different materials. The Hilbert transform extracts the analytical signal from the envelope signal. Then denoising techniques can be applied to the extracted signal to improve the estimation accuracy.

Algorithm 3 Procedure envelope detection method

- 1: **procedure** Threshold detection(*transmittedsignal*, *echosignal*)
- 2: Step-1: Detect ultrasonic transmit time t_0
- 3: Step-2: Extract the envelope from the received echo signal
- 4: Step3: Mark the start time of the rising phase of the signal envelope as t_1 , $ToF = t_1 t_0$, then distance can be calculated

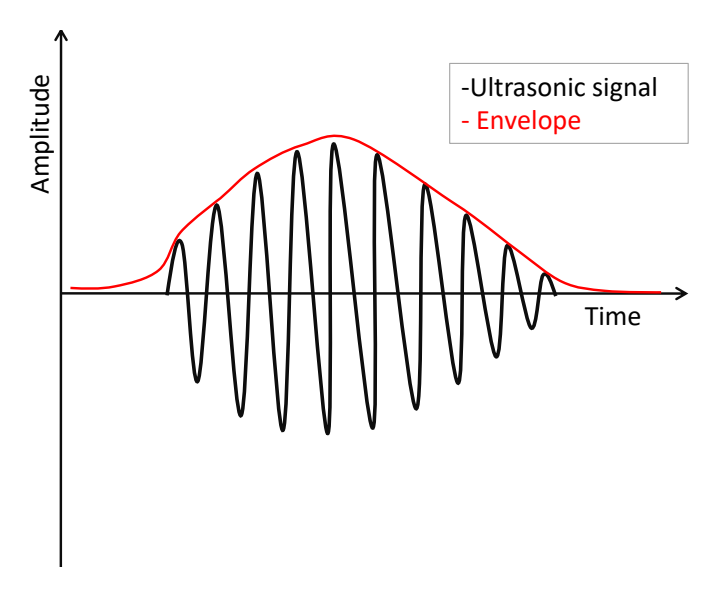


Figure 2.12: Envelope detection method

2.3 Principles and characteristics of sound waves

Ultrasound waves are mechanical waves that require an elastic medium, such as solid, liquid, or gas, to propagate. It is similar to sound waves. The speed of sound waves is different in the different medium through which it travels [26]. In any medium, the particles are packed together because of internal forces. When an object vibrates, it causes movement in the particles of the medium, propagating the sound wave. Piezoelectric transducers can produce longitudinal (compression wave) and transverse waves (shear wave). Most ultrasonic technologies use either longitudinal waves or transverse waves. Ultrasound waves propagate as longitudinal waves in the air and liquid medium and transverse waves in solids.

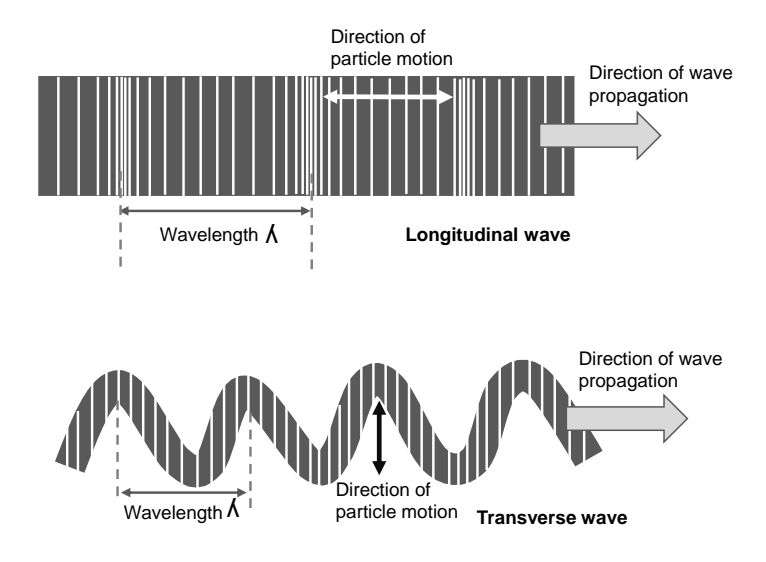


Figure 2.13: longitudinal and transverse waves with direction of particle movement

The motion of particles parallel to the direction of propagation of sound wave in longitudinal waves. The wave travels in the material in alternate compression and rarefaction series. In transverse wave the particle moves perpendicular the direction of propagation of sound wave. Transverse waves consist of crests and troughs.

The speed of sound through a medium is equal to the product of wavelength and frequency. Since frequency is inversely proportional to the period, the speed of the sound wave is related to its frequency and wavelength as follows:

$$c = \lambda f \tag{2.1}$$

Where, c is the speed of sound, λ is the wavelength, and f is the frequency.

The speed of Sound remains the same (nearly independent) for all frequencies in a given medium under the same physical conditions. At constant temperature and humidity the speed of sound remains constant. Ultrasonic waves are reflected at boundaries with a difference in acoustic impendence. The speed of sound is depends on the rigidity and density of the medium.

The speed of sound in air is slower than in solids and liquids because air's rigidity is less than solids and liquids.

The general expression of a mechanical wave's speed depends on the elastic and inertial properties of the medium.

$$v = \sqrt{\frac{elastic\ property}{inertial\ property}}$$
 (2.2)

The speed of sound in a solid medium depends on Young's modulus Y of the medium and the density ρ

$$C_{solid} = \sqrt{\frac{Y}{\rho}} \tag{2.3}$$

In a fluid, the speed of sound depends on the bulk modulus B and the density ρ of the medium,

$$C_{liquid} = \sqrt{\frac{B}{\rho}} \tag{2.4}$$

The adiabatic bulk modulus of an ideal gas at pressure P is $B = \gamma P$. In an ideal gas, the equation for the speed of sound is

$$c_{gas} = \sqrt{\frac{\gamma P}{\rho}} \tag{2.5}$$

where γ is the adiabatic index (ratio of specific heats) and ρ is the density.

In an ideal gas, we can use the ideal gas law:

$$PV = nRT = \frac{mRT}{vM}$$
 (2.6)

R is the universal gas constant, n is number of mole, m is mass of the gas, T is the absolute

Medium	Speed (m/s)
Gases at 0°C	
Air	331.45
Hydrogen	1290
Helium	965
Carbon dioxide	259
Oxygen	316
Liquids at 20°C	
Sea water	1540
Water, fresh	1480
Ethanol	1160
Mercury	1450
Human tissue	1540
Solids (longitudinal or bulk)	
Steel	5960
Marble	3810
Aluminum	5120
Glass	5640
Vulcanized rubber	54
Polyethylene	920
Lead	1960

temperature and M is the molecular mass.

$$P = \frac{m}{M}RT = \rho \frac{RT}{M} \tag{2.7}$$

$$c_{gas} = \sqrt{\frac{\gamma P}{\rho}} = \sqrt{\frac{\gamma RT}{M}}$$
 (2.8)

The speed of sound is independent of pressure for a fixed temperature. Increase in humidity in air is the result of increase of the moisture content thus decreases its density. Hence, the speed of sound increases with the increase in moisture content in air. The velocity and wavelength of the ultrasonic wave depend on the material's elastic properties. Ultrasonic waves will be reflected, and some will be transmitted when there is a change in elastic

properties.

Ultrasound waves

Sound waves with a frequency of 20 kHz and above are referred to as ultrasound waves. A mechanical wave (or vibrations) requires a medium (solid, liquid, or gas) to propagate. The sound waves are classified into three types based on their frequencies as shown in Figure 2.14. Sound waves with a frequency below 20 kHz are known as infrasonic waves; audible sound frequency lies between 20 Hz and 20 kHz, and frequency above 20 kHz is known as ultrasonic waves.

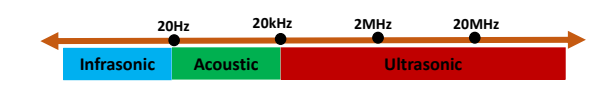


Figure 2.14: Frequency ranges of sound waves

2.3.1 Characteristics of ultrasonic waves

As sound waves go away from the source, the sound's intensity decreases. The intensity of sound is directly proportional to the square amplitude. Therefore, the amplitude of the sound decreases with distance as shown in the Figure 2.15. The frequency does not change with distance as it is a characteristic of the source. The frequency of sound depends upon the source of the sound, not the propagation medium. Hence, it does not change. The amplitude depicts the amount of energy the wave carries.

As an ultrasound wave propagates through a medium, the intensity reduces with the distance traveled [10, 12, 27, 28]. Attenuation increases linearly with frequency. Ultrasound beam intensity decreases exponentially due to attenuation (scattering, diffraction, and absorption), according to:

The expression for the acoustic pressure in a medium with attenuation is expressed as

follows, where α is taken to be the attenuation coefficient. In negligible or no scattering cases, α represents the absorption coefficient. The intensity (assuming plane wave) is:

$$I = I_0 e^{-\alpha d} \tag{2.9}$$

Where I is the amplitude of sound pressure at distance d from the source, I_0 is the initial sound pressure.

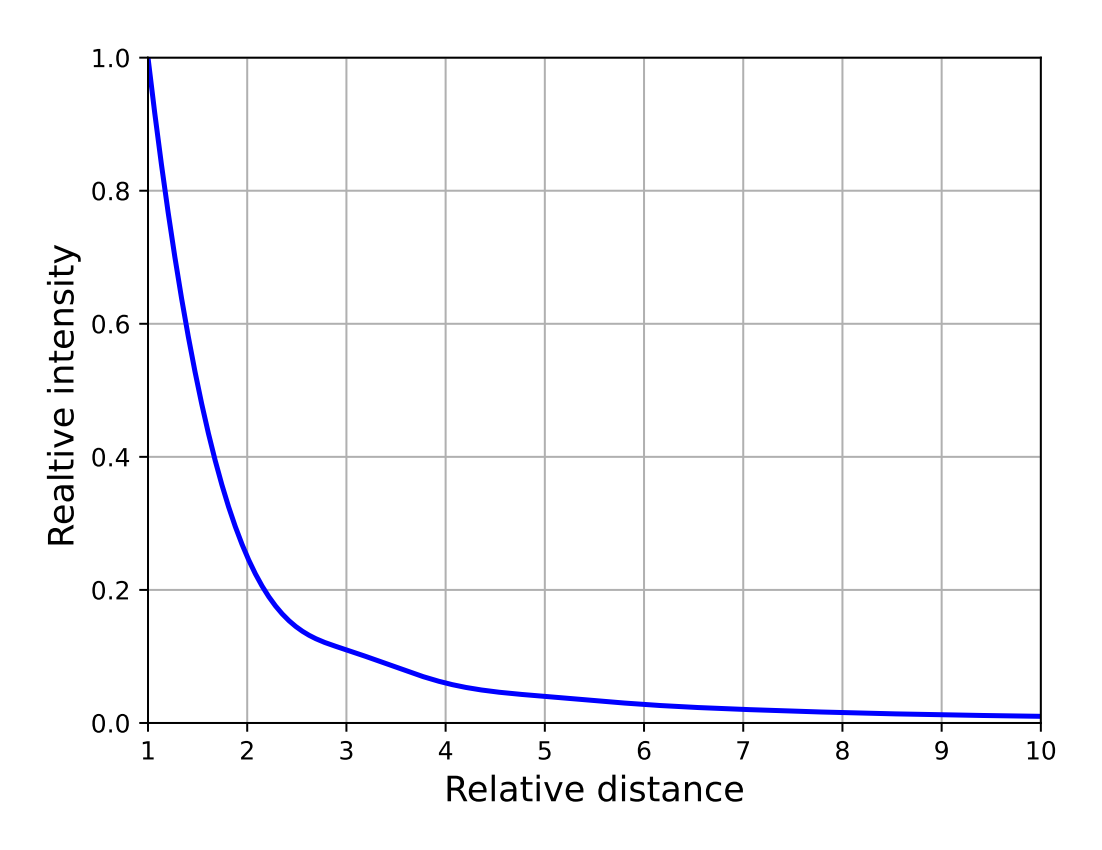


Figure 2.15: Sound intensity with distance

Attenuation

The attenuation of sound wave in air medium mainly due to scattering and absorption of the sound waves. When sound propagates through a medium, the sound pressure decreases with distance. **Acoustic impedance:** The acoustic impedance is computes as the product of speed of sound and density of the material.

$$Z = \rho c \tag{2.10}$$

Where Z is the acoustic impedance of the material, ρ is the material density, and c is the speed of the sound wave in the material.

Reflection: The amount of reflection of the ultrasonic wave depends on the acoustic impedance of two different materials.

$$R = \left(\frac{Z_2 - Z_1}{Z_2 + Z_1}\right)^2 \tag{2.11}$$

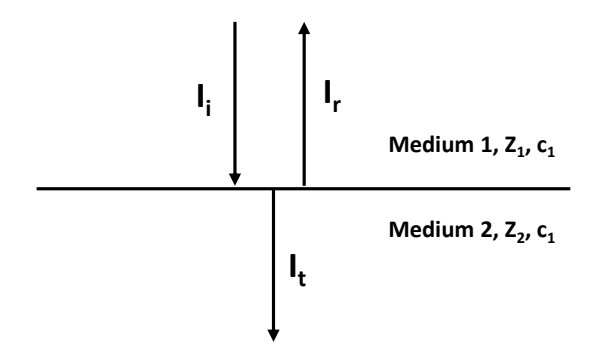


Figure 2.16: Reflection, incident, and transmitted ultrasonic waves

Diffraction: The diffraction is the change in the direction of sound wave as they travelling through a medium. The amount of diffraction (the bending of wave) increases with increase in wavelength and decreases with decrease in wavelength.

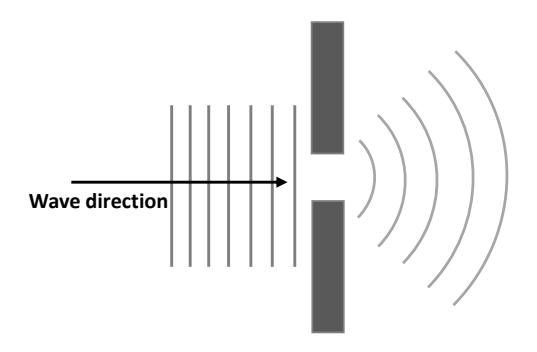


Figure 2.17: Diffraction in sound wave

Refraction: The refraction is due to the different velocities of the ultrasound waves as they pass from one medium to another.

$$\frac{\sin \theta_1}{\sin \theta_2} = \frac{c_1}{c_2} \tag{2.12}$$

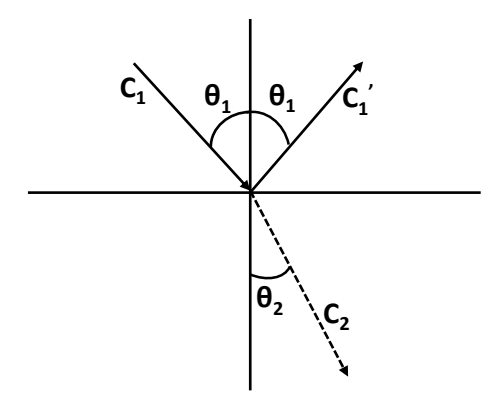


Figure 2.18: Refraction of the sound wave in different medium

Influence of environmental parameters on sound wave

There is a near linear relationship between speed of sound and the air temperature (2.8). As the temperature increases the speed of sound also increases. Temperature is one of the most important environmental parameter that influence the ultrasonic measurement system. Figure 2.19 shows the variation of speed of sound with temperature.

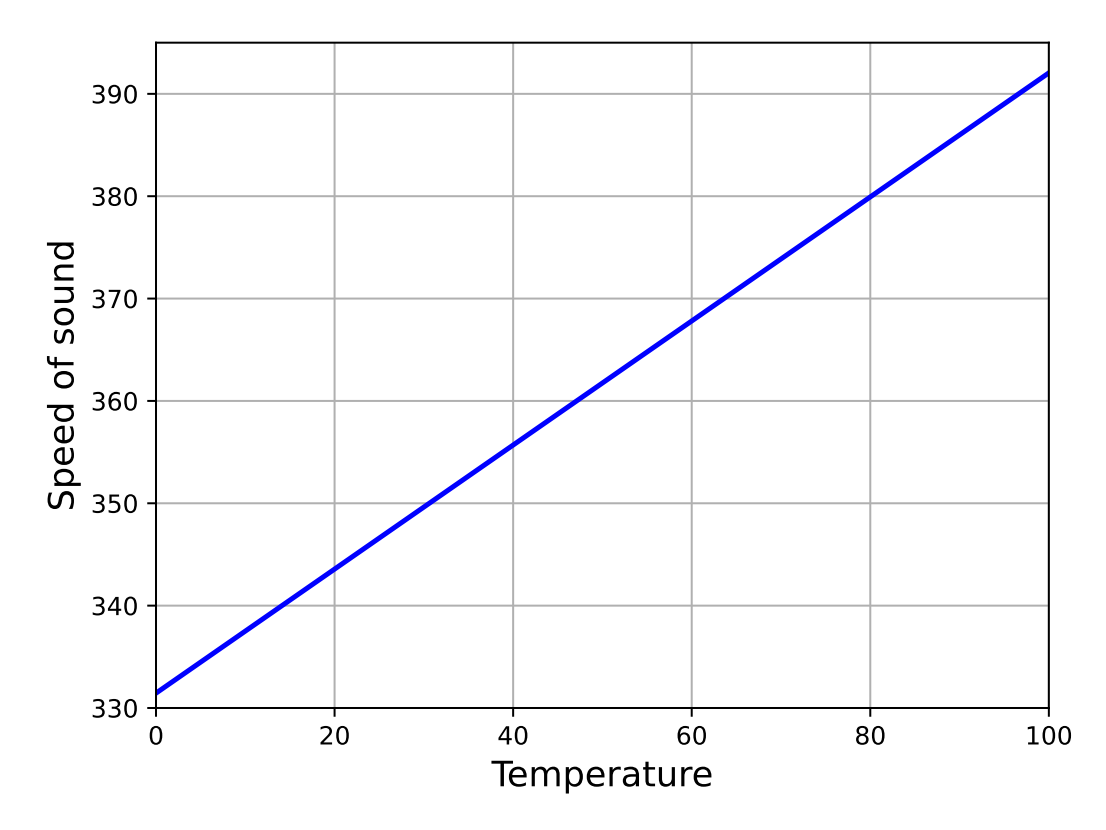


Figure 2.19: Variation of temperature *versus* speed of sound in dry air

Relative Humidity (RH) effect on speed of sound, but the effect is less compared to temperature. Thus, in presence of both temperature and humidity the speed of sound is non-linear. Figure 2.20 shows the speed of sound in air changes with temperature and relative humidity. Hence, for range measurement systems using airborne ultrasonic sensors, it is necessary to compensate the temperature and relative humidity.

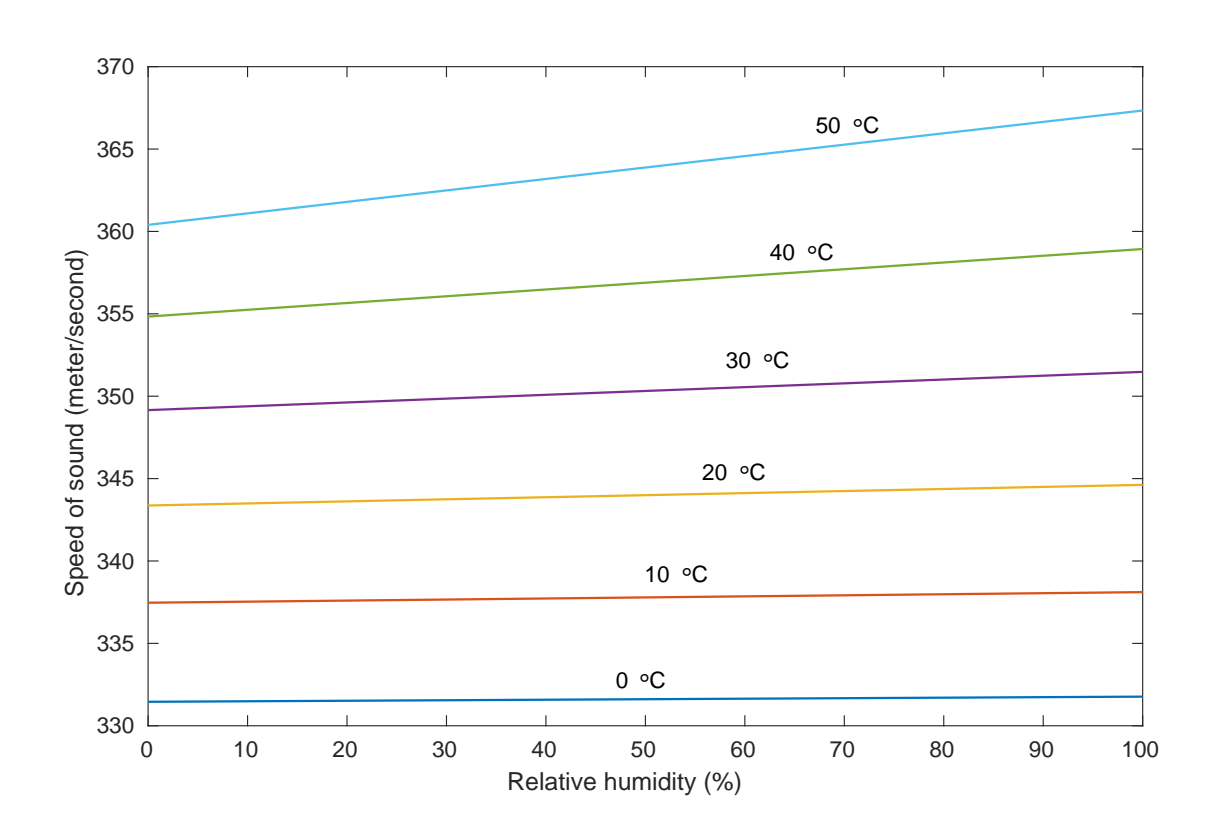


Figure 2.20: Variation of speed of sound with relative humidity at different temperatures

The ultrasonic wave intensity undergoes an attenuation when propagating through air medium, and the intensity decreases with the square of the distance from the source [29, 30, 31, 32]. So, attenuation is directly proportional to propagation distance. As the ultrasonic wave travels through the air medium, a combination of absorption and scattering gives rise to an overall attenuation level. Absorption is the loss of amplitude with an increase in temperature and humidity in the propagation medium. Figure 2.21 shows the attenuation coefficient versus relative humidity for frequencies between 5 and 50 kHz in the air at 20°C.

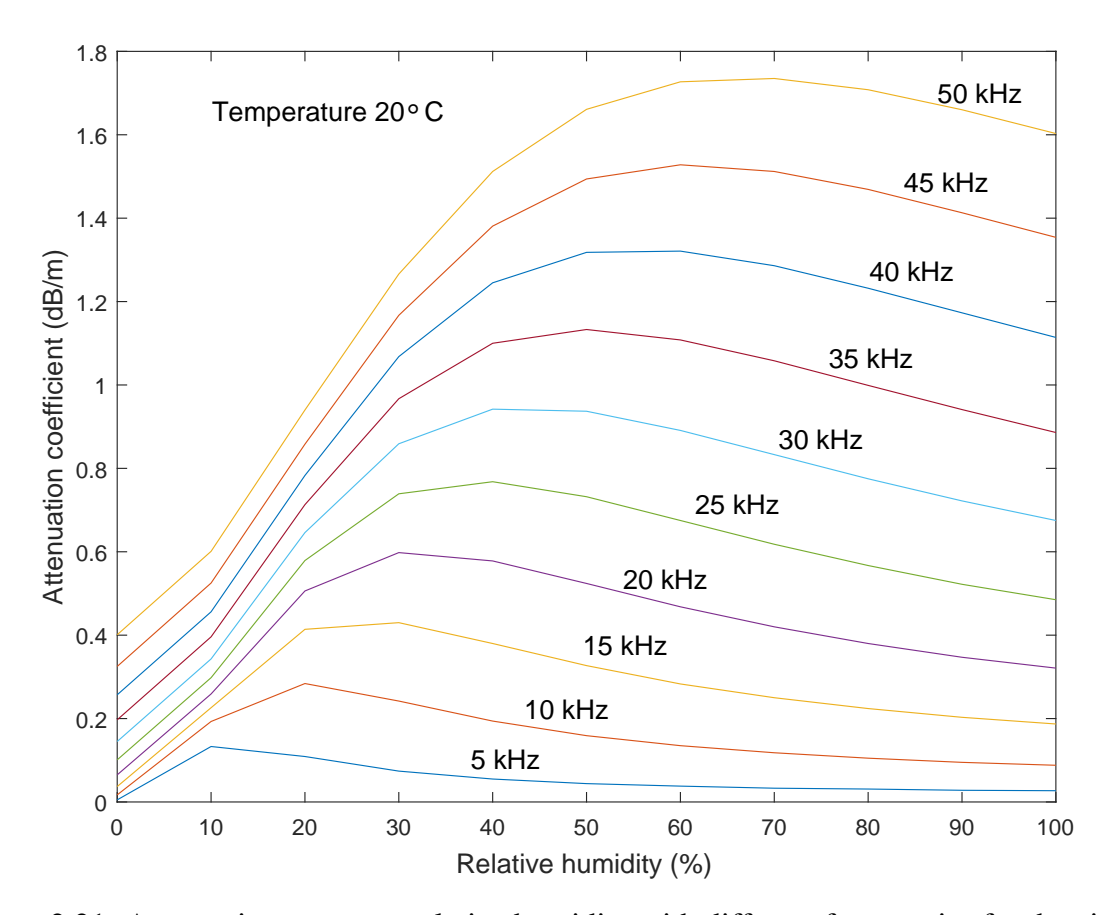


Figure 2.21: Attenuation versus relative humidity with different frequencies for the air temperature at 20 ^{o}C

Sound attenuation depends not only on the frequency but also on temperature and relative humidity. Attenuation as a function of relative humidity for various temperatures is shown in Figure 2.22.

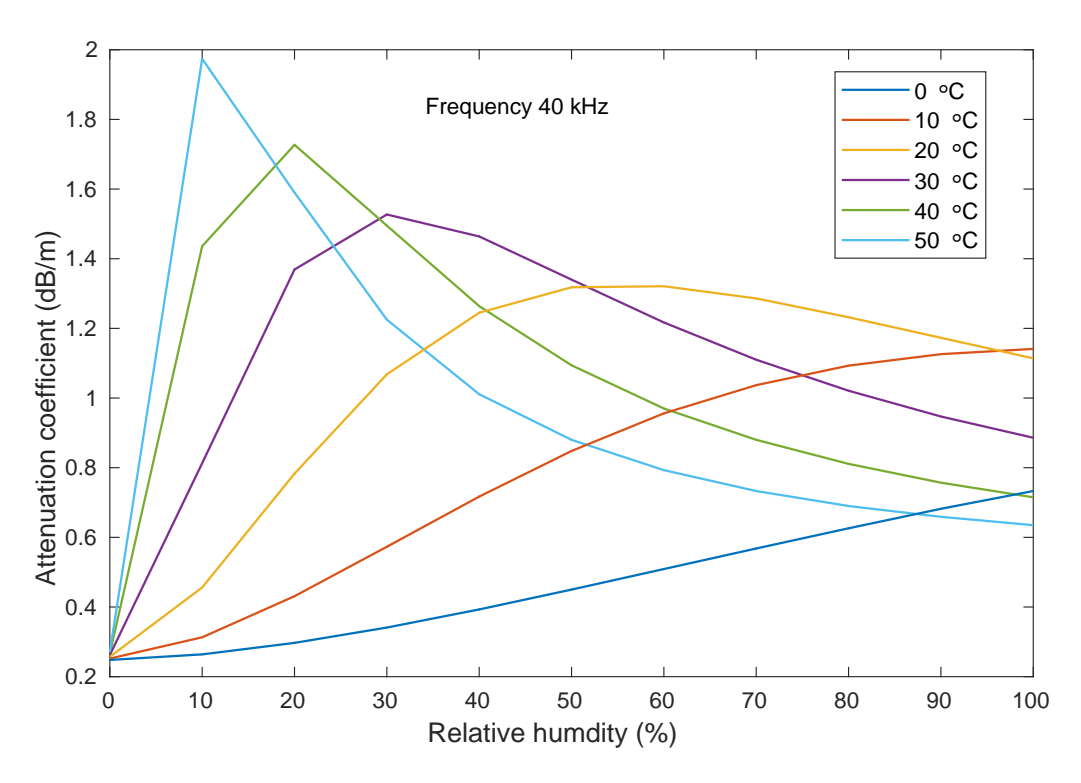


Figure 2.22: Attenuation coefficient of the sound wave as a function relative humidity with different temperatures at frequency 40kHz

Attenuation by absorption of a sound wave in the air medium is directly proportional to the propagation distance. Absorption in the air is less at low frequencies and smaller distances, while at larger distances, atmospheric attenuation becomes more, as shown in figure Figure 2.23. The attenuation rate is approximately $6 \, dB$ per doubling distance from a simple point source.

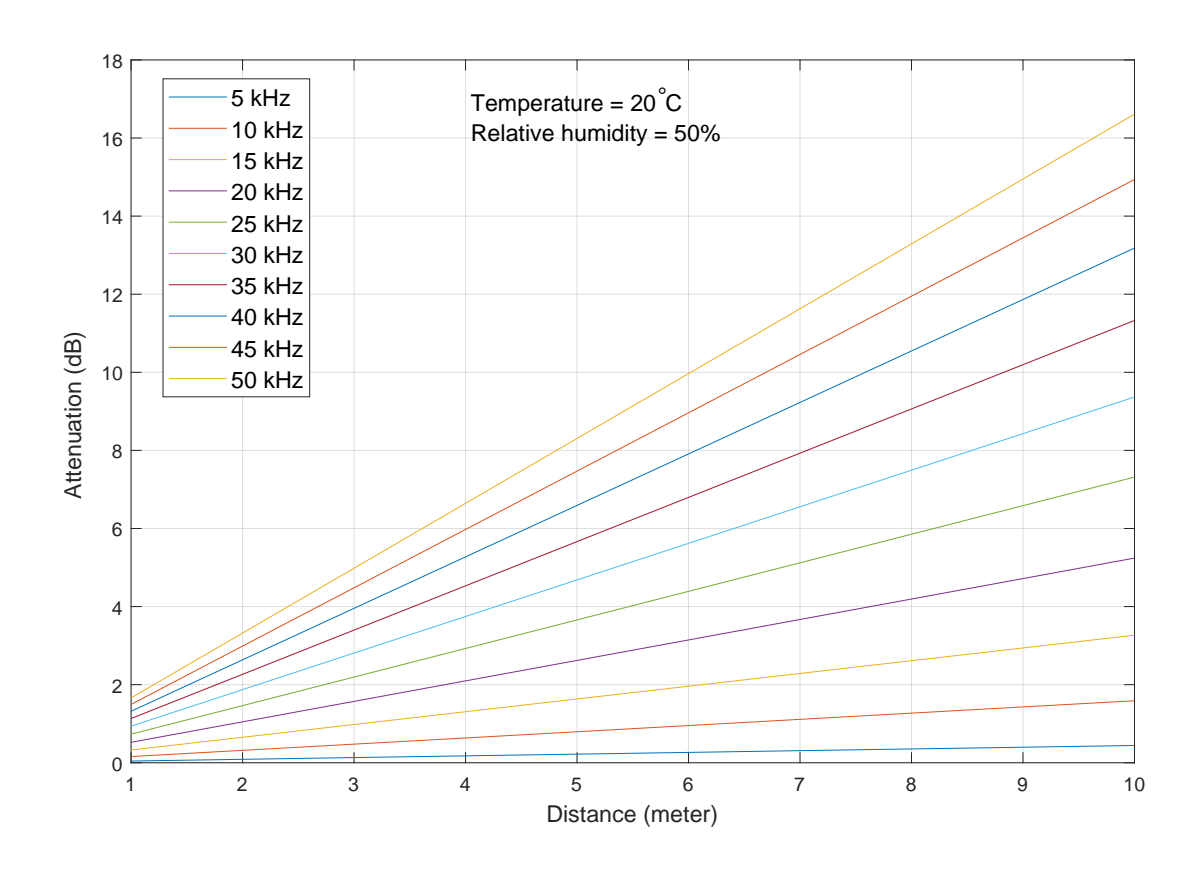


Figure 2.23: Atmospheric attenuation of the speed of sound in air varies with distances for different frequencies at temperature $20 \, ^{o}C$ and relative humidity 50%

Uncertainty in ultrasonic sensor-based measurement

The distance *d* to be measured by means of ToF is obtained by the simple relation:

$$d = k \cdot c \cdot T_f \tag{2.13}$$

Where d is the distance measured between the ultrasonic transducer and the object, k is a constant whose value depends on the path geometry and is 0.5 in this case. c is the speed of sound in the measurement medium (air medium), and T_f is the time-of-flight of the ultrasonic signal.

Several sources of uncertainty are involved in ToF-based distance measurement [33, 34]. The three main components of uncertainty is given in equation (2.13) can be reformulated as

$$\epsilon_d = \epsilon_k + \epsilon_C + \epsilon_{T_f} \tag{2.14}$$

Where ϵ_k is the uncertainty term associated with the geometry of the signal path and is negligible in this case, the term ϵ_C is due to several factors, including the sound wave frequency and propagation medium properties. This ϵ_C term depends on the air temperature and relative humidity for airborne ultrasonic sensors. The uncertainty term ϵ_{T_f} is mainly because acoustic noise results delay in the echo detection and the frequency of the ultrasonic sensor; the higher the frequency more minor the error.

CHAPTER 3

Liquid level measurement using intelligent ultrasonic sensor

Ultrasonic sensors are low-cost and widely used for contactless distance measurement and proximity detection applications in airborne mode. These sensors use sound waves at a frequency above the human hearing range. The speed of sound wave propagation is affected by temperature, relative humidity, and other environmental parameters. The ultrasonic measurement system can also be affected by acoustic and electronic noise. Standard level measurement techniques assumes uniform temperature and relative humidity along the measurement medium. Using the standard ultrasonic measurement technique, we estimate water level in different sized water containers and storage tanks. It is seen that there exists a non-uniform temperature and relative humidity throughout in the measurement medium. Hence, the standard measurement technique is not able to estimate distance accurately. In this study, an modified neural network architecture based algorithm is proposed to enhance the accuracy of the level measurement using ultrasonic measurement system. With this proposed approach, the standard operating range of the ultrasonic sensor is extended. The Levenberg-Marquardt Back-Propagation Artificial Neural Network (LMBP-ANN) algorithm is used to reduce the measurement error. In order to validate the proposed model, we conducted several experiments at various depths of water level in dynamic environmental conditions.

3.1 Introduction

Ultrasonic sensors are reliable, cost-effective devices to sense proximity and measure levels with high reliability. The major advantages of the ultrasonic sensor compared to other similar sensors are mainly it is small in size, portable, low-cost, non-contact, non-intrusive, robust in harsh environments, has longer functional life, simplicity of use, and safe. The principle behind the ultrasonic measurement system is based on the Time-of-Flight (ToF), the amount of time it takes to send and receive a reflected ultrasonic sound wave in the propagation medium [35, 36]. The low-cost piezoelectric ultrasonic sensor consists of an ultrasonic transmitter and a receiver housed on the same circuit and the operating frequency is 40 kHz [34, 37]. Ultrasonic rangefinder use time of flight and speed of sound to measure distance. The distance d can be determined based on the equation, d = (ToF * c)/2, where c is the speed of sound (m/s) [2, 36, 38]. The speed of sound in dry air at Standard Temperature and Pressure (STP) is 331.45 $m/s \pm 0.05$ [10, 39]. (STP: 273.15 K, 1.01325 × 10⁵ Pa = 1 atm)

Environmental parameters that influence the speed of ultrasonic sound waves in the air medium are temperature, relative humidity and to some extent, other gases present in the medium [10, 40]. In addition to environmental parameters, acoustic interference and electronic noise also affect the performance of the system [37]. Both external and internal noise induce uncertainty in ultrasonic measurement systems.

Nowadays, water is scarce and a more valuable resource as the imbalance between demand and supply growing day by day. Therefore, proper management of water resources using intelligent sensor technology is the need of the hour. Storage tanks and containers are used to store high volumes of water to manage the demand. Monitoring the water level in storage tanks and sumps is very important for efficient water management. The water level

in a container of the storage tank can be determined using the following equation

$$L = H - D \tag{3.1}$$

where L is the water level, H is the height of the tank measured from ultrasonic sensor position to zero level, and D represents the distance or depth from the measuring device (ultrasonic sensor) to the water level or surface. The parameter D calculated using ToF and C.

Ultrasonic sound waves are very sensitive to variations in environmental temperature, humidity, and some extent other gases present in the environment. The speed of sound in air medium increases as the temperature increases and it will lead to incorrect distance or level measurements [10]. The effect of temperature and relative humidity can be compensated using observations of temperature and humidity sensors along with the ultrasonic sensor. Ultrasonic level measurement system will be accurate if temperature and relative humidity remain consistent or uniform between the sensor position and the water surface. Despite this, some parameters induce errors in ultrasonic measurement, which is significant for many level measurement applications. This error is due to the parameters like electronic noise, interference, and the variation (gradient) of temperature and relative humidity throughout the measurement medium or path between the sensor location and the water surface. Especially, when the water tank diameter is larger, a small variation in level measurement will result in an erroneous volume measurement of water contained in the tank. Moreover, when the tank is exposed to the sun, the variation of temperature and relative humidity increases and this leads to significant errors in level measurement.

Most of the existing works on ultrasonic-based level or distance measurement in the literature focused on compensating the effect of medium temperature only [41, 42, 43]. In this work, an extensive review of existing ultrasonic measurement techniques for liquid level

monitoring is presented and a novel Artificial Neural Network (ANN) technique to effectively compensate the environmental parameters that affect the performance accuracy of ultrasonic measurement is proposed. The main objective of this work is to enhance the accuracy of the ultrasonic-based measurement system, which is adaptive to the environmental changes in the measurement path. The proposed method can minimize the error substantially. This model also extends the operating range of the ultrasonic sensor.

The organization of the chapter is as follows. In Section 3.2, we discuss the existing techniques for liquid level monitoring along with ultrasonic-based level measurement. Theory of sound wave propagation concerning environmental parameters such as temperature and relative humidity are described in Section 3.3. The mathematical expression of parameter uncertainties in ultrasonic distance measurement is presented in Section 3.4. Proposed modified artificial neural network model used in the development of intelligent ultrasonic systems is described in Section 3.5. Section 3.6 contains the specification of electronic components used in designing the experiment, experimental setup, experimental procedure, and data collection. In Section 3.7, the detailed experimental results are presented to signify the effectiveness of the proposed approach. The complexity of the proposed method, performance comparisons, and limitations are discussed in Section 3.8. Finally, Section 3.9 concludes the paper with a discussion on the future scope of the work.

3.2 Related works

This section reviews existing liquid level measurement techniques and highlights the works related to ultrasonic-based level measurement. There are various level measurement techniques used to measure liquid level [36, 44]. The level measurement methods are classified as contact and non-contact types [8]. Contact-type level measurement sensors include capacitive sensors, floating gauges, optical, and hydrostatic level sensors. On the other side, the non-contact level measurement includes radar, laser, and ultrasonic sensors.

The capacitive sensors measure the liquid level by measuring the capacitance between the conducting two copper plates [45, 46, 47, 48]. The dielectric constant observed between two plates is proportional to the water level [49]. The capacitance and dielectric constant are directly proportional; thus raising the liquid content will increase the capacitance. The advantage of capacitive level sensors has a broad application range and good accuracy [50]. Capacitive sensors get affected by the change in the dielectric constant, which varies with the temperature of the liquid to be measured. These sensors are well-suited for both point and continuous-level measurements. The floating type level switch uses a hollow float switch attached to the arm. The arm will get pushed up when the liquid content increases and goes down when liquid content decreases [51, 52, 53, 54, 55]. These level devices are contact-type point-level sensors. However, float-level sensors suffer from low accuracy and frequent maintenance. The disadvantage of this method is that float actuation relies on liquid contact and moving parts vulnerable to clogging, wear and tear, and damage. The principle of the hydrostatic level sensors is to measure the hydrostatic pressure which is proportional to the measured liquid height [56, 57, 58, 59]. The disadvantage of this method is direct contact with the medium, and regular maintenance is required.

Optical sensors are solid-state sensors that use the reflective property of light exploited for the measurement of liquid level [60, 61, 62, 63, 64]. Optical level sensor comprises a light-emitting diode (LED) and a light receiver. Light from the LED is directed to a prism and is reflected from the prism to the receiver when there is no liquid. When the sensor is immersed in liquid, the light is refracted out into the liquid, leaving little or no light to reach the receiver. The amount of received light by the receiver phototransistors indicates the liquid level. It is also a contact-type and point-level detection sensor. The optical type requires frequent maintenance and it is adversely affected by the change in the reflective property of the medium [65].

A radar level gauge is a non-contact measurement technique based on the calculation of time-of-flight. The distance between the emitted pulse source and the material surface can

be calculated as the product of one-half the time-of-flight and the speed of light [66, 67, 68, 69, 70]. This measurement system is not affected by the process material's state, such as agitation, corrosiveness, tackiness, temperature, pressure, etc. The main advantages of radar level sensors are high accuracy, non-contact type, and continuous level measurement. The disadvantage of radar level sensors are sensitive to interference and are high cost. The cost increases exponentially with an increase in the desired accuracy.

Laser level measurement is used to measure the level basically upon the same operating principle as ultrasonic level sensors [71, 72, 73, 74]. The only difference is that it uses the speed of light whereas the ultrasonic makes use of sound waves speed. This method is not cost-effective, proper calibration must be maintained to get an accurate level measurement. The presence of dust, dirt, and surface material seriously affects the performance of these devices.

Ultrasonic sensors are low-cost, non-intrusive, non-contact range measurement devices. These sensors are extensively used in many applications because of their simplicity of use, high level of safety, ease of installation and require less maintenance [4, 7, 34, 36, 37, 38]. Non-contact ultrasonic level sensors use sound waves for level measurement. The speed of sound depends on the medium parameters, so the influence of the environmental parameters must be taken into account for level measurement [42, 43, 75, 76, 77].

Rocchi *et al.* [4] characterized a low-cost ultrasonic sensor SRF05 for sea surface level measurement under the influence of temperature variations. They estimate the position of the water surface to determine the thickness and depth of the pollutant layer. Qiu *et al.* [7] presented a detailed review of ultrasonic ranging technology including signal processing methodologies, recent developments, current challenges, and future trends.

Carullo and Parvis [34] described an ultrasonic measurement technique for automotive applications to measure the height from the ground to a vehicle body based on the measurement of the reflected signal from the ground. The conducted experiment was in the range of $100-600 \ mm$ and the temperature range of $0-40 \ ^{\circ}C$. The standard distance

measurement uncertainty achieved in the experiment is 1 *mm*. Loizou and Koutroulis [50] presented an extensive review of the existing state-of-the-art techniques for water level sensing monitoring using capacitive and ultrasonic level sensors. Terzic *et al.* [42] designed and developed a fluid level measurement system based on a single ultrasonic sensor and Support Vector Machines (SVM) for dynamic environments, in particular automotive applications. Bucci and Landi [76] presented a novel algorithm for water level measurement in a water tank using ultrasonic sensor with a mean error of 0.5 *mm* for levels ranging from 100 *mm* to 1000 *mm* in ambient temperature conditions.

Mousa *et al.* [43] presented an ultrasonic-based wireless sensor platform to predict urban flash floods using ANN. Canali *et al.* [41] designed an airborne ultrasonic measurement system to accurately measure distance. Matsuya *et al.* [78] proposed a new method for liquid-level measurement based on the echo method. Zhang *et al.* [79] developed a novel method for an ultrasonic measurement system for level measurement using reflected ultrasonic echo energy. Carullo *et al.* [80] described a technique to improve the performance of ultrasonic distance sensors using two-level neural networks. Terzic *et al.* [81] developed a SVM based model using single ultrasonic sensor to measure the fluid level in dynamic environment by compensating the slosh and temperature effect.

Valentin Magori [82] differentiated the ultrasonic sensors into two types; 1) ultrasonic propagation sensors - decodes the parameters that are affected by the speed of sound propagation, local changes of propagation (diffraction and refraction), directional and frequency dependency, propagation attenuation, acoustic impedance, scattering and wave guiding coefficients. 2) Distance sensors- based on principles of use time of flight and amplitude of the received echo signal to derive the presence, distance, and type of a sound-reflecting object. Intelligent algorithms can be used to enhance the measurement range and resolutions.

Brudka and Pacut [83] presented an intelligent robot control system that employs

ultrasonic distance measurements. Shin and Kim [84] introduced a method for measuring the distance with crosstalk rejection at a high measurement rate using the CPPM signal and single-bit signal processing in a single ultrasonic sensor system. Shen *et al.* [85] proposed a new positioning method based on multiple ultrasonic sensors for the autonomous mobile robot and realized higher accuracy without considering temperature information. Majchrzak *et al.* [86] presented an ultrasonic proximity measurement system for mobile robots. Zhao *et al.* [87] designed a high-precision ultrasonic ranging system based on a single-chip microcomputer for the stability of ranging and the improvement of measurement accuracy. Krenik *et al.* [88] explored three different methods for an ultrasound-based positioning system for locating and controlling smart tools. Queiros *et al.* [89] presented a method for ultrasonic ranging based on the cross-correlation of two multi-frequency signals. Xiang and shi [90] analyzed that cause the error of ultrasonic distance measurement and designed the module by selecting the appropriate microprocessor and transducer to eliminate or reduce the effects of error for completing the system in the 1000 mm range from the precision requirement of 1 mm.

Ultrasonic liquid level measurement techniques discussed above have different application areas, different measurement ranges, and varied ranges of temperatures. None of the aforesaid methods explicitly considered the effect of relative humidity and gradient of temperature and humidity in the measurement in the measurement medium. In this work, we propose a novel ANN-based adaptive method to measure the level or distance with higher accuracy wherein, the error is limited to the millimeter range.

3.3 Speed of sound in air medium with temperature and relative humidity

This section describes the dependence of temperature and relative humidity on the sound wave. The speed of sound in an ideal gas is

$$c_{ideal} = \sqrt{\frac{\gamma \times p}{\rho}} = \sqrt{\frac{\gamma RT}{M}} = \sqrt{\frac{\gamma RT}{M}} \left(\frac{273K}{273K}\right)$$

$$\sqrt{\frac{(273K)\gamma R}{M}} \sqrt{\frac{T}{273K}} \approx 331.45\sqrt{\frac{T}{273K}}$$
(3.2)

Where C_{ideal} is the speed of sound (in m/s) in ideal gases. p is the ambient pressure. γ is the ratio of the specific heat capacity of a gas at a constant pressure (C_p) to the specific heat capacity of a gas at a constant volume (C_V) ($\gamma = C_p/C_V$). ρ is the gas density. $R = 8.31 \text{ J/mol} \cdot K$ is the universal gas constant, T is the absolute temperature in kelvins, and M is the molecular mass. t is the temperature in degree Celsius.

Applying Taylor series expansion to equation (3.2), the simplified version is represented as

$$c \approx 331.45 \sqrt{1 + \frac{t}{273.15}} = 331.45 + 0.607 \times t$$
 (3.3)

Where 331.45 m/s is the speed of sound in dry air at 0 °C [39]. t is the temperature in degree Celsius. It is evident from equation (3.3), the speed of sound increases with increase in temperature. For every 1 °C increase in temperature speed of sound increases by 0.607 m/s. Figure 3.1 shows the relationship between the speed of sound and temperature.

The effect of relative humidity on the speed of sound is less compared to temperature. Relative humidity is the amount of moisture that is present in the air compared to the maximum amount the air can hold at that temperature. According to equation (3.2), the speed of sound in air is inversely proportional to the square root of density. Moist air

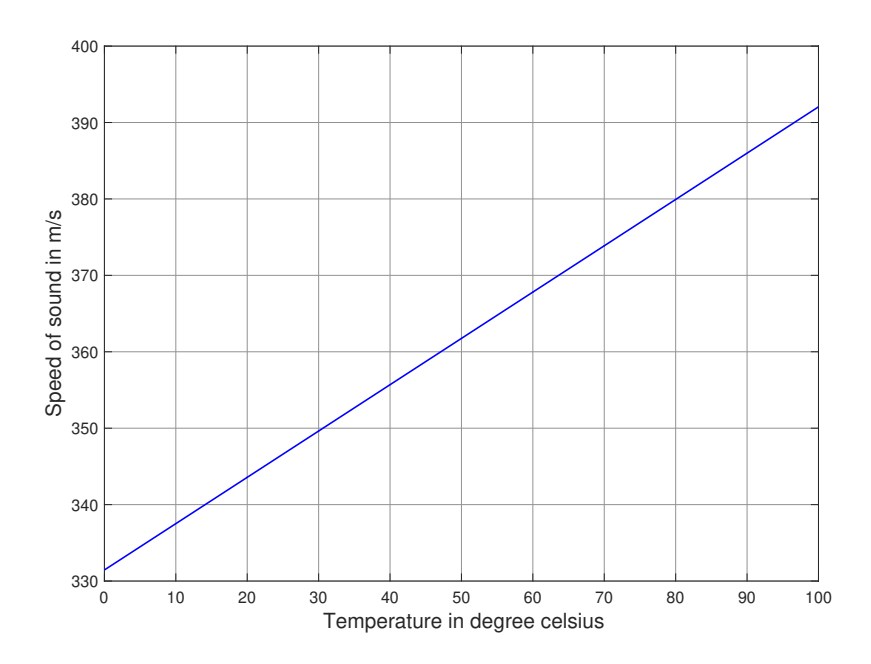


Figure 3.1: Variation of speed of sound with temperature in air medium

contains water molecules and the mass of water molecules is less than oxygen, nitrogen and CO_2 molecules. Therefore, the sound wave travels faster in humid air (moist air) than in dry air. Sound waves travel slower in cooler air than they do in warmer air. According to [40, 91], speed of sound in gas can be defined as

$$c^2 = \gamma \, \frac{RT}{M} \left(1 + \frac{2pB}{RT} \right) \tag{3.4}$$

Where C is the speed of sound. T is the temperature on an absolute scale (e.g. Kelvin). γ , p, R, M, B represent the specific heat ratio, pressure, the universal gas constant, molecular mass and second virial coefficient respectively. The relationship between the speed of sound, temperature, and relative humidity is represented in equation (3.4). As stated in [39, 40, 91], an approximate equation is given in equation (3.5) can be used to calculate C as a function

of temperature, pressure, CO_2 concentration and water vapor mole fraction.

$$c(t, p, x_w, x_c) = a_0 + a_1 t + a_2 t^2 + (a_3 + a_4 t + a_5 t^2) x_w$$

$$+ (a_6 + a_7 t + a_8 t^2) p + (a_9 + a_{10} t + a_{11} t^2) x_c$$

$$+ a_{12} x_w^2 + a_{13} p^2 + a_{14} x_c^2 + a_{15} x_w p x_c \quad (3.5)$$

Coefficients a_i are determined by calibration in reference air of known temperature t in degree Celsius, known relative humidity RH (expressed in percentage), and known speed of sound at the measurement frequency. x_w represents the water vapor mole fraction, x_c is the carbon dioxide mole fraction and p is the pressure. Figure 3.2 represents the change in speed of sound with temperature and relative humidity based on equation (3.5), where the value of $p = 101.3 \ kPa$, and $CO_2 = 314 \ parts \ per \ million \ (ppm)$.

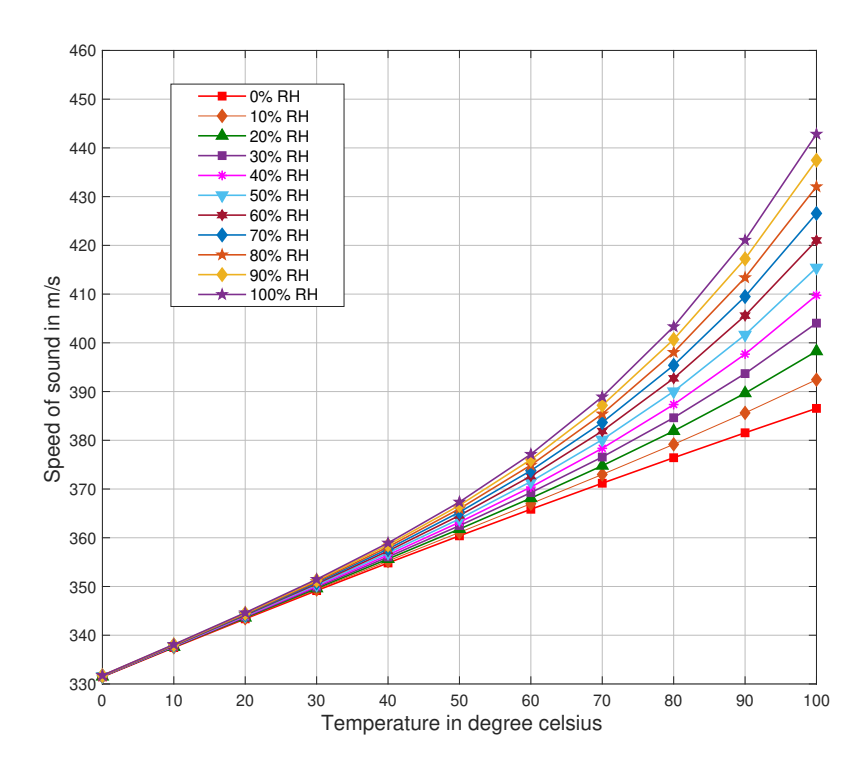


Figure 3.2: Variation of speed of sound in presence of both temperature and relative humidity

3.4 Uncertainty in distance measurement

Every measurement is subject to some uncertainty. As mentioned in [34, 80, 92], ultrasonic sensor measures the distance as

$$d = k T_f c (3.6)$$

Where T_f is the ToF of an ultrasonic signal, c is the speed of sound in air medium, d is the distance to be measured and k is a constant with value 0.5. k value is chosen to be 0.5 as ultrasonic sound covers twice the distance in the time T_f . Thus, distance measurement uncertainty $u_c^2(d)$ is represented as

$$u_c^2(d) = \sum_{i} (g_i u(x_i))^2$$
 (3.7)

Where g_i are the partial derivatives of equation (3.6) with respect to all x_i 's that significantly affect the distance measurement. According to [93, 94], the standard uncertainty associated with distance measurement is obtained from equation (3.7) and can be represented as

$$u_i^2(d) = (k T_f)^2 u^2(c) + (k c)^2 u^2(T_f)$$
(3.8)

Where $u^2(c)$ and $u^2(T_f)$ are the standard uncertainties of speed of sound and ToF respectively. The speed of sound in air medium can be represented as function of temperature t and relative humidity h.

$$c = f(t, h) \tag{3.9}$$

According to [93], uncertainty in measurement shown in equation (3.8) can be reformu-

lated as

$$u_i^2(d) = (k T_f)^2 \left[\left(\frac{\partial f}{\partial t} \right)^2 u^2(t) + \left(\frac{\partial f}{\partial h} \right)^2 u^2(h) \right] + (k c)^2 u^2(T_f) \quad (3.10)$$

$$u_{i}^{2}(d) = (k T_{f})^{2} \left(\frac{\partial f}{\partial t}\right)^{2} u^{2}(t) + (k T_{f})^{2} \left(\frac{\partial f}{\partial h}\right)^{2} u^{2}(h) + (k c)^{2} u^{2}(T_{f})$$
(3.11)

Uncertainty in ToF ($u^2(T_f)$) is mainly because of the influence of noise and attenuation. Uncertainty in the measurement is mainly due to: (i) gradient of temperature in the measurement path; (ii) gradient of relative humidity (more in the case of water tanks); (iii) presence of other gases in the medium; (iv) crosstalk or interference; and (v) electronic noise (which includes shot noise and thermal noise). Water storage tanks located outdoors are directly exposed to sunlight and experience a temperature swing hence, there is a variation in temperature and humidity inside the storage tank. A sample observation of change in temperature and humidity level from the point of measurement to the water surface is shown in Table 3.7. It is not possible to accurately determine the speed of the sound wave in air medium considering all the above factors simultaneously. In this work, we propose an ANN-based approach to compensate all types of uncertainties that influence the ultrasonic-based level measurement.

3.5 Methods

3.5.1 General scheme of the proposed method

Multilayer Perceptrons (MLPs) are neural network models with a single hidden layer that can approximate any continuous function [19, 20, 95]. The main objective of function approximation is to improve the accuracy of the estimation model. An MLP is a class of feedforward ANN, which consists of an input layer, several hidden layers, and an output layer. MLP network used one of the most popular training algorithms called the backpropagation training algorithm. Backpropagation aims to minimize the cost function (minimize the error) by modifying the network's weights and biases. A simple single node MLP network structure is shown in Figure 3.3. Node i in the figure is referred to as a neuron. It includes a summation and an activation function f. The inputs x_j , j = 1, 2...n to the neuron are multiplied by weights w_{ji} and summed up together with the constant bias b_i . The resulting o_i is the input to the activation function f. The activation function can be a linear, threshold, or sigmoid function. A sigmoid activation function is usually used for hidden layers and a linear function is used for the output layer.

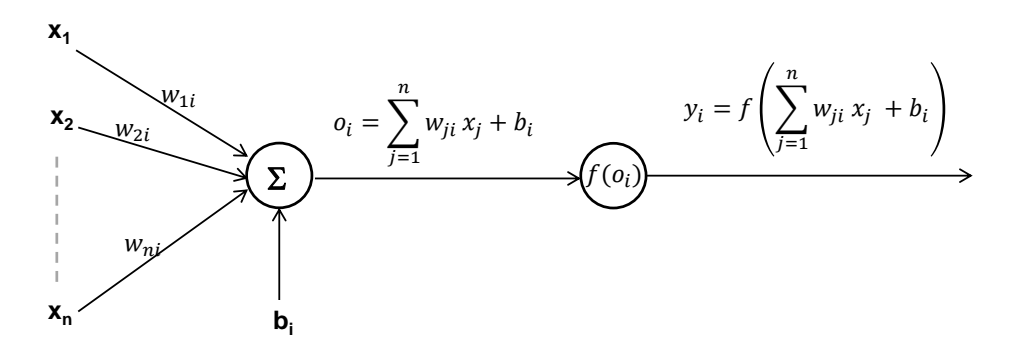


Figure 3.3: Structure of a simple neural network with single node

The output of node i becomes

$$y_i = f\left(\sum_{j=1}^n w_{ji} x_j + b_i\right)$$
(3.12)

Neural networks with at least one hidden layer are necessary and sufficient to estimate an arbitrary nonlinear function with desired accuracy [19, 20]. ANN-based function approximations find the pattern within input-output data without the need for predetermined models. In this work, we used an MLP with three layers as shown in Figure 3.4, which comprises one input layer, one hidden layer, and one output layer. For training the ANN model, transfer function tansig sigmoid function (3.13) is used for hidden layer neurons, and purelin linear transfer function (3.14) is used for the output layer. Four input variables namely temperature (t), relative humidity (h), speed of sound (s), and measured distance

 (m_d) are presented to the input layer. There is only one output neuron at the output layer of the neural network that predicts the estimated output (y_i) . w_{ij}^k represents the weight associated between i^{th} and j^{th} node of two consecutive layers, and k represents the input space. The inputs to the neuron are multiplied by weights w_{ij}^k and summed up together with biases b_j^k . The notation \sum is used for summation. The resulting summation value is the input to the activation function f_h in the hidden layer and f_o to the output layer.

$$f(z) = tansig(z) = \frac{2}{1 + e^{-2(z)}} - 1$$
 (3.13)

$$y_i = purelin\left[w_{ji}^2\left(tansig\left(w_{ji}^1x_j + b_j^1\right)\right) + b_j^2\right]$$
(3.14)

Where *z* is the summation of the weighted input values to the processing node.

The Levenberg-Marquardt Backpropagation (LMBP) algorithm is used for training of MLP network. This algorithm is a variation of Newton's method and uses the back-Propagation procedure [96]. Network performance is evaluated using Mean Squared Error (MSE) according to equation (3.15), where n is the number of inputs, t is the target value (actual value), and y is the network prediction (estimated value).

$$MSE = \frac{1}{n} \sum_{i=1}^{n} (e_i)^2 = \frac{1}{n} \sum_{i=1}^{n} (y_i - t_i)^2$$
 (3.15)

In the back-propagation technique, the input is presented to the input layer which then propagates in the forward direction to the output layer. At the output layer, the result is compared with the desired output to get the error signal. The error signal is then propagated back to the input layer while adjusting the weights and biases in hidden layers to minimize output errors.

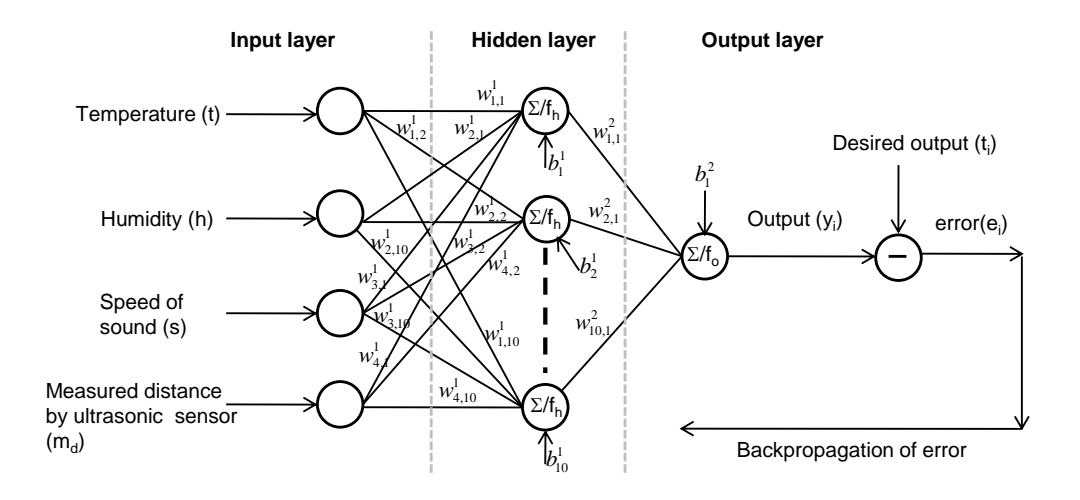


Figure 3.4: Back-propagation neural network with one hidden layer used in this proposed model

3.5.2 Proposed neural network architecture

The standard neural network architecture performs well if the error characteristics remain constant over the entire data range. However, as described in Section VII, we observed from experimental data that the measurement error (3.16) increases with an increase in depth. The error characteristics are also different for different ranges and the traditional ANN architecture could not give a satisfactory result. It is also noticed from the data analysis that a single ANN model fails to minimize the distance error. To reduce the error to the desired accuracy, we proposed a novel and modified ANN architecture in this work. As error characteristics are different for different distance segments, we performed a clustering analysis on the observed measurement errors to divide the data into different subgroups. Figure 3.5 represents the number of groups (clusters) and corresponding within-groups sum of squares. It is observed that within-group sum of squares decreases with an increase in the number of subgroups up to five subgroups and after that it remains almost constant. The elbow point in the plot (Figure 3.5) is found at the number of subgroups equal to 5, which is the optimal number of subgroups according to elbow method [97, 98]. Moreover, we also performed statistical analysis to verify the optimal number of subgroups using Mean

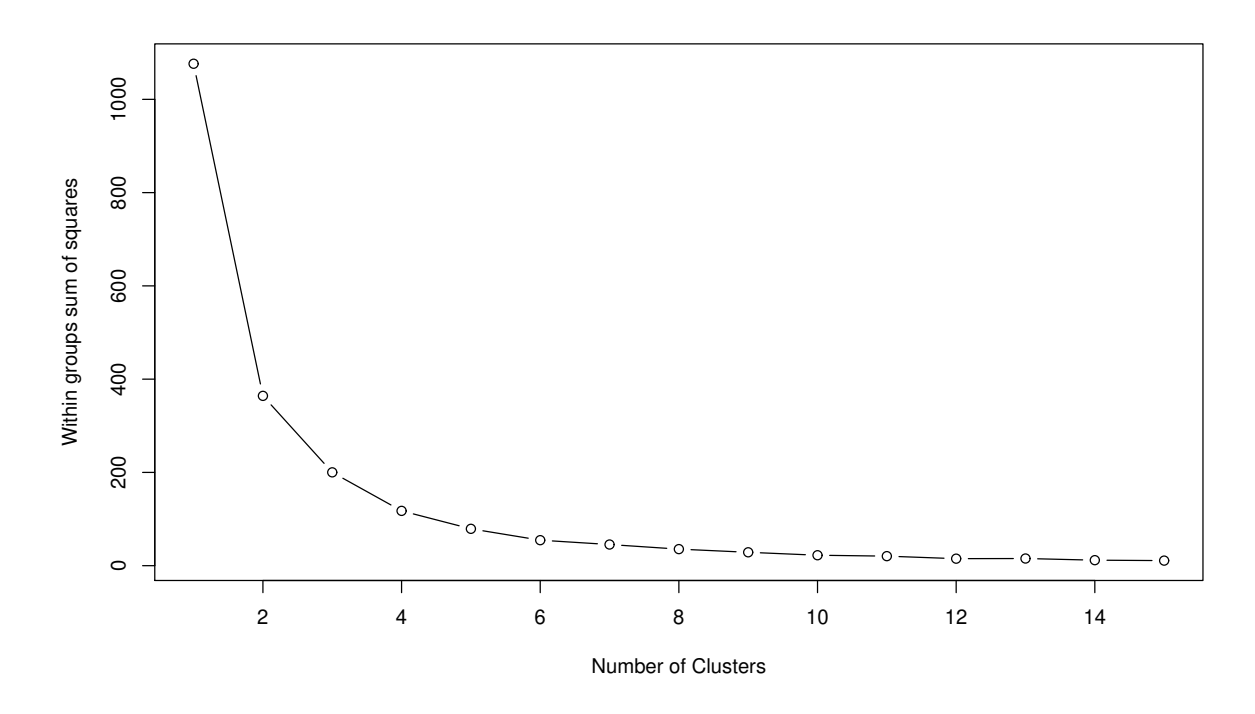


Figure 3.5: Segmentation of measurements errors using k-means clustering method

Absolute Error (MAE) and Standard Deviation (SD) of measurement errors for five different distance (x_d) ranges which are tabulated in Table 3.1 and are distinguishable. Based on observations from Figure 3.5 and Table 3.1, the entire distance measurement range is divided into five different segments. The architecture of the proposed neural network is shown in Figure 3.6. This model is an aggregation of five ANN in which each of the sub-network is a three-layer feed-forward MLP as described in subsection 3.5.1. The speed of sound is calculated based on equation (3.5). The input parameters and the transfer functions are the same for each of these neural sub-networks. For each input that satisfies a particular distance interval condition, the corresponding neural network is selected.

Table 3.1: Mean absolute error and standard deviation of all five segments

Ranges	Mean Absolute Error (MAE)	Standard Deviation (SD)
$2 cm \le x_d \le 100 cm$	0.1142	0.1755
$100 \ cm < x_d \le 200 \ cm$	0.4856	0.3597
$200 \ cm < x_d \le 300 \ cm$	0.6497	0.4407
$300 \ cm < x_d \le 400 \ cm$	0.8255	0.5426
$400 \ cm < x_d \le 500 \ cm$	1.1532	0.7482

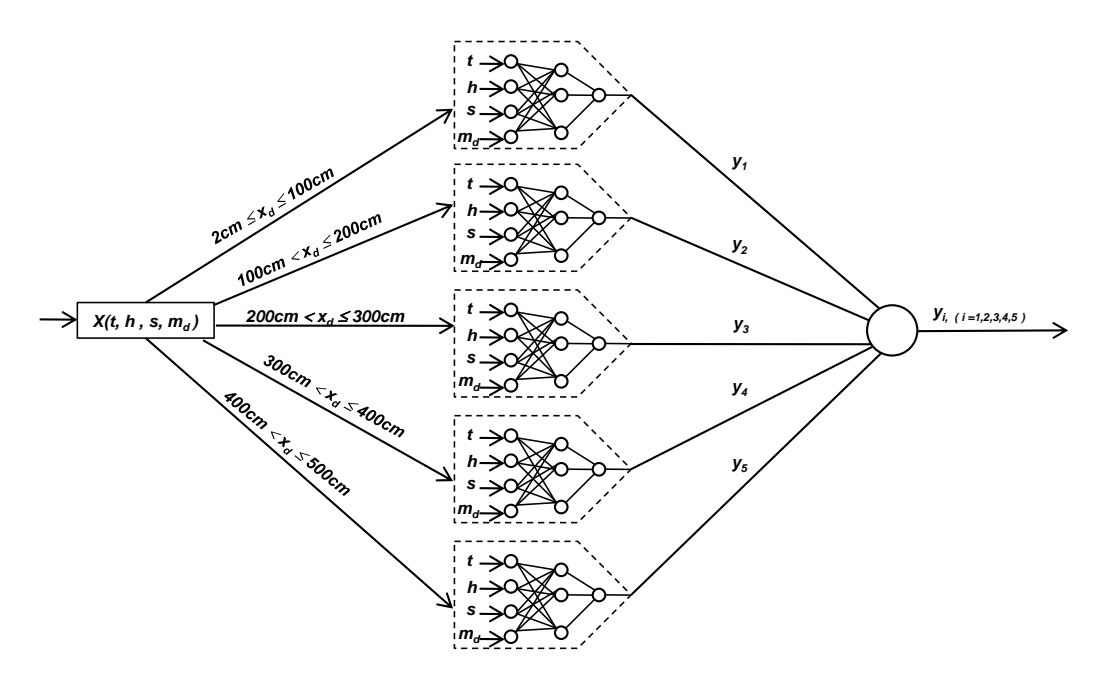


Figure 3.6: Proposed modified ANN model with five sub-network for different ranges

3.5.3 Training of the neural network

The proposed MLP model is trained using the LMBP algorithm. Each recorded data point consists of temperature, relative humidity, speed of sound, and measured distance. The Min-Max normalization method is used to normalize the data. The entire data is divided randomly into training, validation, and test sets. The training set is used to train the ANN model and to adjust the weights and biases in the hidden layer. The validation data set is used to validate the training model by tuning the model parameters. The test set is used to test the accuracy of the trained model. The training process is repeated until the MSE value is below a threshold value or does not change for a pre-specified number of epochs is considered to be the optimal model.

The dataset contains 1555 observations after removing the errors in pre-processing step. The entire observations were divided into five different segments based on the error segmentation analysis. Each of these segments contains around 300 to 330 data points. The intervals are (i) 2 cm $< x_d \le 100$ cm, (ii) 100 cm $< x_d \le 200$ cm, (iii) 200 cm

 $< x_d \le 300$ cm, (iv) 300 cm $< x_d \le 400$ cm, (v) 400 cm $< x_d \le 500$ cm, where x_d represents the distance.

The detailed list of parameters and functions used for training these five neural subnetworks are listed in Table 3.2. Input vector X is represented as $X = (t, h, s, m_d)$ in Figure 3.6. Neural network output y_i represents the estimated distance. Each of these five neural networks is trained several times to obtain the best performance. The parameters of neural networks have been determined empirically by trial and error after multiple runs.

Table 3.2: The parameters and the corresponding values used to train the ANN model

Training parameters	Values	
Neural network model	Feed forward	
Training algorithm	LMBP	
Performance function	MSE	
Total number of layers	3	
Input layer nodes	4	
Hidden layer	1	
Hidden layer neurons	10	
Output layer nodes	1	
Hidden layer transfer function	tansig	
Output layer transfer function	purelin	
Training percentage	70	
Testing percentage	15	
Validation percentage	15	
Data division	random	
Maximum no. of epochs	1000	
Validation check iterations	6	
Minimum performance gradient	1e-7	
Performance goal	0	
Maximum <i>mu</i>	1e10	

Each data segment is randomly divided, 70 % of the data is considered for training, 15 % for validation, and 15 % for testing the model. Three-fold cross-validation is performed on the data to avoid the over-fitting problem. The neural network model is implemented using Matlab software [99]. The model is designed and trained offline on a computer system based on the experimental data. Then, the model is deployed on the micro-controller unit of the ultrasonic module to accurately estimate the level or distance.

3.6 Experimental setup

This section describes the components used to develop the ultrasonic measurement module. The components used in the development of the ultrasonic module are shown in Figure 3.7. The specifications of the HC-SR04 ultrasonic sensor, DHT22 temperature, and humidity sensor are mentioned in Table 3.3. The Bluetooth module (HC-05) is used to send the measured data to end users. All sensors are connected to the 8-bit Arduino ATmega328P microcontroller. This microcontroller has 32 KB of flash memory with a 16 MHz clock speed which is sufficient for this experiment. The physical components used in designing the measurement module are shown in Figure 3.8.

Table 3.3: Specifications of the ultrasonic sensor, temperature and humidity sensor used in the experiment

Ultrasonic sensor (HC-SR04)	Value/Range		
Operating voltage	5V DC		
Operating frequency	40 kHz		
Operating range	2 cm - 400 cm		
Resolution	3 mm		
Operating temperature	-15 °C to $+70$ °C		
Measuring angle	15 degree		
Temperature and humidity sensor (DHT22)	Value/Range		
Operating voltage	3.3-6V DC		
Operating range (Humidity)	0 - 100 %RH		
Operating range (Temperature)	-40 °C to $+80$ °C		
Accuracy (Humidity)	±0.2 %RH		
Accuracy(Temperature)	±0.5 °C		
Resolution (Humidity)	0.1 %RH		
Resolution (Temperature)	0.1 °C		

Several experiments were conducted at different temperatures ranges from 22 °C to 45 °C and relative humidity ranges from 25 %RH to 80 %RH. The level measurement readings were recorded with varying water levels in different storage tanks and sumps ranging from 2 cm to 500 cm. Experiments were also carried out at different time

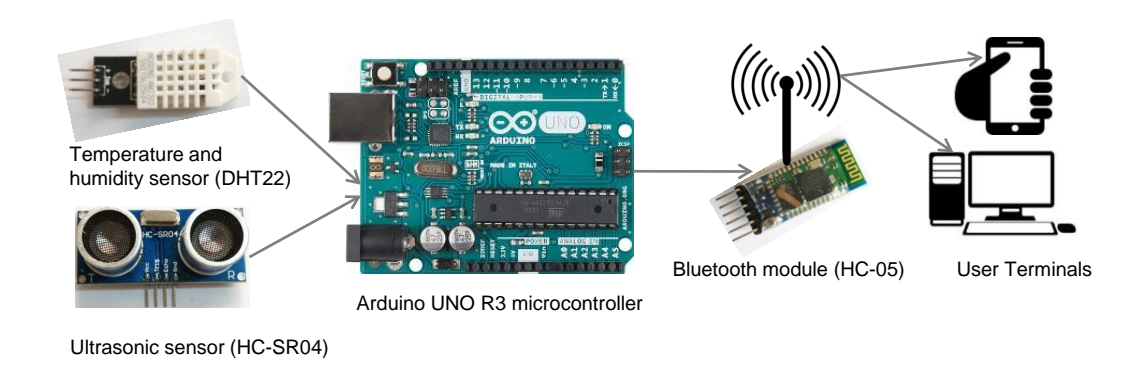


Figure 3.7: Components used in ultrasonic measurement system

intervals during the day time to acquire variations of temperature and humidity data in the measurement medium. The data from the ultrasonic sensor, temperature sensor, and humidity sensor, was used to compute the speed of sound and the water level inside the micron-controller unit and send it to the end user machine through a communication module (HC-05) for further analysis. Actual distance measurements were taken using a metric ruler with a resolution of 1 *mm* to compute the measurement error. The ultrasonic module was installed on the water tank at the top center position with the ultrasonic transducers facing downwards, perpendicular to the water surface. The level measured with the developed ultrasonic module is termed as estimated distance. To validate the accuracy of the developed ultrasonic module, experiments were conducted in dynamic environmental conditions. Experiments were also conducted by blowing hot air into the medium to monitor the effect of temperature and humidity on the developed measurement module. Experiments were performed with the experimental seup module shown in Figure 9.

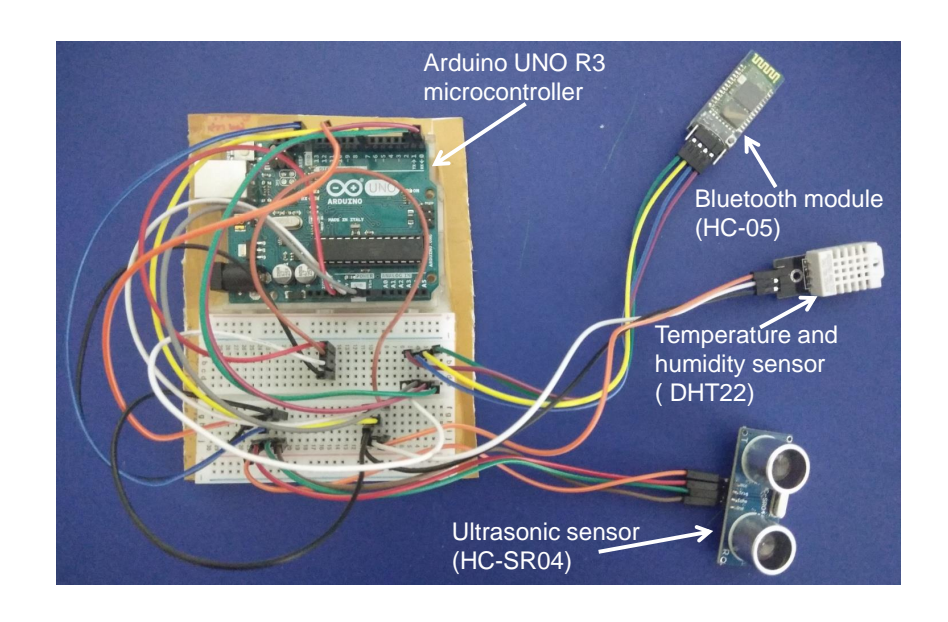


Figure 3.8: Physical components of the ultrasonic measurement module

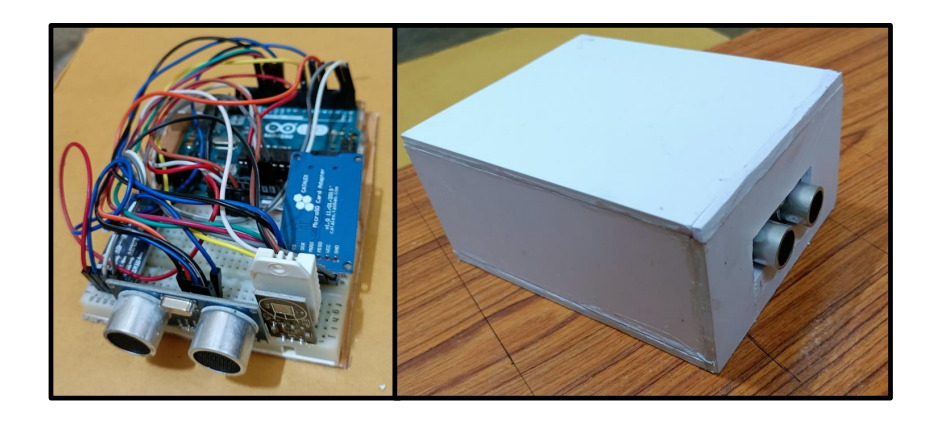


Figure 3.9: Experimental setup module used in liquid level measurement

3.7 Results

3.7.1 Standard approach analysis

According to Bohn [10], the speed of sound increases with an increase in temperature and humidity. However, other environmental parameters affect the speed of sound and are considered in (3.5). We performed experiments and calculated the speed of sound based on equation (3.5) using temperature and humidity values. Still, it is observed that the measured distance deviates more from the actual distance with the increase in depth or level. The deviation of measured distance from an actual distance is shown in Figure 3.10. Despite considering all important environmental parameters, some amount of uncertainty exists due to the gradient of temperature, humidity, and electronic noise that affect the distance measurement accuracy. The measurement error (e_m) given in (3.16) is the difference between measured distance (m_d) and corresponding actual distance (α_d) . To address this measurement uncertainty, an ANN model is used as described earlier in Section 3.5.

Measurement error
$$(e_m) = m_d - a_d$$
 (3.16)

3.7.2 Proposed ANN result analysis

This section analyzes the results of experiments carried out for development of the neural network model for UMS. For training the neural network, all data points were categorized into five segments and for each of these segments, there is a corresponding neural subnetwork model. The reason for the segmentation and number of segments are discussed in subsection 3.5.2. The details of each segment range, total number of data points, data points used for training, validation and testing are presented in Table 3.4.

The data points for each neural sub-networks were randomly divided into three sets

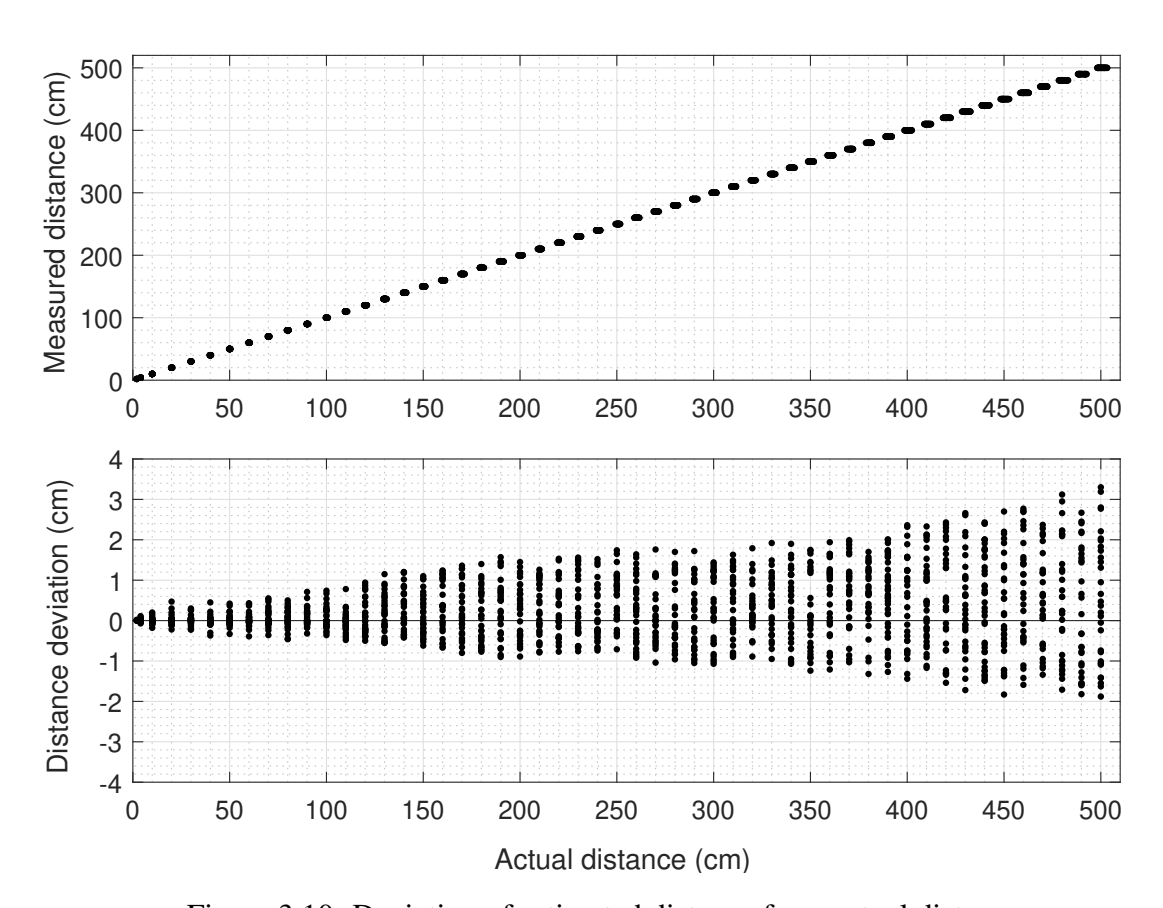


Figure 3.10: Deviation of estimated distance from actual distance

Table 3.4: Training, validation and test datasets of each segment of all five neural subnetworks

Segments	Data points	Training (70%)	Validation (15%)	Test (15%)
Segment-I				
$(2 \text{ cm} \le x_d \le 100 \text{ cm})$	330	230	50	50
Segment-II				
$(100 \text{ cm} < x_d \le 200 \text{ cm})$	300	210	45	45
Segment-III				
$(200 \text{ cm} < x_d \le 300 \text{ cm})$	300	210	45	45
Segment-IV				
$(300 \text{ cm} < x_d \le 400 \text{ cm})$	310	216	47	47
Segment-V				
$(400 \text{ cm} < x_d \le 500 \text{ cm})$	315	221	47	47

namely training, validation, and test sets as described in subsection 3.5.3. The parameters defined in Table 3.2 were used to train each of these neural sub-networks. The best training performance, best validation performance, and best test performance corresponding to each neural sub-network are noted and listed in Table 3.5. MSE and correlation coefficient (R) are used to evaluate the performance of the proposed ANN model.

It can be observed from the performance plots shown in Figure 3.11, that for each neural sub-network corresponding to different distance segments, the MSE of all sub-networks decreases with an increase in the number of epochs. The performance plots of all five neural sub-networks are shown in Figures 11(a)-(e). ANN model was trained and very low MSE was observed for all these neural sub-networks. This implies that desired outputs and the ANN model outputs for the training set are almost similar. The results with very low MSE values show high confidence in model-predicted values.

Table 3.5: The performance results of all five neural sub-networks.

Ranges of data	MSE	Training performance	Validation performance	Test performance
$2 \text{ cm} \le x_d \le 100 \text{ cm}$	2.6768e-06	2.6768e-06	2.9820e-06	1.6234e-06
$100 \text{ cm} < x_d \le 200 \text{ cm}$	3.3422e-05	2.9346e-05	3.9913e-05	4.5953e-05
$200 \text{ cm} < x_d \le 300 \text{ cm}$	6.3413e-05	5.4750e-05	7.0521e-05	9.6731e-05
$300 \text{ cm} < x_d \le 400 \text{ cm}$	8.1793e-05	6.5728e-05	1.1731e-04	1.2011e-04
$400 \text{ cm} < x_d \le 500 \text{ cm}$	1.7937e-04	1.6837e-04	1.8239e-04	2.2807e-04

Regression (R) is a measure that performs a linear regression analysis between the network outputs and the corresponding desired outputs. The R-value computed by the neural network determines how robust are the predictions. R = 1 indicates an exact linear

relationship between network outputs and desired outputs. R close to zero indicates no linear relationship exists between network outputs and desired outputs. High R values are an indication of good network performance. Table 3.6 shows R-values of all five neural sub-networks, which reveal that model prediction and actual values are quite similar.

Error histograms are used to show the distribution of the residuals between the desired output and network output. Figures 3.12(a)-(e) show the error histograms of all five neural sub-networks. The blue bars, green bars, and red bars represent training data, validation data, and test data respectively. From the error histogram Figures 3.12(a), it can be observed that the majority of the errors are between -0.00378 and +0.00337 *cm*. In Figures 3.12(b)-(e), it is also observed that estimated errors for the other four segments are distributed almost evenly in negative and positive directions.

Table 3.6: R-values of all, training, validation and testing of the five neural sub-networks

Ranges of data	Training performance	Validation performance	Test performance	All
$2 \text{ cm} \le x_d \le 100 \text{ cm}$	0.99999	0.99998	0.99999	0.99999
$100 \text{ cm} < x_d \le 200 \text{ cm}$	0.99985	0.9998	0.99976	0.99983
$200 \text{ cm} < x_d \le 300 \text{ cm}$	0.99972	0.99967	0.9995	0.99968
$300 \text{ cm} < x_d \le 400 \text{ cm}$	0.99969	0.99921	0.99937	0.99959
$400 \text{ cm} < x_d \le 500 \text{ cm}$	0.99909	0.99923	0.99894	0.99908

Table 3.7: Variation in temperature and relative humidity at three different positions for different storage tanks.

Depth (d) Te	Top position		Middle position		Near water surface	
	Temp (°C)	Humid (%)	Temp (°C)	Humid (%)	Temp (°C)	Humid (%)
100 cm	24	71	23.5	72	23	73
150 cm	30	48	30	51	29	54
200 cm	33	61	33	63	32	64
250 cm	37	54	36.3	57	35.2	59
300 cm	32	68	31	68	30	73
350 cm	34	56	33	58	33	62
400 cm	41	36	40	38	38	42
450 cm	36	44	35.5	47	33	51
500 cm	38	41	37	45	35	49

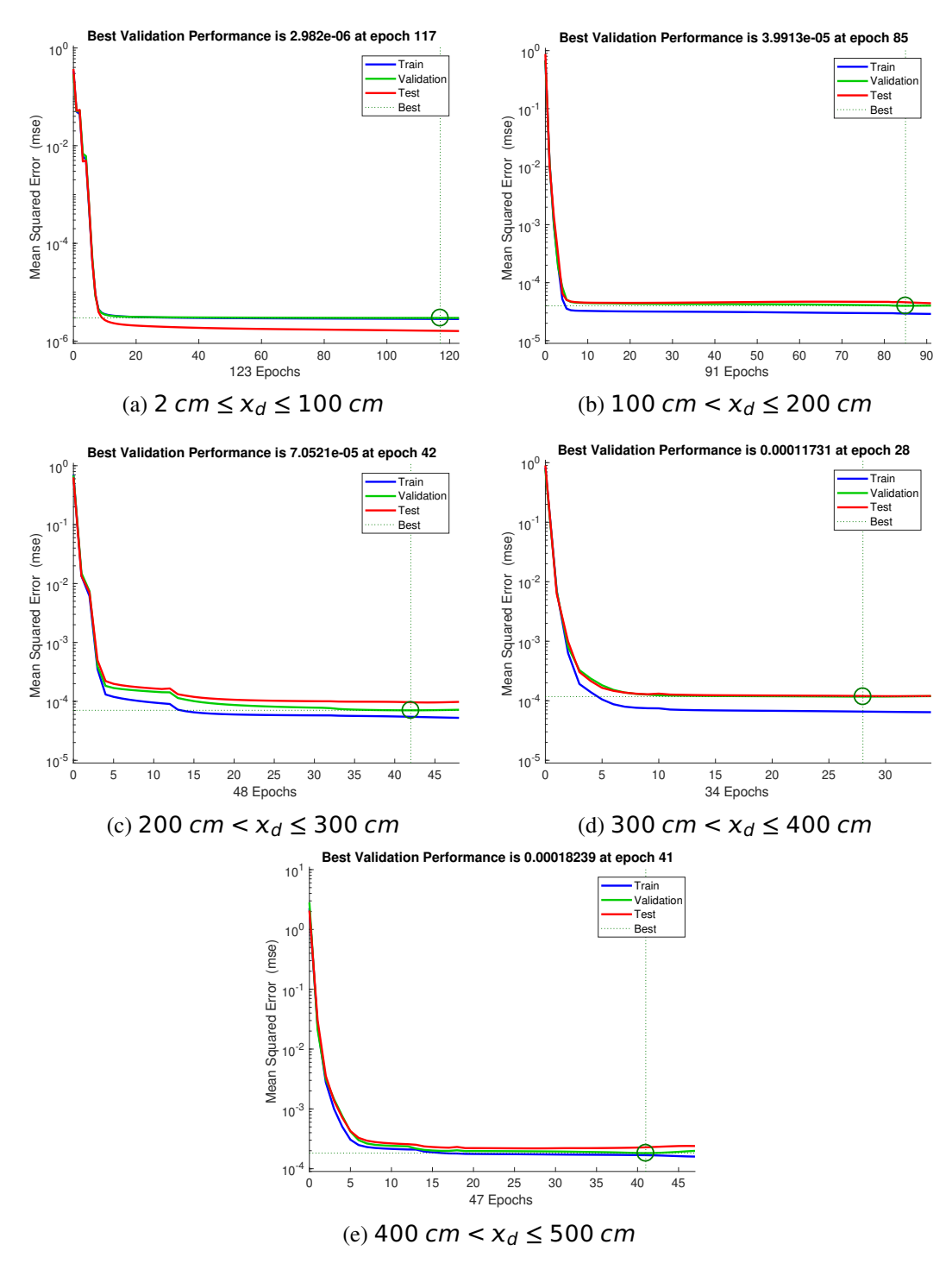


Figure 3.11: The performance plots of all five neural sub-networks

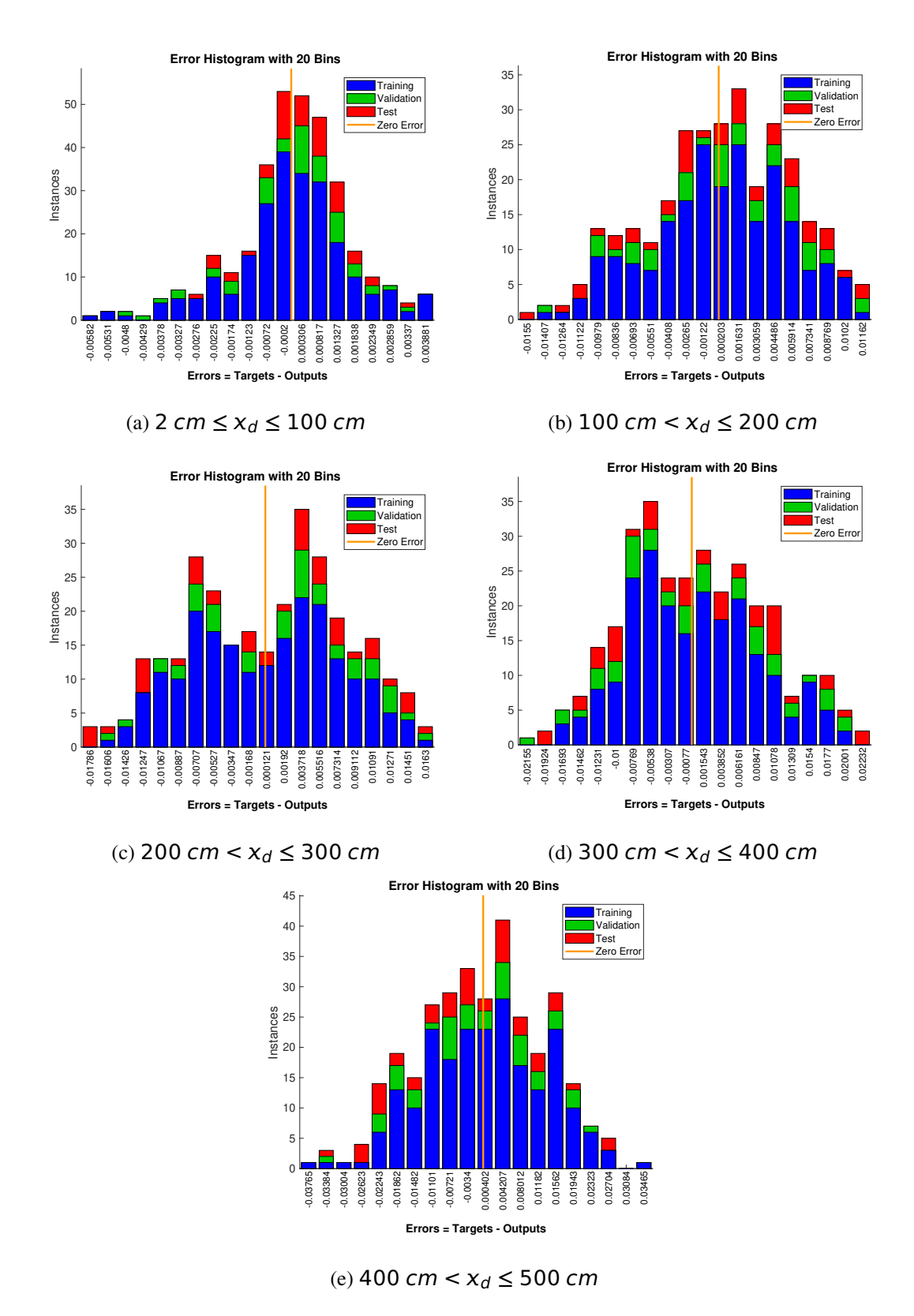


Figure 3.12: Error histograms of all five neural sub-networks

3.7.3 Testing and evaluation of the model with new data sets

The performance of the proposed neural network model is further evaluated with a new data set. The new data set which consists of 508 data points is divided into five segments to evaluate the performance of all five trained neural sub-networks. For segment-I, there are 111 data points for input to the neural sub-network-I, and the output estimated distance error variation lies within ± 0.19 cm which is around 0.2 %. Similarly, segment-II contains 91 data points, segment-III contains 92 data points, segment-IV contains 110 data points and segment-V contains 104 data points. The estimated distance variation for all of these segments is around 0.3 %. Figures. 3.13(a)-(e) show variations in the output of the proposed model and actual distance measurements of all five segments. The results demonstrate that the proposed model works better when there is a variation of temperature and humidity between the UMS and target surface which is observed in real experimental scenarios. A sample of experimental observations to depict the variation in temperature and relative humidity in the measurement medium is shown in Table 3.7. Table 3.7 shows the variation of temperature and relative humidity measured at the top, middle, and near water surface of storage tanks of different depths (100 cm to 500 cm). From this table, it is observed that there is a variation of temperature and humidity level between the point of UMS installation and near to water surface. Although the ultrasonic sensor datasheet mentions that the operating range of distance measurement is restricted to 400 cm, we have tried and used this model for an extended distance range of up to 500 cm. Beyond 400 cm, the error observed was large in the standard theoretical model, but the ANN model can compensate and reduce the distance measurement error to an acceptable limit of ± 1 cm. Thus, the second objective of extending the operating range with the use of the proposed model without upgrading the hardware is also achieved.

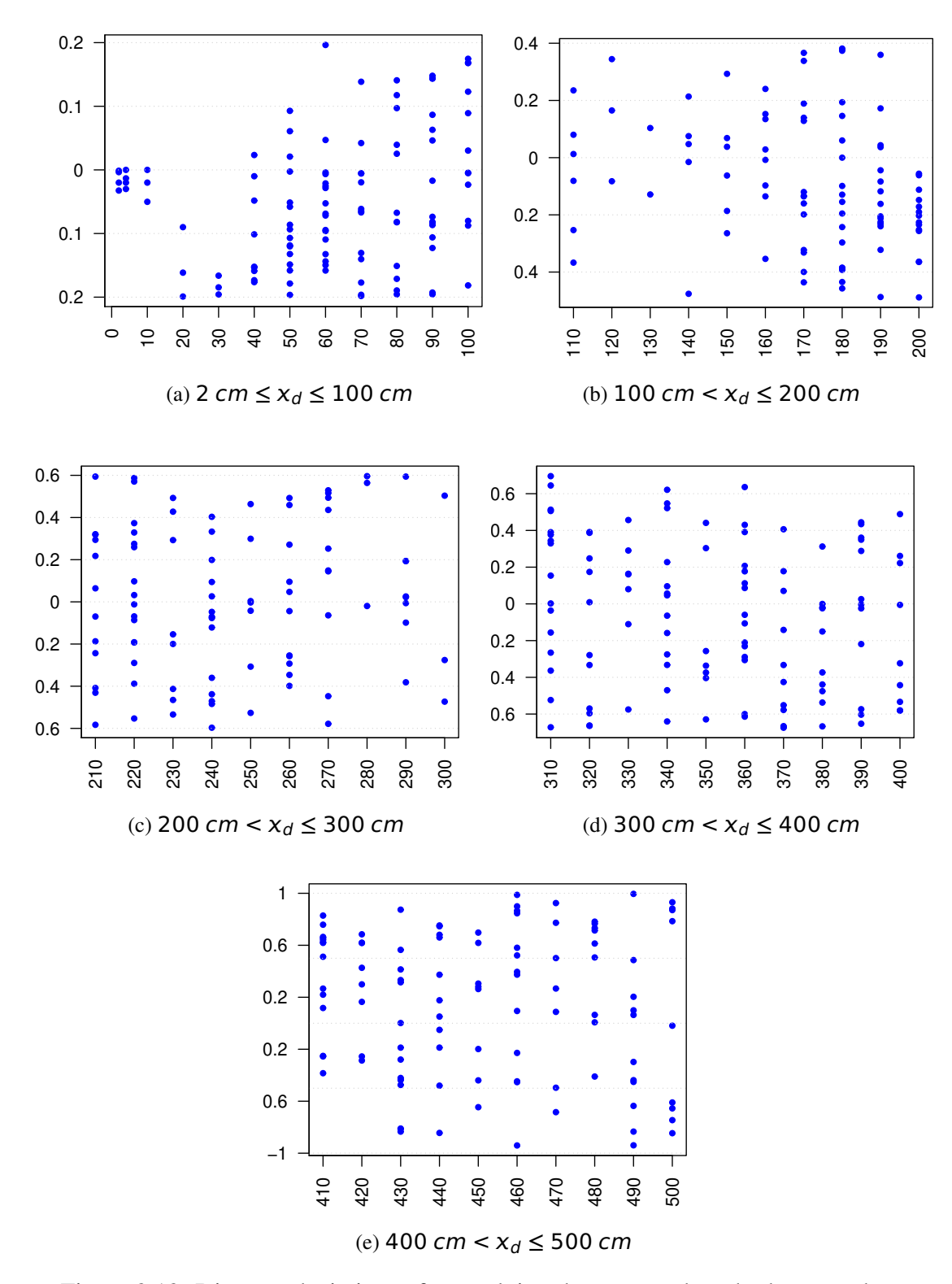


Figure 3.13: Distance deviations after applying the proposed method to new dataset

3.8 Discussions

In this study, we sought to enhance the performance of ultrasonic sensing model using machine learning models (ANNs). The model is first trained offline and then deployed in the ultrasonic measurement system for online level measurement. This developed model bring down the error rate from 1 % to 0.3 % and is also increase the operating range of the ultrasonic sensor by another 100 *cm*, which is almost 25 %. This method significantly enhance the performance of ultrasonic measurement system and can be useful for many industrial applications such as measurement of high-cost liquid level, where the distance measurement accuracy required in millimeter ranges. In general, when the storage tank diameter is more, a small variation in level measurement will lead to incorrect information about the volume of water contained in the tank.

The response time of the DHT22 (AM2302) temperature and humidity sensor is 2 seconds. But, in real-time we observed that the response time of DHT22 is around 380 milliseconds. The computation time of speed of sound formula given in (3.5), time of flight of ultrasonic sensor, and the distance measurement is around 5 milliseconds. The response time of the proposed ANN model implemented on the microcontroller is around 2 to 3 milliseconds. Hence, the overall response time of the developed ultrasonic model is around 400 milliseconds. The ultrasonic sensors are an excellent choice for non-contact distance or level measurement, because of ease of installation, low-cost safe, accurate, and less maintenance cost compared to other non-contact sensors. In some instances such as agitated liquids, turbulent liquids, foam, slosh, and similar other phenomena that absorb ultrasonic waves instead of reflecting can negatively affect the performance of ultrasonic sensors. In some cases like agitated and turbulent liquids, an average of multiple observations may be considered. The proposed low-cost ultrasonic measurement module based on ANN can be used to predict and detect flash floods as it can continuously monitor the level. The same model can be used for different applications and environments by

retraining the ANN model. As the training is always offline, it will not affect the actual measurement time and will not add to the computational complexity of the measurement system.

3.9 Conclusions

This work proposed a modified ANN architecture model to accurately estimate the distance using ultrasonic module with a special case study for water level measurement in different storage tanks. The experimental evidence indicates the effectiveness of the model to make it adaptive to different environmental conditions. The three layer MLP network used for universal approximation and it minimizes the error when an appropriate combination of model parameters are used for the training process. Moreover, the proposed ANN model comprised of five sub-networks for different range to effectively reduce the measurement error across the distance measurement ranges from 2 cm to 500 cm. This model is designed not only to measure the water level but can also be used for other applications, where manual and contact based measurement is difficult or challenging. The developed adaptive ultrasonic model compensates all major environmental parameters under dynamic situations, that affect the ultrasonic sensor measurement. The proposed model also extends the operating range of the used ultrasonic sensor from 400 cm to 500 cm. In future, we want to extend our work for level measurement of liquids like petroleum products, turbulent water, and surfaces that absorb the ultrasonic waves partially. The finding of our current work will be further used to test other algorithms and models to improve the performance of the ultrasonic measurement system for long range measurements.

CHAPTER 4

Temperature estimation using non-contact ultrasonic sensor

Temperature plays a vital role in determining the environmental conditions in addition to humidity and other gases present in the medium. The time of flight of an emitted ultrasonic wave depends on the speed of the sound in the propagation medium. The speed of the sound depends on the characteristics of the medium, which also influences the time of flight. Temperature, humidity, and other gases of the propagation medium significantly affect the speed of sound and time of flight. With proper compensation of the humidity effect, ambient temperature can be estimated using the speed of sound, time of flight, and the object's distance from the ultrasonic sensor. The ultrasonic sensor-based temperature measurement system can determine the medium's average temperature based on the changes in ultrasonic sound speed in the medium of travel. In this work, we propose a non-contact ultrasonic sensor-based ambient temperature estimation system using two machine learning approaches: Multiple Linear Regression (MLR) and Support Vector Machine (SVM) regression. The HC-SR04 ultrasonic sensor module, a low-cost 40 kHz ultrasonic transducer, is used for experimentation to determine the temperature of the medium. The proposed intelligent ultrasonic sensor-based temperature estimation system is designed and effective for measuring temperature in confined spaces such as rooms, boilers, tanks, and other industrial applications where the temperature needs to be measured in a non-contact manner. We conducted experiments in different environmental conditions with temperature ranging from 22 °C to 45 °C and relative humidity ranging from 30% RH to 85% RH to validate the accuracy and effectiveness of the proposed system.

4.1 Introduction

Non-contact ultrasonic measurements are a cost-effective alternative solution for many applications such as industrial, medical, and scientific research [75]. The standard sensors used for temperature measurement are single-point temperature measurements and are usually called sensor-by-contact. These sensors must contact the air and use their radiant energy to change their physical characteristics to measure the environment's temperature. These sensors typically have a larger response time as they do not respond instantly, and their measurement range is limited [100]. A non-contact ultrasonic temperature measurement technique is desirable for instantaneous ambient temperature measurement. The ultrasonic sensor measures the distance based on the ToF measurement. The speed of sound in the air can be computed from the ToF and the distance given in equation (4.5). The ultrasonic sensor can roughly estimate the average ambient temperature from the change observed in the speed of sound, using the relationship between temperature and speed of ultrasonic sound, as described in equation (4.4). However, the speed of sound also depends on the humidity of the propagation medium in addition to the temperature. The estimated ambient temperature is higher than the actual temperature because the sound speed in humid air is faster than that of dry air. Single-point temperature measurement will not give the expected accuracy due to the temperature gradient and humidity present in the measurement medium. Most of the existing work on ultrasonic temperature measurement is based on signal processing techniques, and experiments are performed in a controlled environment and low measurement ranges. This work presents a machine learning approach to accurately estimate the air temperature using a low-cost ultrasonic sensor with different ultrasonic measurement ranges and environmental conditions with temperature ranges from 22 °C to 45 $^{\circ}C$, relative humidity ranges from 30 – 80%RH. In the proposed method, the model is trained using the speed of sound (computed from distance and ToF) and relative humidity as input and actual temperature as the desired output. After proper training, the

sensor node can estimate the ambient temperature more accurately during testing. The main contributions of this study to existing works are summarized below:

- Non-contact temperature measurement based on machine learning approaches without any change in the hardware requirement.
- The proposed system measures the ambient temperature accurately, which is not possible in single point temperature sensors.
- It provides faster response time and long range temperature estimation (less than 100 milliseconds compared to standard temperature sensor response time 2 seconds).

The remainder of the chapter is organized as follows: in Section 4.2 reviews the existing works related to ultrasonic sensor temperature measurements. The basic principles behind the ultrasonic-based measurement are discussed in Section 4.3. The theory behind how the velocity of sound is affected by temperature and humidity is addressed in Section 4.4. The proposed machine learning methods are described in Section 4.5. The detailed experimental procedure and system implementation are covered in Section 4.6. Experimental results and discussions are presented in Section 4.7, followed by conclusions in Section 4.8.

4.2 Related works

Temperature measurements play a vital role in various applications. In the recent past, ultrasonic temperature measurement has evolved as a new temperature measurement technology for environmental monitoring. Many papers use time-of-flight-based techniques for temperature measurement using ultrasound in the air medium [11, 100, 101, 102]. A non-intrusive method for the temperature measurement of stored biomass based on acoustic sensing techniques is proposed in [103]. The accuracy of temperature measurement of stored biomass is estimated with a maximum error of $1.5\,^{\circ}C$ under all test conditions. W-Y Tsai et al. [100] proposed an ultrasonic measurement system to estimate air temperature

with self-correction for humidity without proper humidity correction. It reports an accuracy of ± 0.4 °C, and with humidity correction, it is accurate upto ± 0.3 °C for a temperature range 0 °C to 80 °C. A new microcomputer-based air temperature measurement system using the ultrasonic time-of-flight technique is presented in [11]. The experiment conducted with temperature ranging from 0 to 80 °C, relative humidity range from 20 to 90%RH, and the distance considered is $50 - 200 \, mm$. The standard uncertainty error of the temperature measurement is approximately 0.39 °C. Teh-Lu Liao et al. [104] proposed an ultrasonic temperature sensor system to measure the temperature of an air conditioner (AC) in an automobile with an accuracy of ± 0.4 °C with temperature ranges from 0 to 80 °C and distance of 100 cm with a response time of only 100 ms. T. Motegi et al. [12] demonstrated an acoustic technique for measuring air temperature and humidity in moist air. The measurement accuracy is within 0.5K, the temperature is 293 - 308K, and relative humidity (RH) is 50 - 90% RH. Sahoo et al. [105] proposed an improved neural network algorithm to improve the accuracy of the ultrasonic measurement system with compensation temperature and relative humidity. Rochhi et al. [4] presented an analytical method based on ultrasonic signal reconstruction to improve the measurement accuracy of the ultrasonic measurement method.

Existing ultrasonic temperature measurement methods discussed above are mainly based on ultrasonic signal processing techniques and limited measurement ranges, and the experiments are performed in controlled environments. As there is a presence of a gradient of temperature and humidity in the measurement medium, a single-point measurement will not be able to give accurate temperature measurements. Standard sensors usually respond slowly; thus, they are not ideal for tracking measurements with fast-changing environmental temperatures. Therefore, in this work, we propose machine learning algorithms to increase measurement accuracy and make the ultrasonic measurement system more intelligent to adapt the changing environment. The experiments were conducted at different distances ranging from $100 \, cm - 400 \, cm$ and in other environmental conditions to train, test, and

4.3 Basic principle of ultrasonic measurement

Ultrasonic sensors are a reliable and cost-effective alternative to many non-contact measurement applications. It works based on the principle of measurement of the Timeof-Flight (ToF). ToF is the round trip time of the transmitter-emitted signal and its return received by the receiver after getting reflected by an object. The ultrasonic sensor converts electrical energy into acoustic waves during transmission and vice versa after receiving. The acoustic wave signal is an ultrasonic wave operating at a frequency above 20 kHz that travels at a speed of sound c. We used a 40 kHz ultrasonic sensor HC-SR04 for our experiments. This HC-SR04 sensor has a wide range of non-contact distance measurement capabilities, i.e., from 2 cm to 400 cm. The ultrasonic transmitter (Tx) transmits ultrasonic wave pulses towards the object, and the receiver (Rx) receives an echo signal reflected from the object, as shown in Figure 4.1. A Microcontroller Unit (MCU) communicates with an ultrasonic sensor. The MCU sends a trigger signal to the ultrasonic sensor to measure the distance. A signal of +5V (HIGH) is sent over the trigger pin for around 10μ seconds to trigger the sensor. The ultrasonic sensor generates eight 40 kHz ultrasonic waves, and the echo pin goes high until the ultrasonic wave returns after getting reflected from the object. The total round trip time of an ultrasonic wave transmitted to and reflected from the object determines the distance between the ultrasonic sensor and the object. The distance d from the sensor to the object is denoted by:

$$d = \frac{c \times ToF}{2} \tag{4.1}$$

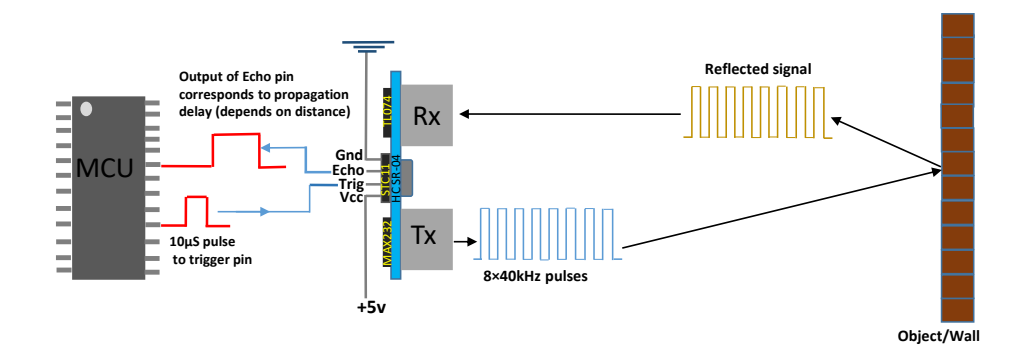


Figure 4.1: Basic working principle of ultrasonic based measurement system

4.4 Theory behind the model

The speed of sound wave traveling in a medium strictly depends on the medium properties [10]. For an ideal gas, the speed of sound can be expressed as

$$c = \sqrt{\frac{\gamma RT}{M}} \tag{4.2}$$

Where γ is the specific heat ratio, R is the universal gas constant ($R = 8.314 \, J/(mol \, K)$), T is the absolute temperature, M is the molecular mass of the gas and C is the speed of sound. For air medium, $\gamma = 1.40$ and $M = 0.02896 \, kg/mol$.

The ultrasonic wave propagation speed at 0 ^{o}C is reported to be 331.45 ± 0.05 m/s. For every 1 ^{o}C increase in temperature, the speed of sound increases 0.607 m/s. The representative graphs of equation (4.3) shown in Figure 4.2 (a) depict the correlation between the speed of sound and medium temperature. When the temperature is known, the formula for computing sound velocity is given in equation (4.3).

$$c = 331.45 + 0.607 * T_c m/s (4.3)$$

Where T_c is the temperature of the medium in degree Celsius. The temperature can be estimated from the speed of sound using equation (4.4).

$$T_c = \frac{c - 331.45}{0.607} \tag{4.4}$$

From equation (4.2), it is observed that the speed of sound increases with an increase in temperature. It is evident from equation (4.1) that ToF depends on the speed of sound. As the speed of sound increases, the ToF decreases (4.3).

$$c = \frac{2 \times d}{Tof} \tag{4.5}$$

Therefore, ToF increases with a decrease in the speed of sound and the medium temperature. An increase in relative humidity in the air increases the speed of sound by a small amount. The combined effect of temperature and relative humidity on the speed of sound is shown in Figure 4.2 (b).

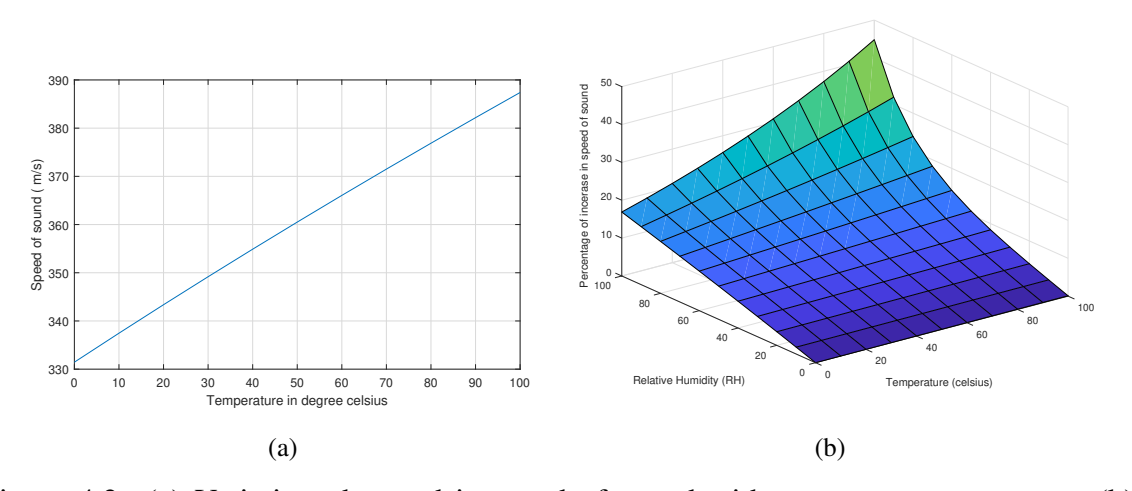


Figure 4.2: (a) Variation observed in speed of sound with respect to temperature, (b) Percentage of increase in speed of sound vs. change in temperature and humidity

4.5 Proposed method

4.5.1 Multiple Linear Regression (MLR)

Multiple linear regression is a machine learning technique used to formulate the complex input-output relationship. The main objective of MLR is to find a linear approximation function between a set of explanatory (independent) variables and the response (dependent) variable.

$$y = \beta_0 + \beta_1 x_1 + \dots + \beta_i x_i + \dots + \beta_m x_m + \epsilon$$
 (4.6)

Where, y is the dependent variable, x_i is the i^{th} independent variable, β_i is the polynomial coefficients corresponding to each x_i , m is the number of independent variables, and ϵ is the model's error term or residuals. In this experiment, the temperature is chosen as the dependent variable, while relative humidity and speed of sound are selected as independent variables.

4.5.2 Support Vector Machine (SVM)

SVM is a popular supervised machine learning method for classification, and regression [21, 106]. It uses a non-linear statistical technique to transform input space into feature spaces of higher dimensionality, which helps in efficient classification. SVM regression is an extension of the SVM technique for predicting numerical values. Instead of generating a hyperplane, a different function is derived based on training data to predict the numerical values of the dependent variable. Given a set of training data points $(x_1, y_1), (x_2, y_2), ..., (x_i, y_i), ..., (x_n, y_n) \subset \mathcal{X} \times \mathbb{R}$, \mathcal{X} is the input vector space, x_i is the input vector, y_i is the observed output value corresponds to input vector x_i , and n is the number of samples. The regression function can be represented as follows:

$$f(\mathbf{w}_1, \mathbf{w}_2, ..., \mathbf{w}_n, b) = y = \langle \mathbf{w}, \mathbf{x} \rangle + b + \epsilon \tag{4.7}$$

Where $\mathbf{w} \in \mathcal{X}$, represents coefficients, $b \in \mathbb{R}$ is the intercept and $\langle ., . \rangle$ denotes dot product. The main aim is to find a function f(x) that has at most ϵ deviation from target y_i . The regression problem can be expressed as a process to minimize the following function with ϵ -insensitivity loss function:

Minimize
$$\frac{1}{2} \| \mathbf{w} \|^2 + C \sum_{i=1}^{n} (\xi + \xi^*)$$
 (4.8)

Subject to
$$\begin{cases} y_{i} - \langle \mathbf{w}, x_{i} \rangle - b \leq \epsilon + \xi_{i} \\ \langle \mathbf{w}, x_{i} \rangle + b - y_{i} \leq \epsilon + \xi_{i}^{*} \\ \xi, \xi_{i}^{*} \geq 0, i = 1, 2, ...n \end{cases}$$
(4.9)

Where C > 0 is a constant that determines the penalty for the prediction error higher than ϵ . Two slack variables ξ and ξ_i^* estimate the distance from actual values corresponding to the boundary values of ϵ . The above optimization problem can be stated in quadratic programming form by using Lagrangian multipliers as follows:

$$f(\mathbf{x}) = \sum_{i=1}^{n} (\alpha_i - \alpha_i^*) \mathcal{K}(\mathbf{x}, \mathbf{x_i}) + b$$
 (4.10)

Subject to
$$\begin{cases} \sum_{i=1}^{n} (\alpha_{i} - \alpha_{i}^{*}) = 0 \\ 0 \leq \alpha_{i} \leq C \\ 0 \leq \alpha_{i}^{*} \leq C \end{cases}$$
 (4.11)

Where $\mathcal{K}(\mathbf{x}, \mathbf{x_i})$ is the kernel function defined as an inner product of the points $\phi(x_i)$ and $\phi(x_i)$. The function ϕ is the mapping from input data to higher dimension feature

space. α_i and α_i^* are the non-negative Lagrange multipliers.

The kernel function plays an important role in the SVM performance. We used the SVM model's Radial Basis kernel Function (RBF) for its better generalization ability than other kernel functions.

4.5.3 Performance evaluation metric

The performances of MLR and SVM-regression were evaluated based on the ambient temperature estimation. Five standard statistical performance evaluation metrics, namely, Root Mean Squared Error (RMSE), Mean Square Error (MSE), Mean Absolute Error (MAE), Mean Absolute Percentage Error (MAPE), and coefficient of determination (R^2) were calculated on test data samples.

4.6 System implementation

The experimental setup of the ultrasonic temperature measurement system is shown in Figure 4.3, which comprises a 40 kHz ultrasonic sensor, a temperature and humidity sensor (DHT22), a Bluetooth module, and a micro-controller. Bluetooth module is used to communicate the measurement result to the personal computer to examine the measurement result and for further processing. Detailed specifications of these components are listed in Table 4.1. The ultrasonic sensor consists of two transducers, one for emitting sound pulses at 40 kHz frequency and the other to detect the sound wave (echo signal) reflected from the target object's surface. As per the datasheet, the operating distance range of the ultrasonic sensor is 2 cm to 400 cm.

For testing, the ultrasonic transducer was fixed at some height on one wall of a room, and time-of-flight measured values were collected at four different distances: 100 cm, 200 cm, 300 cm, and 400 cm. Experiments were performed at various temperature and relative humidity levels, with temperature ranging from 22 ^{o}C – 45 ^{o}C and relative humidity

ranging from 30% RH - 85% RH. Nearly 11,000 data sample points are collected consisting of ToF, temperature, and relative humidity for this experiment at four different ranges of distances: 100 cm, 200 cm, 300 cm, and 400 cm.

4.7 Results and discussions

This section presents the statistical results of the experiments using the MLR and SVM-regression machine learning models. The dataset consisting of 11000 samples is randomly divided into a training dataset (8250 data points, which is 75% of the total data) and the test dataset (2750 data points, which is 25% of the total information). Each training sample data point consists of three variables, namely, temperature (t), relative humidity (h), and speed of sound (s). The raw data of both the training and testing set are normalized using max-min normalization to mitigate the magnitude bias during the training phase. The SVM-regression model parameters are optimized using the cross-validation method. To evaluate the performance and generalization capabilities of MLR and SVM-regression models, we used both models to estimate the temperature on the test dataset and then compare their performance.

The results of MLR and SVM models are shown in Figure 4.4 and Figure 4.5, respectively. Statistical evaluation parameters (RMSE, MSE, MAE, MAPE, and R^2) of MLR and SVM model on the test data is listed in Table 4.2 and Table 4.3 respectively.

In the case of MLR, Figure 4.4 (a)-(d), the histogram of residual values depicts the frequency of residual values of the trained model. Most residual errors are concentrated around zero, which shows a good fit of the model to the observed data. But in the case of SVM, most of the residual errors are more dispersed in comparison to the MLR model, as shown in Figure 4.5 (a)-(d). Similar observations can be seen in Figure 4.4 (e)-(h) of MLR and Figure 4.5 (e)-(h) of the SVM model. The coefficients of determination (R^2) values of both models indicate that the MLR model performs better than the SVM-regression model.

It can be concluded that the MLR model outperforms the SVM model for this study.

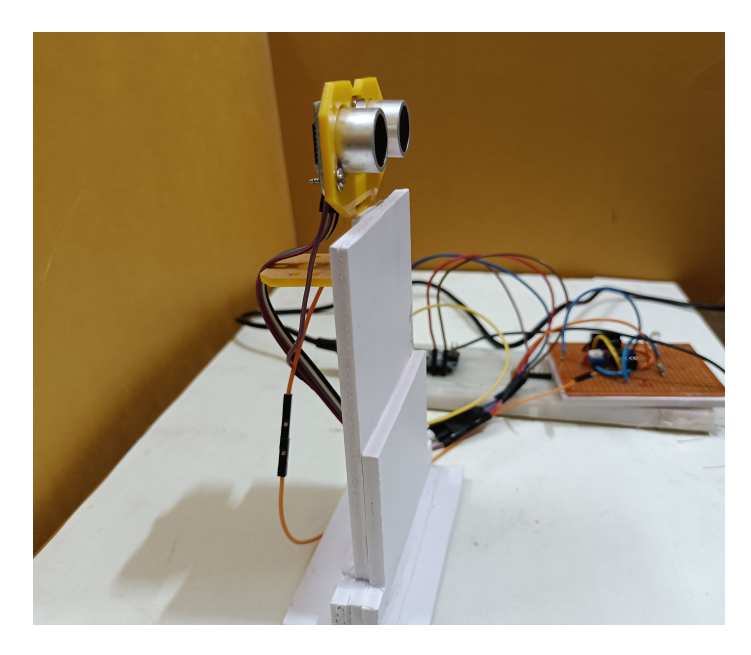


Figure 4.3: Experimental setup of ultrasonic module for temperature measurement

Table 4.1: Components used in this experiment with specifications

Components	Specifications
Microcontroller	Arduino nano (ATmega328)
Ultrasonic sensor	HC-SR04
Temperature and humidity sensor	DHT22 (AM2302)
Bluetooth module	HC-05

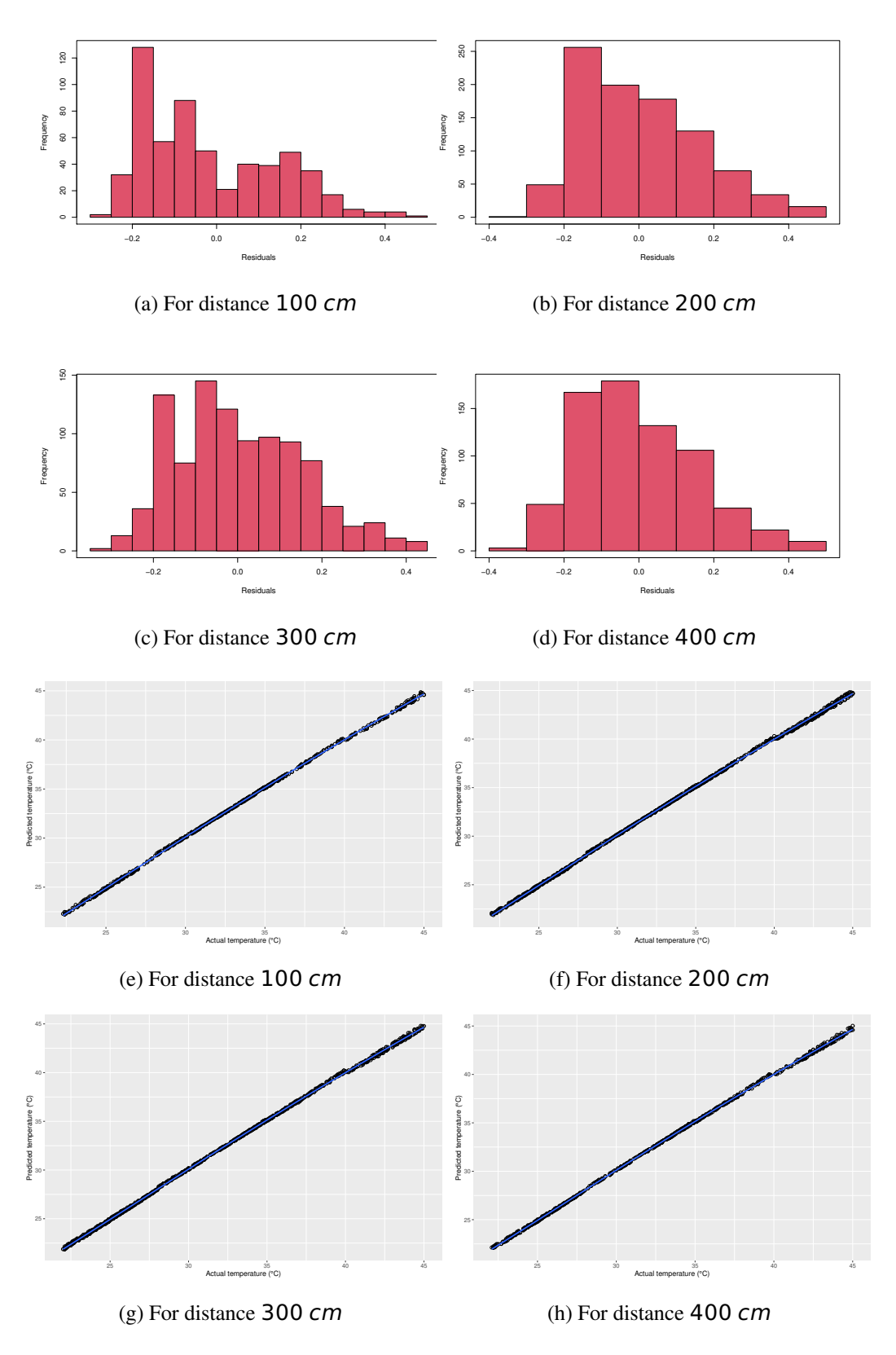


Figure 4.4: Performance plots of MLR, Fig.(a)-(d) histogram plots of residuals and Fig.(e)-(h) actual versus predicted temperature

Table 4.2: Performance metric (RMSE, MSE, MAE and MAPE and \mathbb{R}^2) of MLR

Measurement Ranges	RMSE	MSE	MAE	MAPE	R-Square
100 cm	0.1605	0.0257	0.1406	0.0043	0.9993
200 cm	0.1619	0.0262	0.1332	0.0040	0.9994
300 cm	0.1511	0.0228	0.1244	0.0038	0.9994
400 cm	0.1590	0.0253	0.1317	0.0039	0.9994

Table 4.3: SVM-regression model performance metric (RMSE, MSE, MAE, MAPE, \mathbb{R}^2)

Measurement Ranges	RMSE	MSE	MAE	MAPE	R-Square
100 cm	0.3257	0.1061	0.2616	0.0082	0.9973
200 cm	0.3187	0.1016	0.2590	0.0081	0.9976
300 cm	0.3733	0.1394	0.3043	0.0099	0.9969
400 cm	0.3256	0.1060	0.2776	0.0089	0.9975

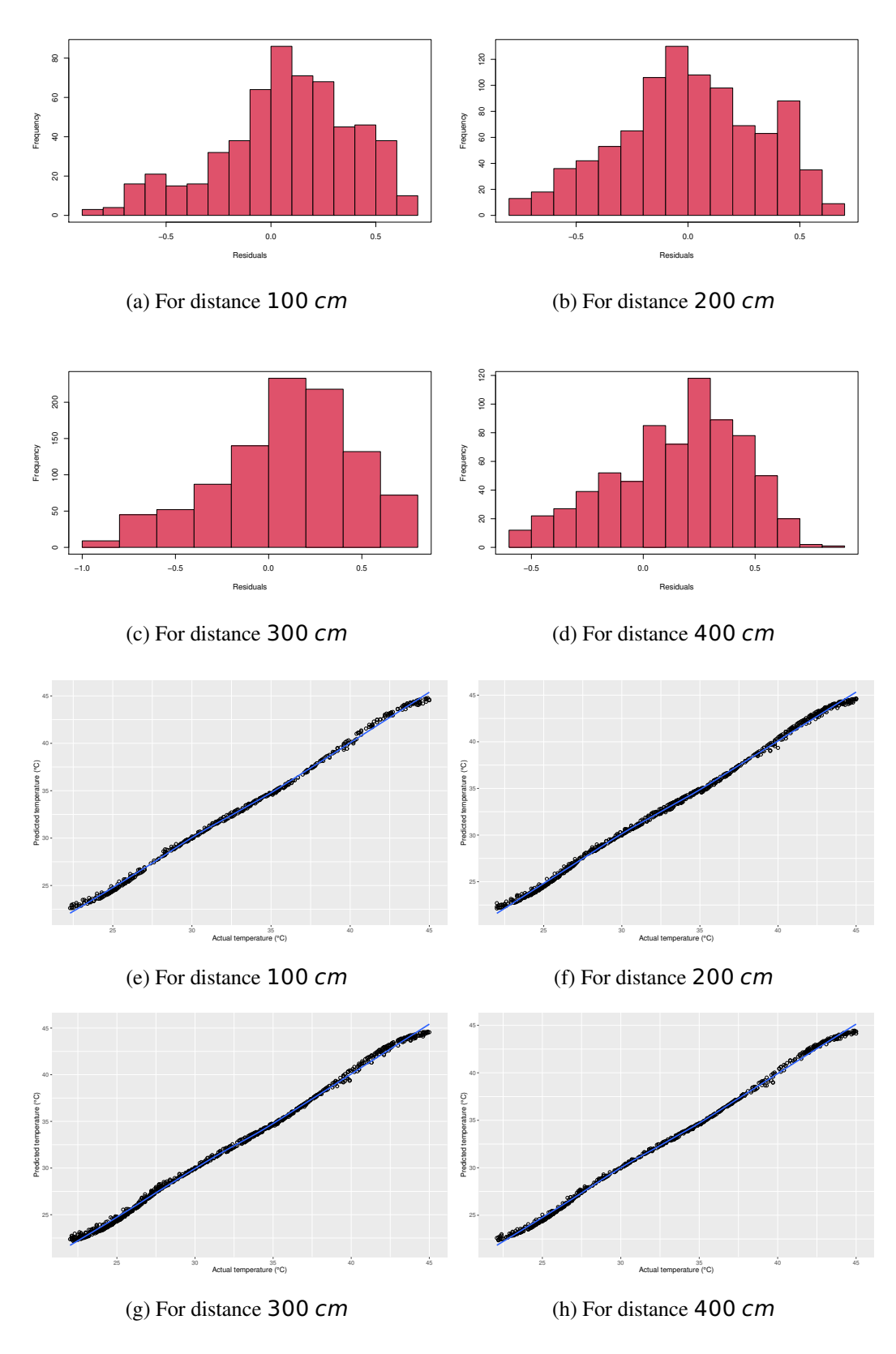


Figure 4.5: Performance plots of SVM Regression, Fig.(a)-(d) histogram of residuals and Fig.(e)-(h) actual versus predicted temperature

4.8 Conclusions

The propagation medium temperature affects the speed of sound in the medium. We use this property and the machine learning-based ultrasonic temperature measurement system to accurately measure the average ambient temperature with a reasonable accuracy bounded by a maximum of ± 0.4 °C under the experimental conditions. The response time of the proposed system is 100 ms, which is much less than the response time of standard temperature sensors, around ± 2 °C. The proposed system can accurately measure the temperature, especially in an environment with fluctuations in temperature and humidity levels. The results indicate that the MLR machine learning model outperforms the SVM model.

This proposed system's main advantages are: i) non-contact measurement, ii) ease of implementation, iii) longer ranges of measurement, and iv) software-enhanced high resolution in measurements. Faster response time without any up-gradation of hardware. The measurement accuracy depends on the surface of the object from which the ToF signal is reflected and the angle of the ultrasonic sensor. Ultrasonic waves depend on temperature and humidity, and other parameters and gases present in the environment. In the future, we propose to study the estimation of relative humidity in consideration of other environmental parameters using the ultrasonic sensor. We also propose to study different machine learning algorithms to improve the accuracy of the proposed system.

CHAPTER 5

Relative humidity estimation using non-contact ultrasonic sensor

The speed of sound depends on the humidity of the propagation medium in addition to the temperature. The combined dependency of both relative humidity and temperature becomes non-linear and makes the estimation difficult. In chapter-4, we discussed the ultrasonic measurement system for estimating ambient temperature in a non-contact manner. In this work, we will discuss an ultrasonic Time-of-Flight (ToF) based technique to estimate the relative humidity of the environment accurately. The ultrasonic time-of-flight measurement technique is based on ultrasonic sound wave propagation in the medium. As the temperature and relative humidity highly influence the speed of sound in the air medium, a highly accurate ambient relative humidity measurement system can be realized using an ultrasonic sensor with proper compensation of temperature.

The non-contact ultrasonic measurement system depends on sound speed, and the sound's speed changes with changes in temperature and relative humidity. Thus, the ultrasonic sensor can be used for the prediction of both temperature and relative humidity of the medium [12, 40, 107].

We straightforwardly explored different machine learning algorithms but only achieved a little success. In this work, we propose a combination of fuzzy logic and an artificial neural network approach for estimating relative humidity using ultrasonic sensors. The framework of the proposed model is the following; (1) a fuzzy controller used to classify the input sample data into different segments, (2) based on the fuzzy output, each segment of the data range is fed into a specific pre-trained neural network to predict the relative humidity.

We experimented with and compared a few other popular machine learning approaches, like Support Vector Regression (SVM), K-Nearest Neighbor (KNN), and Random Forest Regression (RFR), with the proposed method's accuracy.

5.1 Introduction

Monitoring relative humidity in the indoor environment is essential for maintaining the health of the buildings and occupants. Relative humidity is a measure of the air's water vapor content at a given temperature [27]. Thus, the amount of moisture in the air also depends on air temperature [10]. Very high humidity can cause condensation and affects the ambience and health of the human beings. A very low humidity can trigger static electricity around the room, and affects the proper functioning of electronic modules. Monitoring temperature and humidity level of the room or building is required for good air conditioning and fire warning system. Conventional humidity measurement sensors are single-point measurement devices and can not estimate the distribution of relative humidity in a room. A non-contact method for measuring relative humidity is a requirement for estimating the distribution properly. The ultrasonic measurement technique is an alternate solution for non-contact based air temperature and humidity measurement. Airborne ultrasonic measurement systems use the speed of sound for different sensing applications. The ultrasonic sound propagation speed depends on the temperature and humidity of the transmitting medium [10, 28, 31].

Non-contact ultrasonic sensors are low-cost, easy to implement, less response time and capable of high performance [37]. The fundamental operating principle of the ultrasonic sensing system is based on calculating the time of flight. Time of flight is the time for an ultrasonic pulse wave to travel from the transmitter of the sensor and the reflected echo received at the receiver [4, 105, 108]. The object distance d from the sensor is

$$d = \frac{tof * c}{2} \tag{5.1}$$

Where *c* is the speed of sound and *tof* is the time-of-flight.

For a known location of the object, the distance d between the ultrasonic sensor and the object can be calculated. Using equation (5.1), we can calculate the speed of sound using the time-of-flight, and distance [109].

$$c = \frac{2d}{tof} \tag{5.2}$$

If the speed of sound increases, the time of flight decreases. According to Bohn [10], the air temperature affects the speed of sound according to the following equation.

$$c = 331.45 + 0.6 * t \tag{5.3}$$

Where 331.45 is the speed of sound (m/s) in air medium at 0 °C and t is the temperature in (°C)

Standard ultrasonic sensors compute the time of flight, assuming the constant speed of sound at a fixed air temperature during wave propagation. From equation (5.3), it is observed that the speed of sound in air increases with an increase in air temperature. There is a relationship between the speed of sound and temperature [31]. Thus, air temperature can be estimated from the speed of sound and can be expressed as follows.

$$c = f(t) \tag{5.4}$$

$$t = f^{-1}(c) (5.5)$$

By substituting equation (5.2), we can estimate the temperature from time-of-flight, and traveled distance [110].

$$t = f^{-1} \left(\frac{2d}{tof}\right) \tag{5.6}$$

As the speed of sound is affected by air temperature, humidity and other environmental

parameters, estimating temperature only from the speed of sound will not be accurate. Thus, we propose machine learning models to get accurate air temperature of the measurement medium [109]. The speed of sound also increases with an increase in relative humidity. The speed of sound in the air medium is expressed as a function of temperature and relative humidity.

$$c = f(t, h) \tag{5.7}$$

Where t is the temperature (${}^{\circ}C$) and h is the relative humidity (%).

An approximate equation for the speed of sound ratio over temperature and humidity is [28]

$$c_h/c_0 = 1 + h (9.66 \times 10^{-4} + 7.6 \times 10^{-5} t + 1.8 \times 10^{-6} t^2 + 7.2 \times 10^{-8} t^3 + 6.5 \times 10^{-11} t^4)$$
 (5.8)

Where C_h the speed of sound in humid air, C_0 the speed of sound in dry air, relative humidity h from 0 to 1.0 and temperature t from 0 to $50^{\circ}C$.

Relative humidity estimation using the ultrasonic technique has been proposed in the literature in the recent past. These methods have limitations like a restricted distance range, experiments performed in a controlled environment, and high implementation costs. Existing research on estimating air temperature and relative humidity using ultrasonic time-of-flight techniques is described in Section 5.2. Usually, an ultrasonic measurement system assumes uniform temperature and relative humidity throughout the measurement medium. In reality, the medium temperature and humidity are mostly not uniform, and there is normally a gradient of temperature and relative humidity. Ultrasonic signal time-of-flight encodes the spatial distribution of the temperature and relative humidity along the propagation path. The relationship between the time-of-flight, humidity distribution h(z), and temperature distribution t(z) is given by the following equation [38]:

$$tof = 2 \int_0^d \frac{dz}{f(t(z), h(z))}$$
 (5.9)

In this work, our objective is to estimate the relative humidity of the air medium using the ultrasonic time-of-flight technique. To estimate relative humidity, using (5.7) is not feasible because relative humidity has relatively less effect on the speed of sound compared to the effect of temperature. Moreover, as there is no significant correlation between temperature and relative humidity, just by substituting temperature value in (5.7), one can not accurately estimate relative humidity. We propose a combination of fuzzy logic and a neural network approach to estimating relative humidity. The conceptual framework of this proposed two-phase method is shown in Figure 5.1. In addition to the proposed model-based relative humidity estimation, we also used other machine-learning methods to estimate the relative humidity for comparison purposes. We found that the proposed method for estimating relative humidity is more accurate than other methods. The main contributions of this work are summarized as follows:

- A new and novel hybrid model is proposed for estimating relative humidity using ultrasonic sensors.
- Use of fuzzy logic and fuzzification of the experimental sample data to find different relative humidity ranges in the first phase.
- A set of ANN sub-modules corresponding to different ranges of relative humidity integrated into one ANN model is proposed to estimate relative humidity accurately.
- To measure the relative humidity of a larger space quickly and in a continuous manner compared to the conventional single-point measurement sensors, which are discrete having slower response times.
- The proposed model can accurately estimate the relative humidity of the entire medium in the presence of a gradient of temperature and humidity.
- The proposed model can work in extreme and dynamic environments where singlepoint measurement may not be feasible.

The remainder of the chapter is organized as follows. Section 5.2 briefly reviews the related works followed by proposed methodology in Section 5.3. Experimental setup, experiment, and data acquisition procedures are described in Section 5.4. The detailed analysis of experimental results of the proposed method and its comparison with other models are discussed in Section 5.5. Finally, the concluding remarks and future works are discussed in Section 5.6.

5.2 Related works

We present the related works on non-contact ultrasonic sensor based measurement methods, effect of the environmental conditions like temperature and relative humidity in this section. It is already known from research papers that sound wave propagation in the air is affected by several environmental parameters [10, 27, 28, 31, 91]. Bohn [10] mentions the effect of temperature and humidity on sound speed in air medium. Harris [27] performed experiments and reported results on the absorption of the speed of sound at different frequencies, humidity, and temperature ranges. Wong *et al.* [28] conducted experiments and analyzed the impact of relative humidity on the speed of sound in the air over a temperature range from $0-30\,^{\circ}C$. Attenborough [31] discussed the influence of geometric spreading, air absorption, refraction, and temperature gradients on the propagation of sound wave in air medium. Cramer [91] measured specific heat ratio and speed of sound in air medium considering temperature, pressure, humidity, and CO_2 .

Non-contact ultrasonic range measurement system that depends on the speed of ultrasonic sound in air medium depends on the various environmental parameters [4, 43, 105, 111]. Sahoo *et al.* [105] proposed an ANN-based non-contact ultrasonic level measurement system to accurately measure the liquid level while compensating temperature and relative humidity gradient along the measurement path. Rocchi *et al.* [4] conducted exhaustive experiments with a non-contact ultrasonic sensor to measure the level and estimate the

position of the water surface to measure the thickness of the pollutant layer. Mousa *et al.* [43] designed a low-powered sensing device based on an ultrasonic sensor that can detect flash floods and traffic congestion. They used multiple machine-learning techniques embedded in the device to estimate water levels with proper compensation for all environmental conditions. Huang *et al.* [111] proposed an ultrasonic range measurement system that compensates the air temperature with the average temperature in air medium instead of single point measurement.

Airborne non-contact ultrasonic sensor is used for temperature measurement using time-of-flight techniques [100, 101, 102, 109, 110, 112, 113]. Sahoo $et\ al.$ [109] proposed a low-cost non-contact ultrasonic-based ambient temperature measurement system using machine learning approaches. Zhou $et\ al.$ [110] proposed an accurate temperature estimation method using the ultrasonic sensor with an error bounded by $\pm 0.04\ ^{\circ}C$. Dobosz $et\ al.$ [101] presented an ultrasonic measurement technique that can measure the gradient of air temperature along the beam axis of the laser interferometer during displacement measurement. Akio $et\ al.$ [112] measured air temperature and its gradient using the acoustic frequency responses. Hu $et\ al.$ [113] presented an acoustic sensing technique to measure the temperature of biomass fuels. Ruixi $et\ al.$ [102] used time of flight of of ultrasonic wave to measure air temperature. Tsai $et\ al.$ [100] ultrasonic ToF to measure the average temperature of the air by detecting the changes in the speed of sound.

Conventional sensors are single-point contact-based measurement systems for measuring temperature and humidity. Whereas non-contact ultrasonic sensors can measure the average relative humidity and temperature because water vapor in the air can influence the speed of sound [107]. Motegi *et al.* [12] presented a technique to measure temperature and relative humidity using sound velocity and its attenuation. Schaik *et al.* [40] developed a device to measure average temperature and humidity using two ultrasonic transducers.

All the related works on estimating the relative humidity using ultrasonic sensors are based on a signal processing and ToF approach, that incurs high implementation costs.

Experiments are limited to specific ranges, confined to the laboratory with controlled environments, and not suitable for real-time applications. In this work, we present a fuzzy inspired two-stage machine learning approach to estimate the relative humidity with temperature compensation accurately.

5.3 Methodology

The main focus of this study is to accurately estimate the relative humidity of the medium using non-contact intelligent ultrasonic sensor. Different machine-learning approaches are investigated to accurately estimate the relative humidity. The idea is to use machine learning to automatically learn and identify the complex patterns from the data samples and make intelligent decisions on new data points. A labeled training dataset is first used in supervised machine learning to train the underlying model. Then the new unlabelled test data samples are fed to the trained model to make accurate predictions [18]. Machine learning-based regression techniques are used to predict continuous dependent variables [114, 115, 116, 117]. The proposed model uses a two-phase model, and the overall framework of the model is depicted in Figure 5.2. The defined fuzzy logic controller ([118, 119, 120]) takes temperate and speed of sound as input and predicts relative humidity ranges. Based on the output ranges of the fuzzy controller, we design four neural networks, and each network is trained on different ranges of temperature and speed of sound to estimate the relative humidity. Other machine learning methods such as Support Vector Regression (SVR), K-Nearest Neighbors (KNN), and Random Forest Regression (RFR) are used to estimate the relative humidity and compare the performances with the proposed method [121].

5.3.1 Support Vector Regression (SVR)

Support vector machine is used for classification problems and also used for regression problems [18, 21, 122]. The regression problem aims to determine a function that

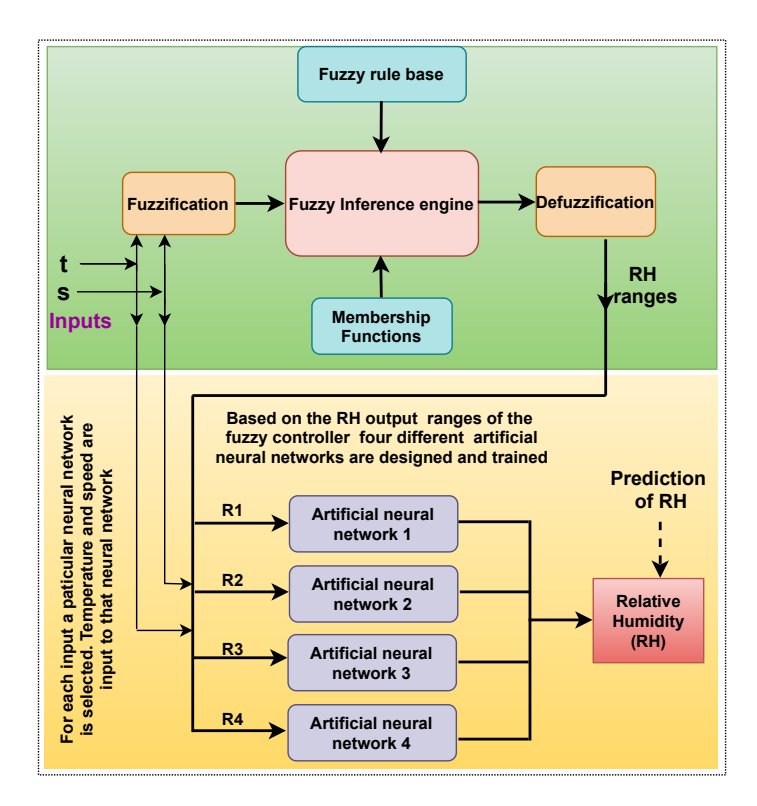


Figure 5.1: The schematic diagram of proposed two-phase method to estimate relative humidity

can accurately approximate dependent variable values. A nonlinear mapping is done to map the n-dimension input samples into a higher dimensional feature space by nonlinear transformation φ , on which linear regression can be performed.

Let a training sample is a set $\{x_i, y_i\}$, where $x_i \in \mathbb{R}$, i = 1...N where x_i represents the n-dimensional input sample space and corresponding target value $y_i \in \mathbb{R}$, where N represents the size of the training data.

The SVR function can be denoted as

$$y = w^{\mathsf{T}} \varphi(x) + b \tag{5.10}$$

The aim is to determine the value of $w \in \mathbb{R}$, $b \in \mathbb{R}$ such that values of x can be computed by minimizing the regression error. The appropriate selection of hyper-parameters values is important for SVR algorithm's robustness and efficiency. To build a more efficient

model, we need proper kernel functions, regularization parameter C, which determines the penalties to estimation errors. The radius ϵ also needs to be determined, such that the data inside the ϵ -tube can be ignored.

In this study, the optimal hyperparameter values are determined after repeated experiments on all data sets. A polynomial kernel is used as the kernel function, the regularization parameter C is set to 1, and the value of ϵ is set to 0.1.

5.3.2 K-Nearest Neighbors Regression(KNNR)

The k-nearest neighbors algorithm is used for classification, and regression problems [18]. KNN algorithms are simple to implement and computationally inexpensive. The KNN regression model is used to predict output values $\mathbf{y} \in \mathbb{R}$ for a given input values $\mathbf{x} \in \mathbb{R}$ is based on N input-output training samples $(\mathbf{x_i}, \mathbf{y_i})_{i=1}^N$, where $\mathbf{x_i} = \{x_1^i, x_2^i, \dots, x_d^i\} \in \mathbb{R}$, is an input sample i from d-dimensional feature space, and the corresponding output value $\mathbf{y_i} \in \mathbb{R}$.

For a new test sample \mathbf{x} , we need to learn a function $(f: x \to y)$ from the training dataset. KNN regression starts computing the distance d between test sample \mathbf{x} and each sample $\mathbf{x_i}$ in the training dataset. In this case, we consider Euclidean distance as a distance metric, among many other distance metrics.

The sample \mathbf{x} , which is a set of k-nearest neighbors, $\mathcal{N}_{K}(\mathbf{x})$, is considered as a test sample taken from training samples based on Euclidean distance. The final estimated output value \hat{y} is calculated by considering the mean of the output values of the nearest neighbors as follows:

$$\hat{y} = \frac{\sum_{i \in \mathcal{N}_K(x)} y_i}{k} \tag{5.11}$$

Selection of k value is important to avoid the over-fitting problem. In this study, we vary the parameter k from 1 to 5 and the lowest error is obtained for k = 1 corresponding to all

training datasets. Therefore, we choose the optimal value of k = 1.

5.3.3 Random Forest Regression (RFR)

Random forest is an ensemble method which constructs multiple decision trees using the bootstrap technique followed by aggregation, which is also known as bagging [18, 22]. A random forest regression contains an ensemble of regression trees and random feature selection during tree induction. Bootstrap sampling is used for constructing regression trees. The random selection of features for partitioning at each node reduces the correlation between the trees. Averaging their predictions reduces the variance and improves overall accuracy. The final output is calculated by aggregating all the predictions across all the trees.

The number of trees are one of the important hyper-parameters in the random forest model. While searching for the best split at each node, number of selected tree helps in optimal selection of a subset of features m from the total number of features M, in each training subset. A typical number of trees m for regression tasks is M/3. In this experiment, the optimal value for a number of trees is taken as 500.

5.3.4 Proposed method

The proposed method comprises two steps as shown in Figure 5.2. In the first step, the fuzzy inference controller is designed, and in the second step, one of the four different artificial neural networks is designed based on the fuzzy output to estimate the relative humidity. The flowchart is shown in Figure 5.6 describes the procedure followed in this study to estimate relative humidity. The input to fuzzy logic is measured temperature and speed of sound, and the output of the fuzzy logic controller is the membership function, which defines the relative humidity range. Based on the fuzzy output, one neural network out of the four is selected, and the same input is fed into the selected neural network to compute the relative humidity.

5.3.5 Fuzzy logic controller

Researchers have applied fuzzy logic systems to numerous real-world applications, particularly in control systems, predictions, and inference engines [118, 119]. Deterministic models are required to be more robust and inadequate to describe the system process. The use of fuzzy systems is one of the effective solutions to these problems. Conventional mathematical models are not efficient in dealing with ill-defined and uncertain systems. The fuzzy inference system uses logical rules based on expert knowledge and can effectively handle uncertain and ill-defined systems. A fuzzy inference system usually consists of a fuzzification module, a knowledge base, the fuzzy inference engine, and the defuzzification module [120]. The fuzzy inference system is shown in Figure 5.2.

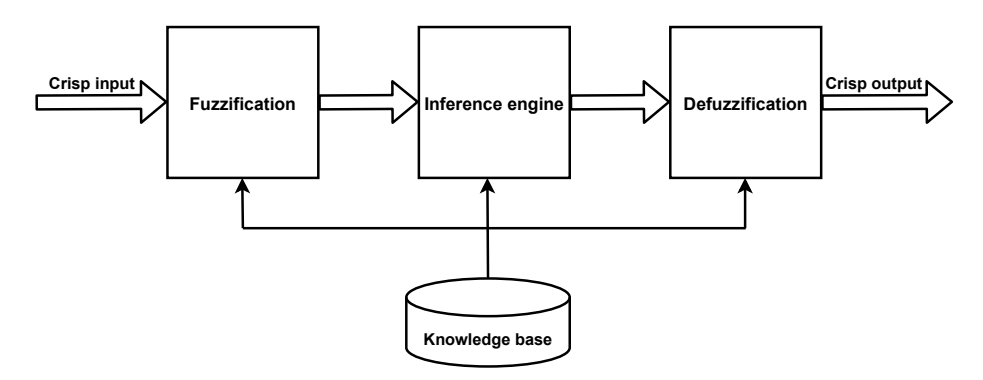


Figure 5.2: Fuzzy inference system architecture

This work uses the Mamdani inference and aggregation method. Fuzzy inference maps the inputs to outputs using fuzzy logic based on the mapping functions. The fuzzy inference process contains membership functions, fuzzy logic operators, and *if-then* rules. Fuzzy membership functions is constructed based on expert knowledge, experience, and real data. Fuzzification is the first step of the fuzzy logic controller, which converts crisp inputs into fuzzy variables (linguistic) using the membership functions. Out of many different membership functions, we zeroed on triangular membership functions to represent the linguistic variables. The inference engine computes the fuzzy output from fuzzy input by using *if-then* rules already stored in the knowledge base. The centroid-based defuzzification

method converts the fuzzy output to a crisp value. The same membership function is used for fuzzification and defuzzification step for consistent output. We designed the fuzzy controller using the Fuzzy Logic Toolbox of Matlab. Two input variables and one output variable are used in this proposed fuzzy logic model. Figure 5.3 and Figure 5.4 represents the membership functions of both input variables, i.e., temperature and speed of sound. The experimental temperature range is 22 - 45 °C, and the speed of sound range varies from 345 - 360 m/s. The output variable is the relative humidity ranges from 30 - 85%. We defined four membership functions for the input air temperature variable, namely, Low Temperature (LT), Normal Temperature (NT), High Temperature (HT), and Very High Temperature (VHT). Similarly, there are four membership functions, Speed1 (S1), Speed2 (S2), Speed3 (S3), and Speed4 (S4), corresponding to the input variable speed of sound. The output variable relative humidity uses four membership functions, namely, Low Humidity (LH), Low Medium Humidity (LMH), Medium Humidity (MHH).

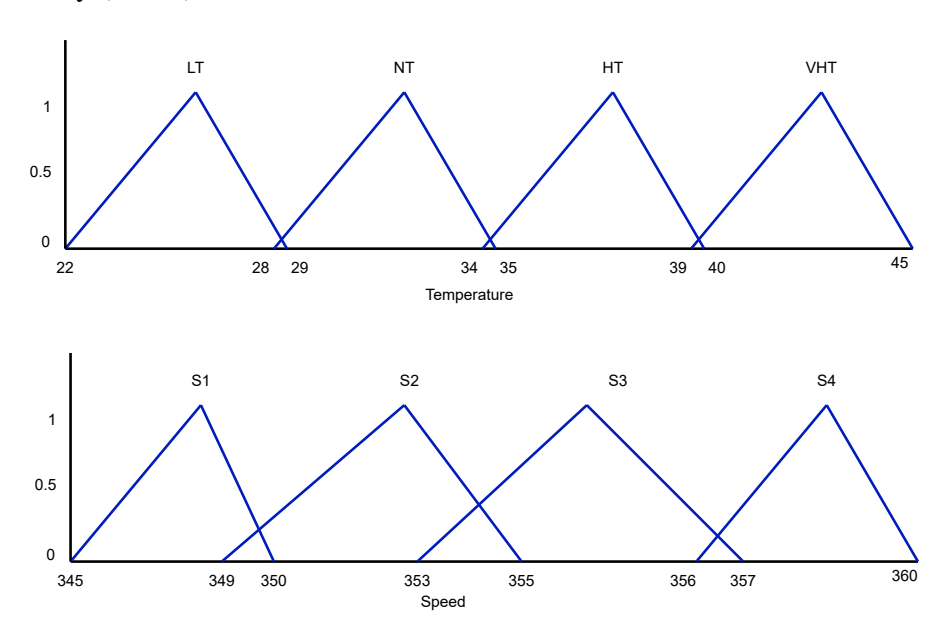


Figure 5.3: Membership functions for input variable temperature and speed of sound

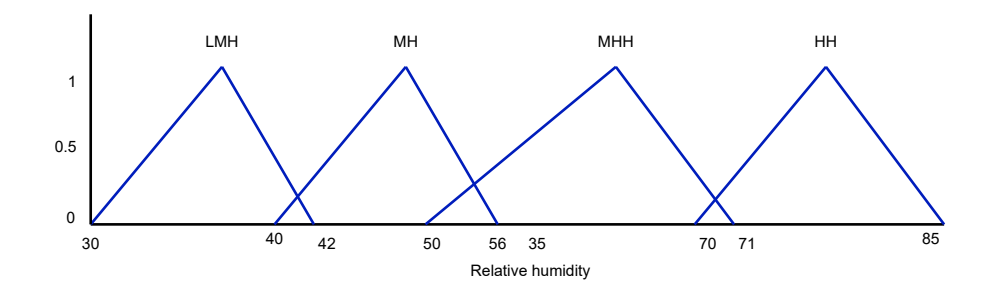


Figure 5.4: Membership functions for output variable relative humidity

5.3.6 Integrated artificial neural network model

An artificial neural network can model and approximate the complex relationships between inputs and outputs. For many years, feedforward neural networks are the most popular and most widely used models in many practical applications [43, 123, 124]. Feedforward neural network contains one or more hidden layers to deal with nonlinear and complex correlations. Multi-Layer Perceptron (MLP) is a class of neural networks consists of one input layer, one hidden layer, and one output layer. Usually, MLP with one hidden layer is sufficient to approximate any continuous nonlinear function [105, 123].

We propose four artificial neural networks based on output ranges of fuzzy inference systems. Each neural network comprises one input layer, one hidden layer, and one output layer. We chose different hidden layer nodes and arrangements to obtain the best production results. The proposed neural network representation is shown in Figure 5.5. The two inputs are ambient temperature and sound speed, and relative humidity is the output of each network.

The neural network function is mathematically formulated as follows:

$$y(x, w) = g\left(\sum_{j=1}^{l} w_{j,1}^{2} f\left(\sum_{i=1}^{k} w_{i,j}^{1} + b_{j}^{1}\right) + b_{1}^{2}\right)$$
(5.12)

Where j=1,...l, and l is the total number of hidden layer neurons. The variable i varies from 1,...k, where k represents the total number of input variables. The parameters $w_{i,j}^1$

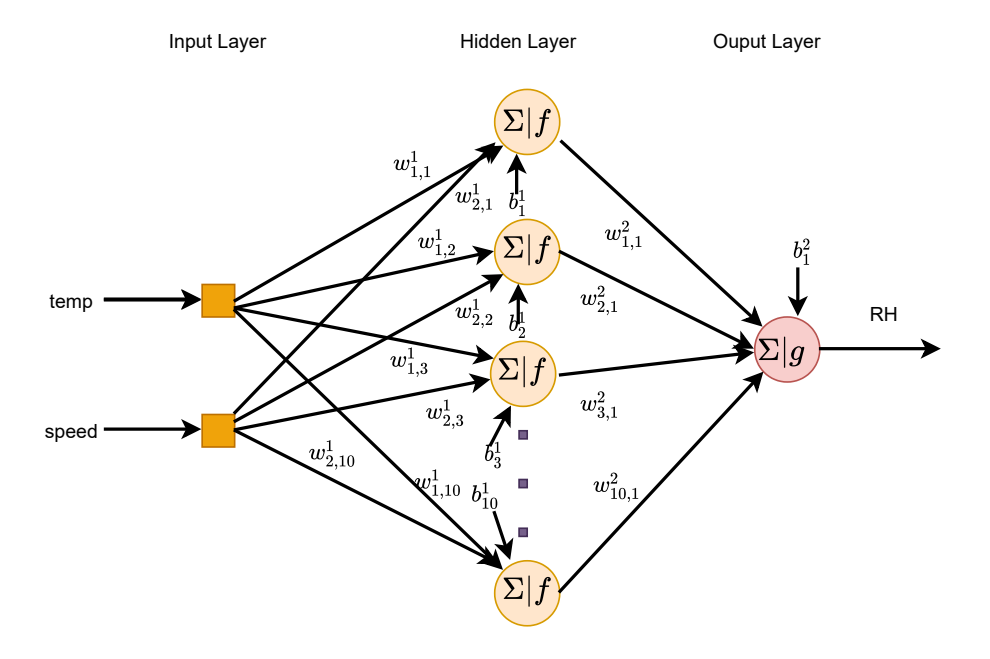


Figure 5.5: Architecture of neural network proposed in this work

and b_j^1 are the weights and biases for input to the hidden layer. Similarly, the parameters $w_{j,1}^2$ and b_1^2 are the weights and the biases from hidden to the output layer. The activation function of the hidden layer is denoted by f(.), and g(.) is the activation function of the output layer.

5.3.7 Training of the neural network

The neural network is trained to learn the complex nonlinear relationship between the input and output. During the testing stage, the trained neural network can compute the output corresponding to the given input data. The backpropagation algorithm is utilized in the training of ANN models. The backpropagation algorithm uses the supervised training technique where the network weights and biases are initialized with random values at the beginning of the training phase. The backpropagation algorithm can be described into two stages:

• Feedforward step: In this step, an input pattern is applied to the input layer and allowed to propagate through the network layers. During the propagation, the inputs

values are modified by current weights and biases and then by the nonlinear activation functions until the final output is produced. The network's estimated output value is then compared to the target output to calculate the loss function.

• Backpropagation: In this step, the output error signals are fed back (backpropagation) through the network layers starting from the output layer, through the hidden layers back to the input layer. The weights are modified in a way that minimizes the error across the entire training input dataset.

In this study, the tan-sigmoid function is used as the nonlinear activation function in the hidden layer. The *purelin* linear transfer function is used in the output layer. The number of neurons in the hidden layer is taken to be 10. The Levenberg-Marquardt backpropagation training algorithm is used to train the neural networks.

Algorithm 4 Proposed hybrid fuzzy-neural network algorithm

INPUT: temperature (t), speed of sound (s)

OUTPUT: relative humidity (h)

function Fuzzy_inference_system(t, s)

for each input i = 1 to 2 do

 $q_i \leftarrow$ universe of discourse input i

 $n_{mf} \leftarrow \text{number of } mfs \text{ for input } i$

for each output do

 $q_0 \leftarrow$ universe of discourse output

 $n_{mf} \leftarrow \text{number of } mfs \text{ for output}$

return output membership functions (*h*)

Require: input set (t, s) and target h

g(): Activation function for hidden and output layers

w, b :Random initialization of weights and biases

repeat

for each input observations (t,s) do

 $R_i \leftarrow \text{FUZZY_INFERENCE_SYSTEM} \left(\mathsf{t}, \mathsf{s} \right)$

$$ANN_i \leftarrow R_i$$

compute net input g(net) to each hidden nodes

if $\hat{h} \neq h$ then update the parameters

$$w \leftarrow w - \alpha \tfrac{\partial L(h,g(net))}{\partial w}$$

$$b \leftarrow b - \alpha \frac{\partial L(h, g(net))}{\partial b}$$

until met the stopping criteria

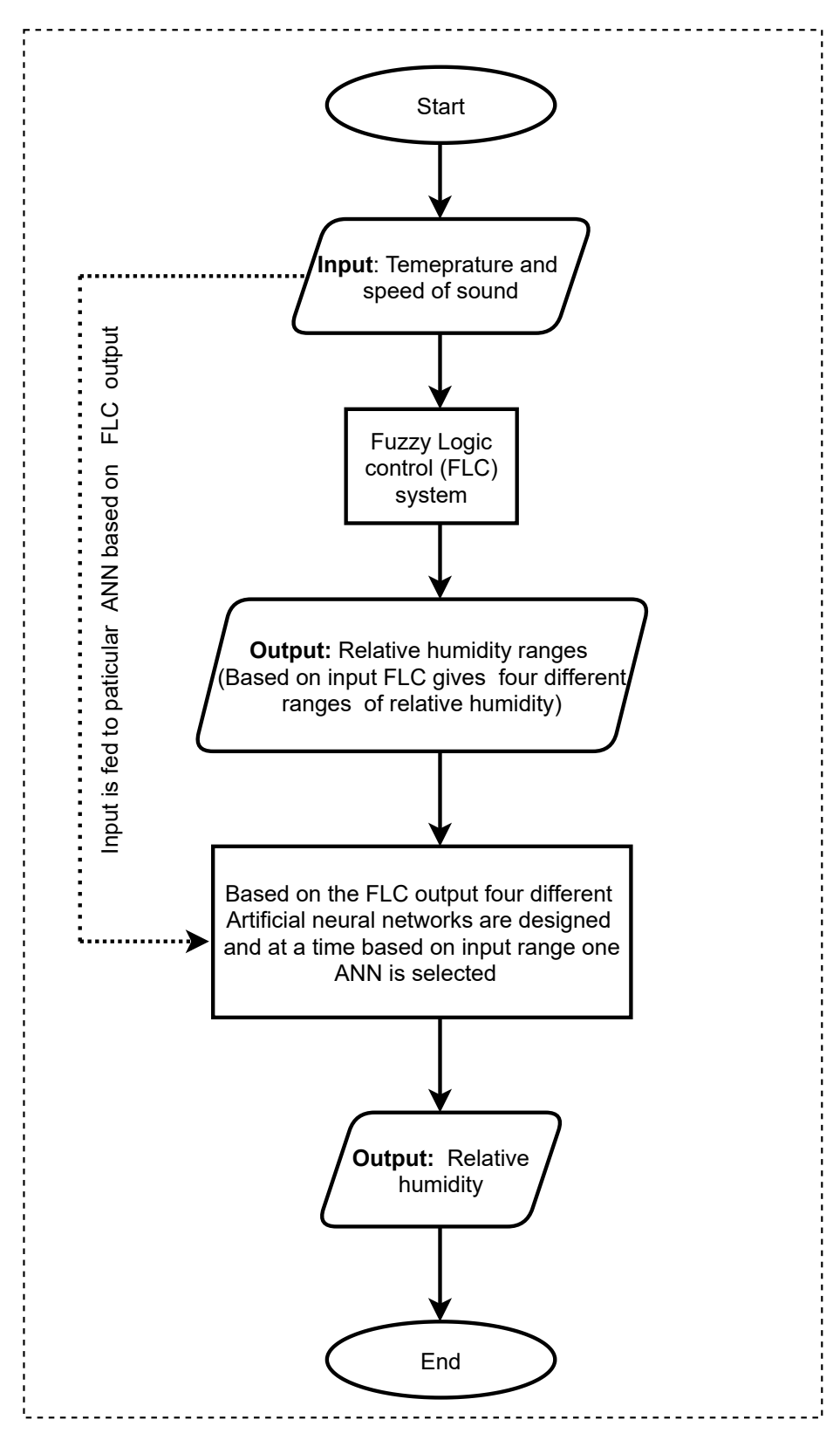


Figure 5.6: Flowchart of the procedure of the proposed method to estimate relative humidity

5.4 Experiment design

5.4.1 Experimental setup

This study used a low-cost non-contact ultrasonic sensor to estimate the relative humidity using two input parameters i.e. temperature and speed of sound. The experimental setup module used for the experimentation is shown in Figure 5.7. The setup module comprises of a temperature sensor (DHT22), a micro-controller (ATmega328p), an ultrasonic sensor (HC-SR04), and a Bluetooth module. Relative humidity sensor is used to collect relative humidity data for training purposes. The 8-bit micro-controller (16 MHz with 32 KB flash memory) is used for data acquisition and processing. The Bluetooth module is used to communicate data to the end user. The HC-SR04 ultrasonic sensor with an operating frequency of 40 kHz is used for transmitting and receiving ultrasonic waves. This ultrasonic sensor module comprises two transducers. One transducer is used for emitting an ultrasonic wave at 40 kHz and the other to receive the wave after getting reflected from the target surface. The operating range of this HC-SR04 sensor is 2 to 400 cm.

We designed four rectangular boxes as shown in the Figure 5.8 with open upper surfaces for carrying out experiments. The height (H) and width (D) of the box are 100 cm and 200 cm, respectively. The four boxes' inner lengths (L) are 100 cm, 200 cm, 300 cm, and 400 cm for experiments with different distance ranges. On one side of the box, we attached the experimental setup module at a height of 60 cm from the bottom. The other side acts as the surface to reflect the ultrasonic waves. We performed repeated experiments in all four different ranges to estimate the relative humidity of the measurement medium using temperature and speed of sound variations in the propagation path of the ultrasound signal.

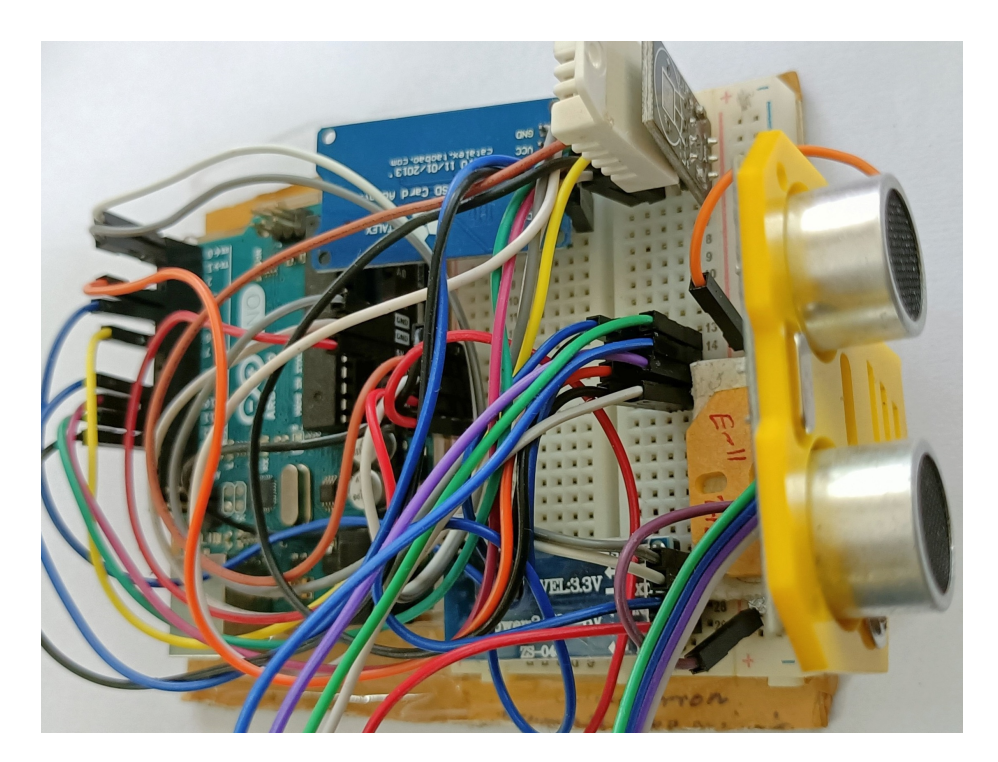


Figure 5.7: The hardware module developed for non-contact humidity measurement

5.4.2 Measurement system

To measure the speed of sound, the absolute distance between the ultrasonic sensor and the object's surface is required. The speed of sound is dependent on air temperature (5.3). However, the speed of sound is also influenced by relative humidity. But, we can not derive relative humidity, given the speed of sound and air temperature directly from (5.8), as the influence of relative humidity on the speed of sound is less compared to the influence of temperature and is also non-linear.

The experiments are performed, and data is collected at 100 cm, 200 cm, 300 cm, and 400 cm range. The temperature and humidity is varied inside the measurement boxes specially designed for this experiment. We use a heat gun and humidifier to vary the temperature (range : $22 - 45 \, ^{\circ}C$) and humidity (range : 30 - 85%RH). Ultrasonic sensors use time-of-flight to measure the distance, encompassing the temperature and humidity variation along the measurement path. Standard temperature and humidity sensors are single-point measurement sensors, and can not capture the variations in the measurement medium. So,

for accurate measurement, multiple temperatures, and humidity sensors are kept on the bottom surface inside the box to capture the temperature and humidity variation in the measurement path.

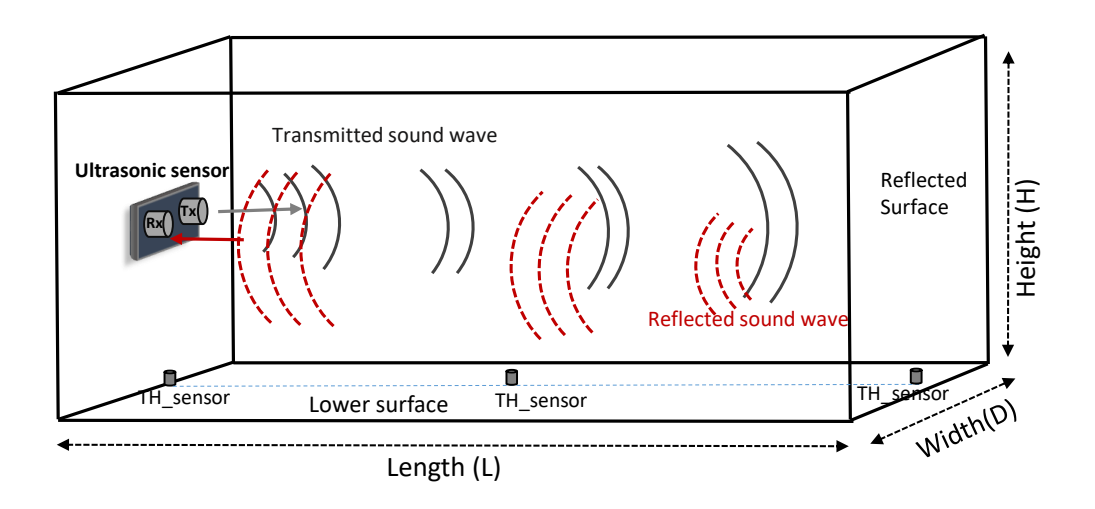


Figure 5.8: Experimental setup for data collection

5.5 Results and discussions

In this section, we described the experimental results and analysis of the proposed two-phase method to estimate relative humidity. At first, the range of possible values for the input and output variables of the fuzzy inference system is described. Then, the performances of all other machine learning methods considered in this work are compared with the proposed two-phase fuzzy logic embedded integrated neural network model. The performance evaluation metric of the backpropagation neural network is compared and contrasted with the other machine learning methods. The overall system performance is discussed in detail.

The training dataset contains 7800 data points after pre-processing. Each tuple of the dataset consists of temperature, speed of sound, and relative humidity. The fuzzy inference system finds input and output variable ranges. As described earlier, there are four

Table 5.1: The different ranges of temperature and relative humidity considered for experimentation

Variables	Range-1 (R1)	Range-2 (R2)	Range-3 (R3)	Range-4 (R4)
Temperature (°C)	22–28	28–35	35–40	40–45
Speed of Sound (<i>m</i> / <i>s</i>)	345–350	349–355	353–357	356–360
Relative humidity (%)	69–85	54–70	40–55	30–41

Table 5.2: Training data samples for each range of temperature and relative humidity (Ref. Table. 5.1)

Distance	R1 (Data)	R2 (Data)	R3 (Data)	R4 (Data)	Total data
100 cm (D1)	578	592	297	333	1800
200 cm (D2)	660	696	322	322	2000
300 cm (D3)	748	590	351	311	2000
400 cm (D4)	698	554	376	372	2000

membership functions corresponding to the input variables i.e. temperature and speed of sound and output variable relative humidity. The fuzzy system decides the ranges of the output relative humidity based on the input variables. We divide the dataset into four groups, and the ranges of each group are described in Table 5.1. We designed an artificial neural network for each group to take the temperature and speed of sound as input and estimate the relative humidity as output. Since we experimented with four distances, the data is divided into four groups corresponding to each distance. Table 5.2 depicts the four distances (D1, D2, D3, and D4) and the number of data points in each range (R1, R2, R3, and R4) as per Table 5.1.

To compare the performance of the different models, we use the training and testing accuracy of the machine learning models. We carried out 10-fold cross-validation for all the methods. To ensure statistical independence, 10-fold cross-validations performed with a repetition of 10 times by shuffling the input data randomly and averaging the results. In the 10-fold cross-validation, the entire dataset is divided into ten subsets, with nine subsets for training and one subset for testing. The cross-validation results of all the models are evaluated using statistical measures; root-mean-squared error, mean absolute error, mean

absolute percentage error, and R-values (coefficient of correlation). Table 5.4 shows the average cross-validation accuracies of the proposed two-phase ANN, SVR, KNN, and RFR methods. This Table 5.4 clearly shows that the proposed ANN model outperforms the other popular machine learning models. We also perform pair wise statistical significance test compared the models. Pair-wise Student's t-test analysis is computed between ANN and other methods at the 5% level of significance. We found that ANN model better compared to other models.

Performance evaluation of the proposed ANN model

The input feature matrix is normalized before training the ANN model. Normalizing the data generally makes faster convergence for neural networks. The data set is normalized using MIN-MAX normalization techniques to normalize and scale the data within 0 and 1. The input variables and the labeled output of the dataset are divided into a training set, a validation set, and a test set. Matlab software is used to develop the neural network model. The two inputs, namely, temperature and speed of sound, make the input layer, one hidden layer is used, comprising ten neurons, and a single neuron output layer is used to estimate the relative humidity. This proposed neural network model is shown in Figure 5.5. We conducted exhaustive experiments to collect data in different environmental conditions and for various distances. The dataset consists of 7800 sample data points for different distances and temperature and relative humidity ranges. We designed and trained the four neural networks depending on the number of output membership functions based on the ranges of the fuzzy logic. Training is done with 10-fold cross-validation to evaluate and compare the training performance of neural networks with other methods and presented in Table 5.4.

Performance evaluation of the neural network with unseen dataset

The effectiveness of the trained neural networks for estimating the relative humidity was further evaluated using unseen input dataset. We use a new input dataset consisting of 3210

Table 5.3: Performance evaluation of the proposed model using unseen dataset

Distance	Range-1	Range-2	Range-3	Range-4	Total
100 cm	151	212	115	95	573
200 cm	261	290	140	219	910
300 cm	369	278	192	166	1005
400 cm	230	214	140	138	722

data points. Each input vector represents the temperature and speed of sound corresponding to a measure at a particular instance. The temperature ranges from 22 - 45 °C, and the speed of sound ranges from 345 - 360 m/s. The total number of input sample data points corresponding to distances (100 - 400 cm) and the corresponding ranges (R1 - R4) are tabulated in Table 5.3. The scatter plot of the observed variations in estimated relative humidity in different distances (D1, D2, D3, and D4) along with ranges of humidity (R1, R2, R3, and R4) are depicted in Figures. 5.9 - 5.12. It can be observed that the estimation variation is a little more for some input data points in the case of D1 - R1 and D3 - R1 combinations, as seen in Figures 5.9 (a), (c). For all other combinations of Distance-Range, the maximum estimation variation is bounded by $\pm 3\%$. The other performance metric that includes Root Means Square Error (RMSE), Mean Absolute Error (MAE), Mean Absolute Percentage Error (MAPE), and correlation of coefficient (R-values) corresponding to the four different neural networks (based on four different ranges R1, R2, R3, and R4) are tabulated in Table 5.5.

Discussions

Ultrasonic sensor-based existing works for estimating relative humidity have high implementation costs and are not suitable for practical applications. The proposed method is based on a machine learning approach, involves low implementation cost, operates in high measurement ranges, and is suitable for wide range of applications. The relative humidity estimation accuracy of the proposed method is bounded by $\pm 3\%$. The achieved

accuracy is comparable to standard commercially available off-the-shelf humidity sensors [125, 126]. Standard sensors for measuring relative humidity are single-point measurements and are restricted to that point of measurement only. The proposed ultrasonic measurement system overcomes these limitations and effectively captures and accurately measures relative humidity variations in the air medium at various distances. The overall response time of the ultrasonic measurement system is 500 milliseconds. However, the response time of the standard humidity sensor is 2 seconds.

There are a few limitations of the proposed work. One of the major limitations is the requirement to use a standard temperature sensor along with the ultrasonic sensor. This is required as we need to compensate for the temperature effect to estimate relative humidity using an ultrasonic measurement system. It is necessary to check that the condensed water vapor is not affecting ultrasonic measurement systems during the experimentation. A minor fluctuation in air temperature gradient may also result in $\pm 1\%$ to $\pm 2\%$ error in relative humidity.

The novelty of the proposed model lies in combining a fuzzy inference system and an integration of backpropagation neural networks to estimate the relative humidity of the air medium. We compared the performance of the proposed model with other well-known supervised machine learning approaches such as support vector regression, random forest regression, and the k-nearest neighbors method. The 10-fold cross-validations are repeated ten times to minimize biases and over-fitting. We evaluated the performance metric as described earlier. Implementation of the model was carried out using Matlab. The training and testing experiments were conducted using a personal computer with an Intel Core i7 CPU (3.6 GHz) and 16 GB of RAM. The proposed method was implemented using C-language. The results reveal that the backpropagation neural network outperforms other methods in terms of accuracy. The proposed combined approach estimate relative humidity more accurately.

Table 5.4: Average performance of 10-fold cross validation of ANN, SVR, KNN and RFR

D1	RMSE	MAE	MAPE	R-value
ANN	1.62	1.36	1.76	0.92
SVM	3.23	2.74	3.58	0.86
KNN	2.04	1.55	1.99	0.88
RFR	1.96	1.53	1.98	0.89
D2	RMSE	MAE	MAPE	R-value
ANN	1.33	1.07	1.78	0.97
SVM	2.19	1.75	2.95	0.95
KNN	1.95	1.50	2.51	0.92
RFR	1.85	1.44	2.41	0.94
D3	RMSE	MAE	MAPE	R-value
ANN	1.17	0.96	2.02	0.95
SVM	1.64	1.34	2.84	0.96
KNN	1.73	1.35	2.84	0.88
RFR	1.60	1.27	2.68	0.91
				0.7 1
D4	RMSE	MAE	MAPE	R-value
D4 ANN	RMSE 0.952			
		MAE	MAPE	R-value
ANN	0.952	MAE 0.777	MAPE 2.28	R-value 0.95

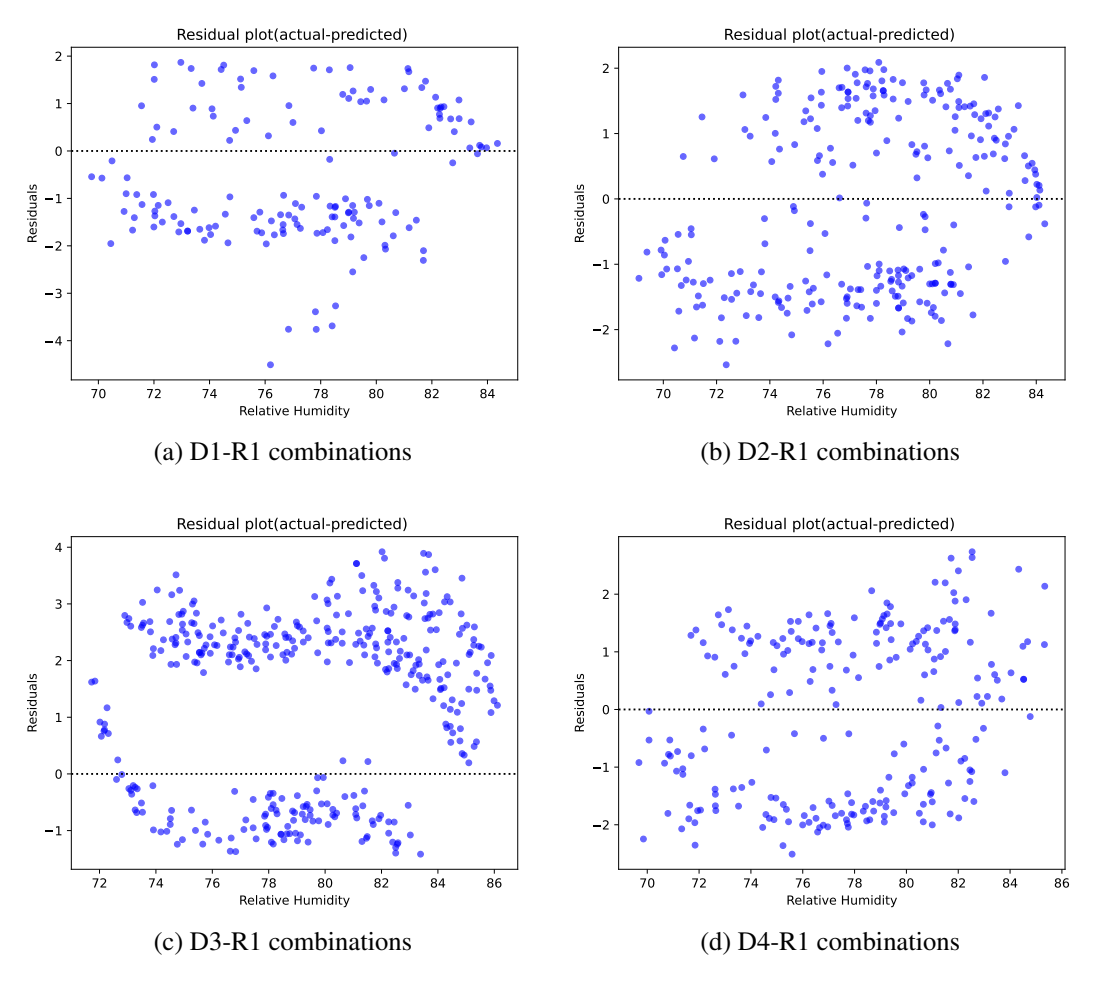


Figure 5.9: The residual scatter plots for unseen dataset and using proposed model. D1-D4 represent distances of 100, 200, 300, and 400 cm respectively. R1 represents the ranges of input and output variables as shown in Table 5.1

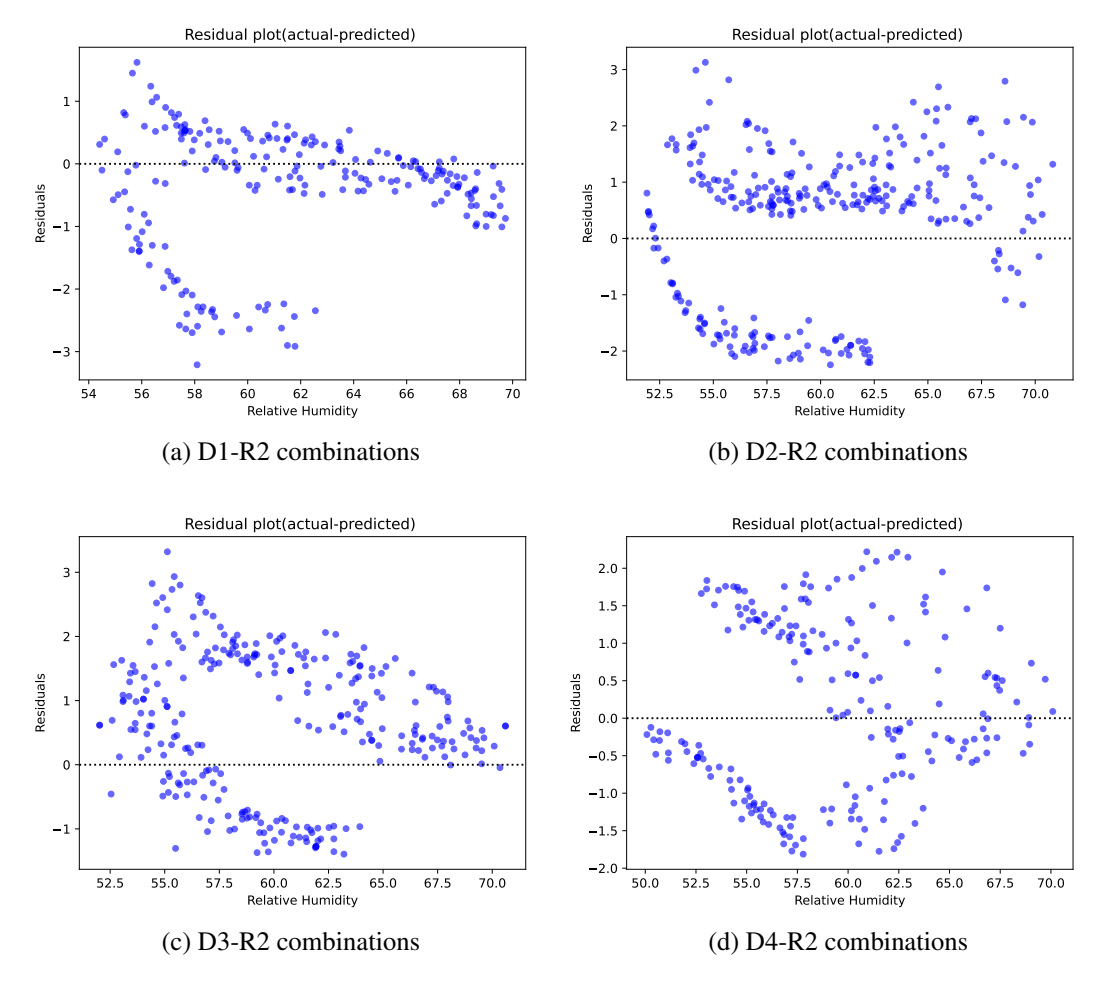


Figure 5.10: The residual scatter plots for unseen dataset and using proposed model. D1-D4 represent distances of 100, 200, 300, and 400 cm respectively. R2 represents the ranges of input and output variables as shown in Table 5.1

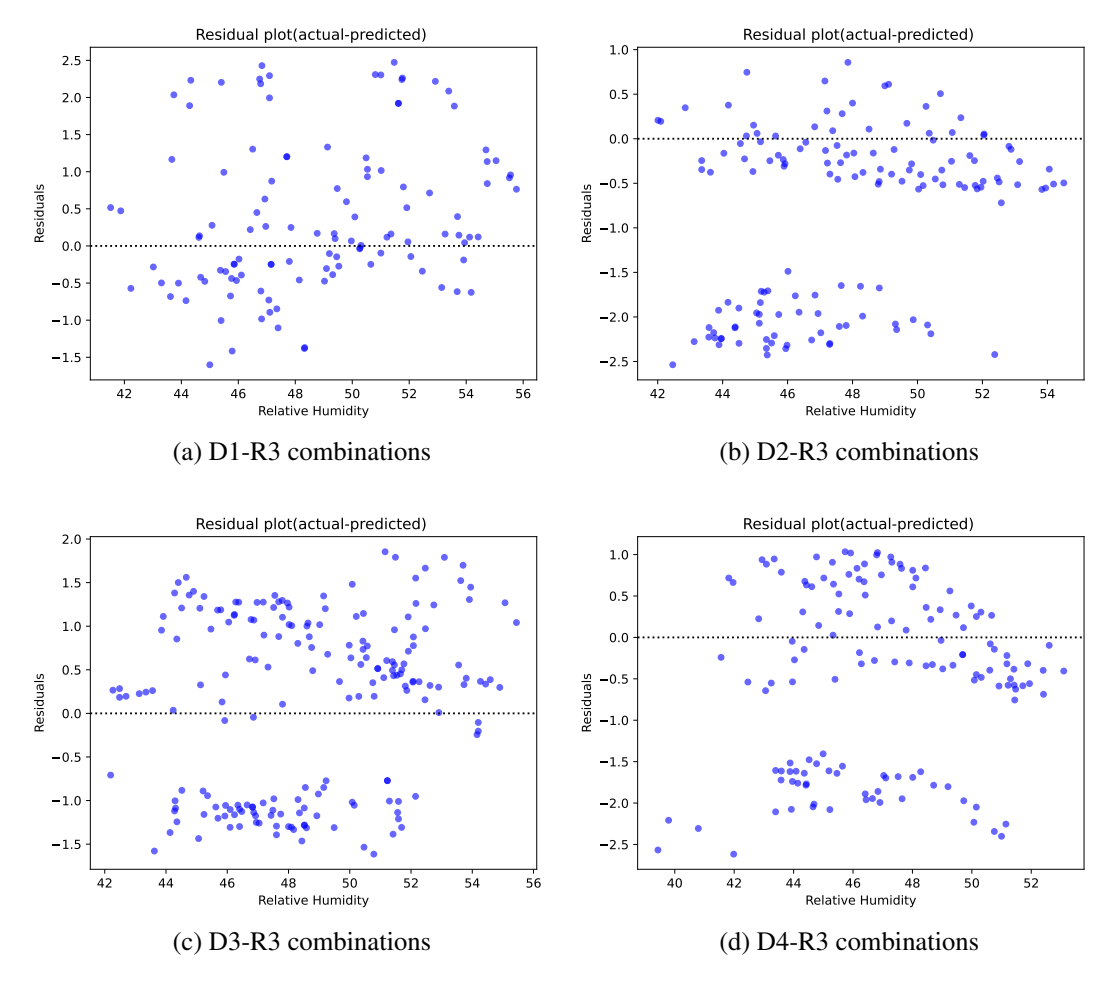


Figure 5.11: The residual scatter plots for unseen dataset and using proposed model. D1-D4 represent distances of 100, 200, 300, and 400 cm respectively. R3 represents the ranges of input and output variables as shown in Table 5.1

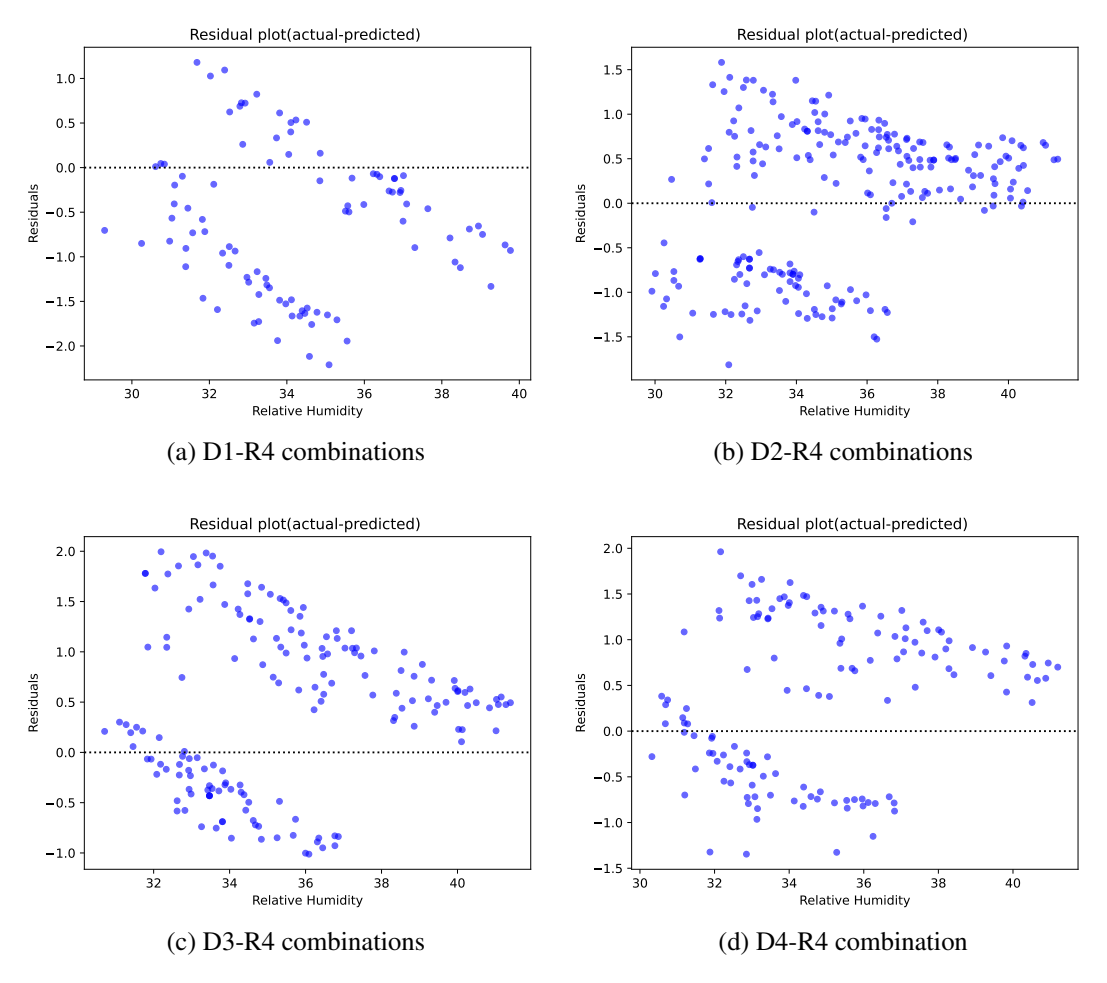


Figure 5.12: The residual scatter plots for unseen dataset and using the proposed model. D1-D4 represent distances of 100, 200, 300, and 400 cm respectively. R4 represent the ranges of input and output variables as shown in Table 5.1

Table 5.5: Performance comparison of proposed hybrid ANN model on unseen dataset for different ranges of temperature and humidity for different distances

ANN	RMSE	MAE	MAPE	R-values
D1_R1	1.51	1.33	1.71	0.93
D1_R2	1.07	0.73	1.20	0.98
D1_R3	1.08	0.82	1.73	0.96
D1_R4	1.02	0.84	2.41	0.95
D2_R1	1.33	1.23	1.58	0.93
D2_R2	1.36	1.21	2.04	0.96
D2_R3	1.30	0.96	1.99	0.95
D2_R4	0.80	0.71	2.06	0.96
D3_R1	2.04	1.81	2.34	0.92
D3_R2	1.26	1.08	1.86	0.98
D3_R3	1.01	0.92	1.90	0.95
D3_R4	0.93	0.78	2.26	0.96
D4_R1	1.42	1.30	1.67	0.93
D4_R2	1.14	0.99	1.71	0.97
D4_R3	1.17	0.94	2.00	0.94
D4_R4	0.92	0.81	2.37	0.95

5.6 Conclusions

In this study, we propose a two-phase fuzzy-neural network approach to estimate the relative humidity of the air medium. The principle of the proposed model or framework was to develop a fuzzy inference system for deriving the relative humidity range based on the temperature and speed of sound. The speed of sound is measured from the time of flight and the distance between the ultrasonic sensor and the reflecting object. As the fuzzy system cannot directly predict the relative humidity of the air medium, it only defines membership functions to represent the output. We determined and trained four backpropagation neural networks based on the output membership function ranges to estimate the relative humidity. The hybrid model consisting of the fuzzy inference system and a neural network can estimate the relative humidity with lesser uncertainty and measurement error. We compared the results of the hybrid neural network model with other machine learning models such as

SVM, KNN, and RFR. The performances of all the machine learning models are compared based on a repeated 10-fold cross-validation procedure and statistical significance test. The reliability of the fuzzy-neural approach was evaluated via RMSE, MAE, MAPE, and R-values between model predictions and experimental results. It is observed that the proposed model outperforms the other machine learning models. Experimental results showed that the developed fuzzy-neural framework could accurately estimate the relative humidity compared to other well-known machine learning models.

CHAPTER 6

Material classification using ultrasonic echo envelope signal

Ultrasonic sensors are frequently used for non-contact range measurements and proximity detection in application areas such as mobile robot navigation and autonomous vehicles. This ultrasonic signal can also be used to recognize and categorize targets or materials. The shape of ultrasonic echo envelope signal contains a significant amount of information. Material identification plays an important role in robotic applications. This information helps robots to detect the material and comply with its behavior accordingly. In this chapter, a machine learning-based technique to classify a few types of materials using the reflected ultrasonic echo signal is proposed. The main idea is to use the feature information of reflected signals to accurately classify the materials. To achieve this classification task, we apply a convolutional neural network approach to the raw echo signal of non-contact ultrasonic sensors to accurately detect and classify materials.

6.1 Introduction

Ultrasonic sensors are widely used for detection tasks and environment perception. These sensors provide a solution to the problems of autonomous mobile robot navigation, mapping, detection, and localization tasks [3, 7]. Ultrasonic sensors have advantages over other sensing techniques because of their low-cost, ease of implementation, low bandwidth for data processing, safe, and are not affected by light. However, the disadvantages of ultrasonic sensors are poor response in presence of electronic noise and environmental

attenuation. Environmental temperature and humidity are the major parameters that affect sensor characteristics. Material information is useful when objects are similar structures and indistinguishable only based on vision. The ultrasonic signal is influenced by the characteristics of the target material. Both the distance and the strength of the reflected echo ultrasonic signal play an important role in characterizing materials accurately, which helps the robot to move seamlessly. Therefore, highly accurate material identification is essential for mobile robot navigation. Classification using conventional machine learning techniques needed multiple sequential steps namely; feature extraction, feature selection, model learning, and classification. Moreover, the performance of machine learning techniques is mostly affected by feature selection. Auto feature extraction is an important characteristic of the CNN model compared to other conventional machine learning techniques [23, 127]. In this work, we use the raw echo envelop signal for the CNN model without any extra feature extraction module

A single ultrasonic sensor can classify four targets (e.g. edge, plan, small cylinder, and corner) in indoor environments [128]. A multi-transducer pulse-echo ranging system is used to differentiate between a plane or a right angle corner [129]. An array of ultrasonic sensors with an artificial neural network is used to detect and classify the different types of objects [130]. Classification of ten different materials using different classification algorithms based on capacitive proximity sensor signal is discussed in [131]. A fuzzy ARTMAP neural network classification system is used to recognize objects at varying distances using ultrasonic echo signal [132]. The raw ultrasonic signal is used to classify various objects by implementing different machine learning algorithms [133]. A novel method for the classification of objects and recognizing the properties of materials such as texture and density information by considering the reflected echo signal is proposed in [134]. In [135] Echo envelope signals are used to locate the object and identify the object using the features of the echo signal. An algorithm is proposed in [136] for distance measurements as well as object identification using the reflected echo of the ultrasonic transducers. A neural

network approach to recognize the object using the features extracted from the echo signal is proposed in [137]. A combination of an array of ultrasonic sensors together with a neural network algorithm is proposed to identify the shape and size of an object in a non-contact manner [138]. In [139], authors have discussed ultrasonic-based detection and identification of objects for robotic applications. Ultrasonic sensor combined with multi-layer perception model to classify different objects [140]. In [141], echo signal feature information is used to identify objects helps to develop ultrasonic mobility aid to assist blind people.

In all the above-discussed work, the methodology includes feature extraction as a preprocessing step. The accuracy of the models is also not that good. In this work, we propose a 1-D CNN model for the classification of five different materials such as glass, steel, wood, cloth, and sponge using the raw ultrasonic echo signal. The remainder of the chapter is organized as follows: Section 6.2 describes the overview of ultrasonic time domain signal processing and covers the detailed architecture of convolutional neural networks. Section 6.3 provides the details of the proposed method used in this work and also describes the network parameters. Section 6.4 describes the experimental setup and procedure for data collection. Section 6.5 presents the results of the experiment to explain the effectiveness of the proposed method. Finally, Section 6.6 summarizes and concludes the work with future research scope.

6.2 Background

Ultrasonic measurements are based on calculation of the time of flight. In addition to range measurement, echo signal contain significant information which can be used for object identification and material classification. The echo waveform ultrasonic signal in time domain can be converted into frequency by using Fast Fourier Transform (FFT). The raw signal of ultrasonic sensor can be processed using time and also frequency domain analysis as shown in Figure 6.1.

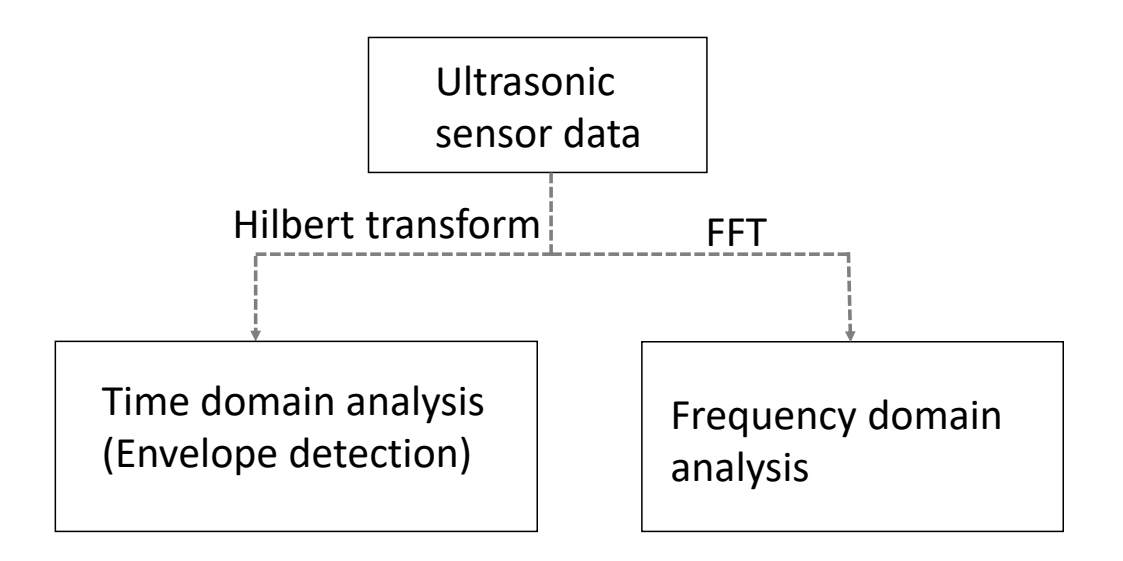


Figure 6.1: Ultrasonic signal processing steps

The time-domain signal is the raw data form of ultrasonic sensor. The envelope contained in the raw ultrasonic signal can be extracted using Hilbert transform [142, 143]. In time domain the envelope of a signal represents the amplitude of the signal. Envelope is the extreme peak points in the waveform within which the signal is contained. The raw signal fed into the Hilbert transform to create analytical signal which helps to determine the envelope of the signal as shown in Figure 6.2. The standard procedure to calculate the envelope from a raw input signal described in Algorithm 1. In time domain the amplitude of the received echo signal is an envelope which starts from baseline reaches to a peak and then back to baseline of the signal.

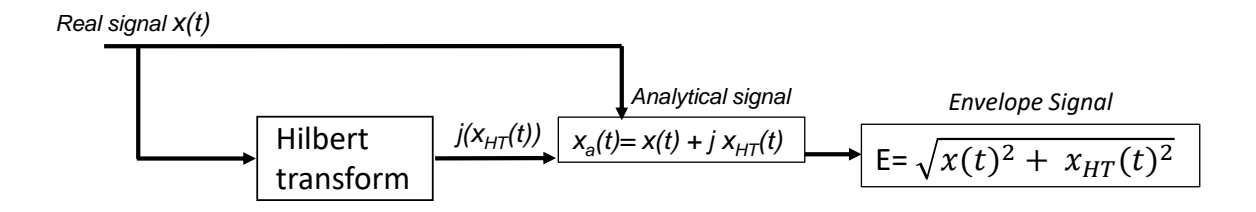


Figure 6.2: Hilbert transform block diagram

```
Algorithm 5 Standard procedure for envelope detection
INPUT: echoSignal

OUTPUT: envelope

peakarray ← []

baseline ← average (echo signal)

for index, value in echoSignal do

if value > baseline then

peakarray.push(index)

return peakarray
```

6.2.1 Hilbert transform

The Hilbert Transform (HT) technique is used for analysis of a variety of non-stationary signal and image processing applications. An analytical signal is the complex-valued representation of real-valued signal. Hilbert transform is used to determine the amplitude envelope of a signal as shown in the Figure 6.3. The essential role of Hilbert transform is to filter out the negative frequency components from the raw input signal without disturbing the phase value. The applications of HT includes biomedical, ultrasonic, radar, and speech recognition system.

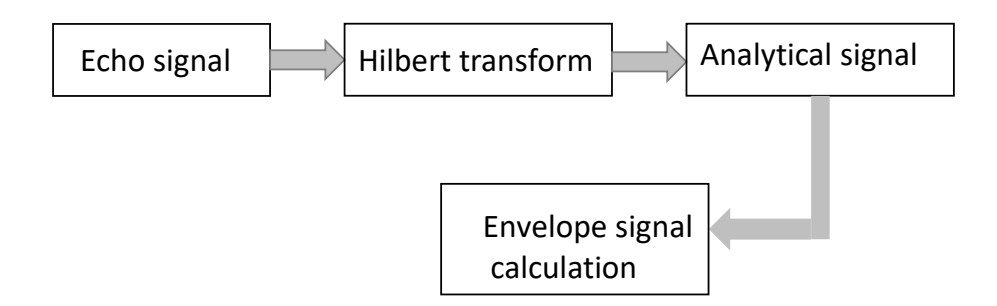


Figure 6.3: Steps involved in calculation of envelope signal using Hilbert transform

The Hilbert transform is defined as follows if y(t) is a original echo signal:

$$h(t) = H\{y(t)\} = \frac{1}{\Pi} \int_{-\infty}^{\infty} \frac{y(\tau)}{t - \tau} d\tau = y(t) * \frac{1}{\pi t}$$
 (6.1)

The input signal y(t) serves as the real component of the input signal, while its Hilbert transform, h(t), serves as the imaginary part, as shown in the following:

$$y_a(t) = y(t) + jh(t)$$
(6.2)

where, $y_a(t)$ is the analytical signal.

The envelope E(t) of the input signal is calculated as follows:

$$E(t) = |y(t) + jh(t)| = \sqrt{y^2(t) + h^2(t)}$$
(6.3)

$$phase(\Phi) = \arctan\left(\frac{h(t)}{y(t)}\right)$$
 (6.4)

In this work, we attempt to differentiate five different materials using ultrasonic echo signal. Hilbert transform is used to calculate the amplitude envelope of the raw ultrasonic signal. Figure 6.4 depicts the ultrasonic echo envelope estimation using Hilbert transform.

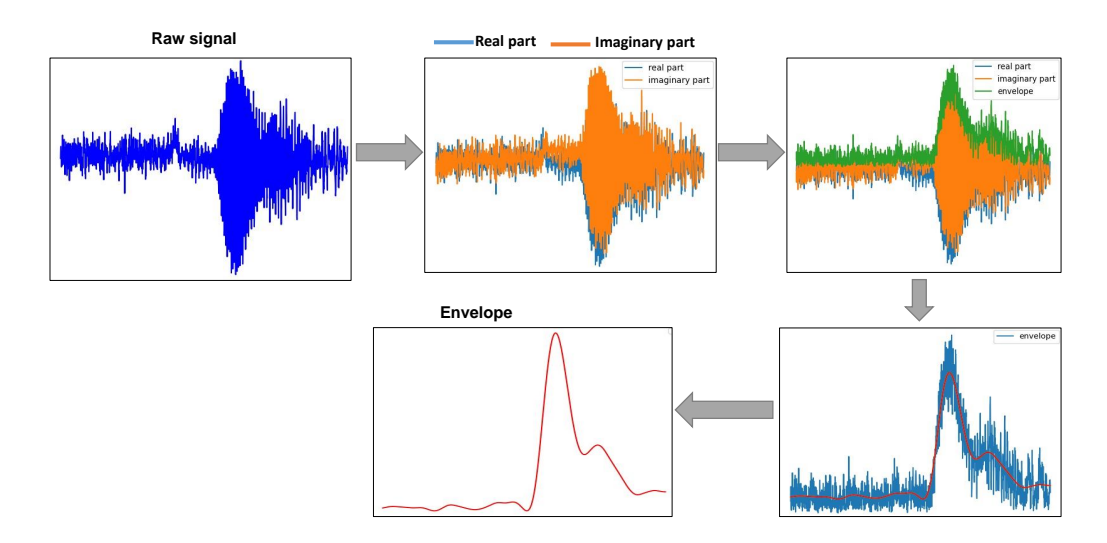


Figure 6.4: The process of extraction of envelope from raw signal using Hilbert transform

The five different materials considered in this experiment are cloth, glass, metal plate, sponge, and wood. We filtered out the dc offset from the signal before applying Hilbert transform. The reflected ultrasonic echo signal from these materials are recorded and fed into the Hilbert transform. The envelopes extracted using Hilbert transform is shown in the Figure 6.5. It is observed from the envelop signals the materials are distinguishable.

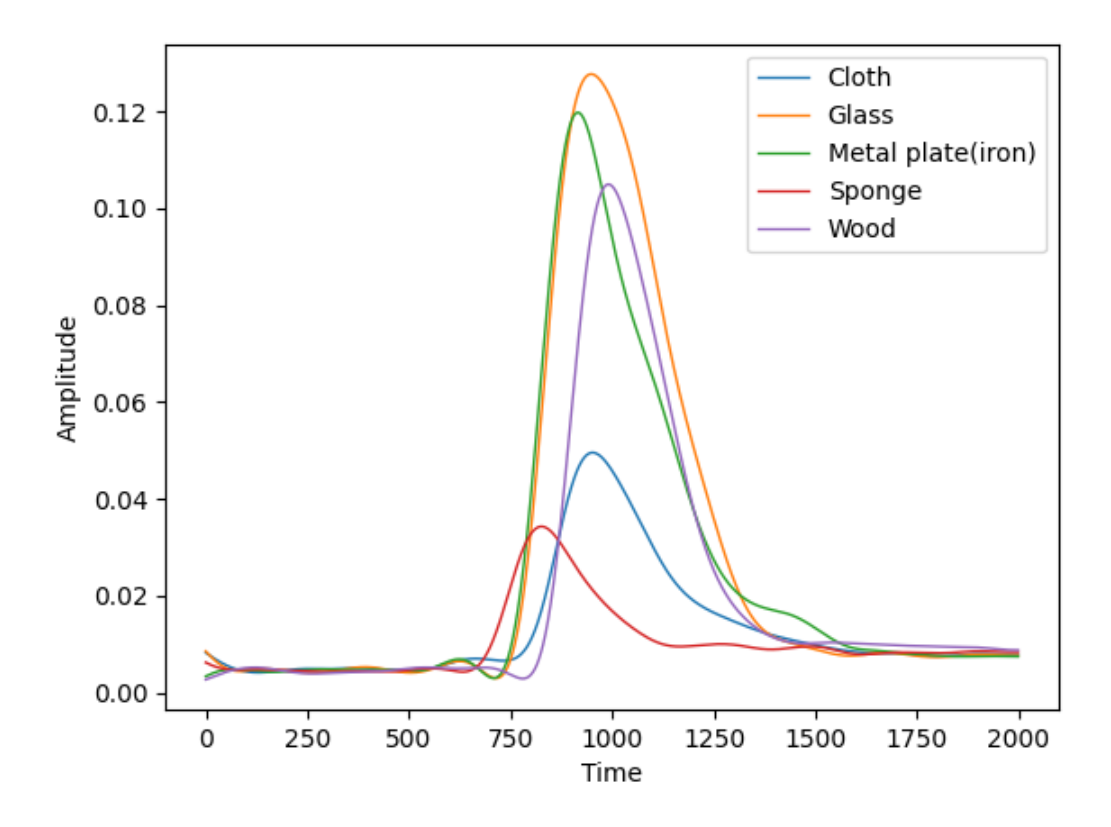


Figure 6.5: Envelope signals for five different class of materials

6.2.2 Convolutional Neural Network (CNN) model

Convolutional neural networks are a type of artificial neural network specifically designed for image classification tasks[23, 127, 144, 145, 146]. They are inspired by the structure and function of the visual cortex in the human brain, which is responsible for processing visual stimuli.

CNNs are composed of multiple layers of interconnected neurons, with each layer responsible for extracting a specific set of features from the input data. The layers at the

beginning of the network typically consist of convolutional layers, which apply a set of filters to the input data to detect various features, such as edges, corners, and patterns. These features are then passed through pooling layers, which reduce the size of the feature map and reduce the computational complexity of the network. The final layers of a CNN are typically fully connected layers, which combine the features extracted by the convolutional and pooling layers to make a final prediction. CNNs are effective at image classification tasks because they can automatically learn and extract the relevant features from the input data, rather than requiring manual feature extraction by the user.

In addition to image classification, CNNs are also used in other applications such as object detection, signal classification, semantic segmentation, and natural language processing. They are widely used in a variety of fields due to their ability to automatically learn useful features from data and their effectiveness at solving complex tasks.

Convolution layer

In a CNN model, a convolutional layer is a type of layer that applies a set of filters to the input data to detect various features, such as edges, corners, and patterns. The filters are small matrices (also known as kernels or weights) that are used to apply a convolution operation to the input data. The convolution operation involves element-wise multiplication of the filter matrix with a small region of the input data (also known as the receptive field), followed by a summation of all elements of the matrix. This process is repeated for every location in the input data, resulting in a feature map that represents the presence of the features detected by the filter.

Convolutional layers are typically followed by non-linear activation functions, such as the ReLU (Rectified Linear Unit) function, which introduces non-linearity to the network and allows it to learn more complex features. The number of filters applied in a convolutional layer is a hyperparameter that can be tuned to control the complexity of the model. Convolutional layers are an important part of the architecture of CNNs and play a key role

in the ability of the network to extract useful features from the input data and perform well on tasks such as image classification and object detection.

Pooling layer

In a convolutional neural network (CNN), a pooling layer is a type of layer that reduces the size of the feature map produced by the convolutional layers by down-sampling the data. Pooling is typically applied after a convolutional layer to reduce the computational complexity of the network and to introduce some degree of spatial invariance, which means that the network is less sensitive to the exact position of features in the input data.

There are several types of pooling layers, but the most common ones are max pooling and average pooling. In max pooling, the output of the pooling layer is the maximum value of the input region. In average pooling, the output is the average of the input region. The size of the pooling region and the stride (the number of pixels to move the pooling window at each step) are hyperparameters that can be tuned to control the complexity of the model and the size of the feature map. Pooling layers are typically followed by additional convolutional layers and fully connected layers in the architecture of a CNN.

Activation function

An activation function is a function that is applied to the output of a neuron in an artificial neural network to determine the output of the neuron and to introduce non-linearity to the network. Activation functions are an important part of the architecture of neural networks and are used to model complex relationships in the data. Activation functions are an important component of the architecture of neural networks and can have a significant impact on the performance of the model. Choosing the right activation function for a particular task can be an important factor in the success of the model.

There are many different types of activation functions, each with its properties and characteristics. In this work, we use ReLU and SoftMax activation functions.

Rectified Linear Unit (ReLU): The ReLU activation function is a type of activation function that maps all negative values to 0 and all positive values to the same value. It is defined as:

$$f(x) = max(0, x)$$

Where max(0, x) returns the maximum of 0 and x.

The ReLU function is simple to compute and has been shown to be effective in many applications. It is often used in the hidden layers of a neural network, where it can introduce non-linearity to the network and allow it to learn more complex features. However, the ReLU function has a number of limitations, including the fact that it can suffer from the "dying ReLU" problem, where a large number of neurons become inactive and do not contribute to the prediction. This can be mitigated by using variants of the ReLU function, such as the leaky ReLU function, which allows a small gradient when the input is negative.

SoftMax: The softmax activation function is a type of activation function that is commonly used in the output layer of a neural network for classification tasks. It maps a vector of real-valued inputs to a vector of values between 0 and 1 that sum to 1, allowing the outputs to be interpreted as probabilities. The softmax function is defined as:

$$f(x) = (\exp(x_i)) / \left(\sum_{i=1}^{n} \exp(x_i)\right)$$
(6.5)

Where x is a vector of inputs, x_i is the i^{th} element of the vector, and n is the number of elements in the vector.

The softmax function is often used in the output layer of a neural network for classification tasks, where it can provide a probability distribution over the possible classes. However, the softmax function has a number of limitations, including the fact that it can be computationally expensive to compute and can suffer from numerical instability when the inputs are very large or very small. In recent years, other activation functions, such as the sigmoid function, have been proposed as alternatives to the softmax function for

classification tasks.

Fully connected layer: A fully connected layer, also known as a dense layer, is a type of layer in a neural network that is composed of neurons that are connected to all the neurons in the preceding layer. In other words, each neuron in a fully connected layer receives input from every neuron in the previous layer and produces an output that is passed to every neuron in the next layer.

A fully connected layer can be thought of as a multi-layer perceptron, where the neurons in the layer are connected to all the neurons in the preceding layer and are fully connected to the next layer. Fully connected layers are often used in the hidden layers of a neural network, where they can learn complex features from the input data. However, they can be computationally expensive to train and can suffer from overfitting if they have too many parameters. In recent years, other types of layers, such as convolutional layers and recurrent layers, have become popular for certain types of tasks due to their improved training performance and ability to learn more complex features.

Loss functions minimization

A loss function is a function that measures the performance of a machine learning model on a given task. It quantifies the difference between the predicted output of the model and the true output, and is used to optimize the model by adjusting the model's parameters to minimize the loss.

There are many different types of loss functions, and the choice of loss function depends on the task at hand. In this work we use cross entropy loss function.

Cross Entropy (CE): Cross-entropy loss is a loss function that is used for classification tasks, and is defined as the negative log likelihood of the true class. It is given by:

$$Loss = -\sum_{i=1}^{n} y_i \log y_{pred,i}$$
 (6.6)

Where y is the true class (represented as a one-hot vector), y_{pred} is the predicted probability distribution over the classes, and the summation is over all classes.

The cross-entropy loss function measures the difference between the predicted probability distribution and the true probability distribution for the classes. It is used to optimize the model by minimizing the loss, which means that the model learns to predict the true class with high probability. The cross-entropy loss function has a number of advantages over other loss functions, including the fact that it is easy to compute and is well-suited for classification tasks with a large number of classes. However, it can be sensitive to the scale of the predictions and can be affected by imbalanced class distributions. In some cases, other loss functions, such as the hinge loss or the focal loss, may be more appropriate for a given task.

Regularization in CNN

Regularization is a technique that is used to prevent overfitting in machine learning models by adding a penalty term to the loss function. The goal of regularization is to encourage the model to learn a simpler, more generalized solution, rather than a complex, overfitted solution.

Regularization can be an effective tool for improving the generalization performance of machine learning models, but it is important to find the right balance between model complexity and regularization strength. Too much regularization can lead to underfitting, while too little regularization can lead to overfitting.

There are several types of regularization techniques that are commonly used in machine learning. In this work we use dropout regularization.

Dropout regularization: Dropout regularization is a technique that is used to prevent overfitting in machine learning models by randomly setting a portion of the model weights to zero during training. The goal of dropout regularization is to encourage the model to learn a simpler, more generalized solution, rather than a complex, overfitted solution. In

practice, dropout regularization is implemented by randomly setting a certain percentage of the model weights to zero at each training iteration. For example, if the dropout rate is set to 0.5, then on average 50% of the weights will be set to zero at each training iteration. This has the effect of preventing the model from relying too heavily on any one feature, and can be useful for improving the generalizability of the model.

Dropout regularization is typically used in neural networks, and can be applied to any layer of the network. It is a simple and effective way to reduce overfitting, and can be used in combination with other regularization techniques, such as L1 or L2 regularization. One of the key benefits of dropout regularization is that it is easy to implement and does not require any additional computational resources. However, it can be less effective at preventing overfitting than other regularization techniques, such as L1 or L2 regularization, and it may require careful tuning of the dropout rate to achieve good results.

Gradient descent

Gradient descent is an optimization algorithm that is used to minimize the loss function of a machine learning model. It works by iteratively adjusting the model's parameters in the direction that reduces the loss.

In each iteration of the algorithm, the model's parameters are updated according to the following formula:

$$w_i = w_i - \alpha \frac{\partial L}{\partial w_i} \tag{6.7}$$

Where L is the loss function, w_i is the i^{th} parameter of the model, and α is the learning rate. The learning rate determines the size of the update to the parameters in each iteration.

The partial derivative $\frac{\partial L}{\partial w_i}$ represents the slope of the loss function with respect to the i^{th} parameter. It tells us how the loss changes as we adjust the i^{th} parameter. The sign of the derivative indicates the direction in which the loss is decreasing, and the magnitude of

the derivative indicates the rate of change.

There are several types of gradient descent algorithms, including:

Adaptive gradient descent algorithm: Adaptive gradient descent is an optimization algorithm that is used to minimize the loss function of a machine learning model. It works by iterative adjusting the model's parameters in the direction that reduces the loss.

In each iteration of the algorithm, the model's parameters are updated according to the following formula:

$$w_i = w_i - \alpha \frac{\partial L}{\partial w_i} \tag{6.8}$$

where L is the loss function, W_i is the i^{th} parameter of the model, and $\frac{\partial L}{\partial W_i}$ is the gradient of the loss function with respect to the i^{th} parameter.

The learning rate α is not a fixed value in adaptive gradient descent but is instead adjusted based on the gradient of the loss function with respect to the parameters. This can help the algorithm to converge more quickly, as it adjusts the learning rate based on the difficulty of the optimization problem.

Adaptive gradient descent algorithms continue to iterate over the entire dataset until the loss function converges to a minimum value, or until a maximum number of iterations is reached.

There are several variants of adaptive gradient descent, including:

- Adaptive Gradient Algorithm (Adagrad): This method adjusts the learning rate based
 on the sum of the squares of the gradients of the loss function with respect to the
 parameters. It can be effective when the gradients have different scales.
- Adadelta: This method adjusts the learning rate based on the average of the squares
 of the gradients of the loss function with respect to the parameters over a moving
 window. It does not require the specification of a learning rate.
- Adam (Adaptive Moment Estimation): This method adjusts the learning rate based on

the exponentially weighted average of the gradients of the loss function with respect to the parameters and an exponentially weighted average of the squares of the gradients. It also includes bias correction terms to improve the performance when the data is sparse.

In this work, we use Adam optimization algorithm. Adam combines the benefits of two other stochastic gradient descent extensions and the adaptive gradient algorithm to improve performance.

6.3 Method

Here, We developed a 1-D CNN model for ultrasonic signal classification. The input to the model is a frame of 1999 features. Hence, each frame size is 1999 and a total of 600 such frames are there. There is a total of five class labels used in this model. We created two different datasets with sizes of 600 for training and 130 for testing. The one-hot encoder is used for encoding each data point before sending it to the model. The first two layers have 16 features of an 8 kernel size and a stride of 2 with the same padding. Then after a max pool layer of size 2 followed by two convolution layers of 64 features of each kernel size 4 and a stride of 2 with the same padding. This is followed by a max-pooling layer of the size 2, which is same as the previous layer. Then there are 2 convolution layers of kernel size 4 and 256 features and a max pool layer of size 2. After that, there are 2 convolution layers and a max pool layer. Each has 512 features of 2 kernel sizes with the same padding and a stride of 2. In all the convolution layers we used ReLu as our activation function. After the stack of convolution and max-pooling layer, There is a Global Average Pooling of size 512 and dropout of 0.3. After that, there is the dense layer (fully connected) of size 5 with the activation function SoftMax. Here, we used categorical cross entropy for the loss function and Adam for the optimizer. We used batch size as 20 and the number of epochs as 20. The proposed 1-D CNN architecture is shown in the Figure 6.7. The detailed parameters for training and validation of the model are described in Table 6.1.

The overall system flow of this work is shown in the Figure 6.6

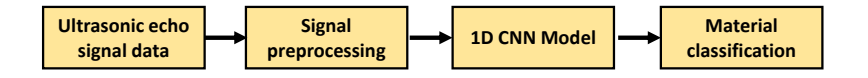


Figure 6.6: System flow of material classification using proposed approach

Table 6.1: Model configuration parameters and the corresponding values

Layers	Configurations	Output Dimensions
Convolution (C1)	16 Filter, 8 Kernel, ReLu	(None, 996, 16)
Convolution (C12)	16 Filter, 8 Kernel, ReLu	(None, 498, 16)
Max Pooling (p1)	2 kernel	(None, 249, 16)
Convolution (C21)	64 Filter, 4 Kernel, ReLu	(None, 125, 64)
Convolution (C21)	64 Filter, 4 Kernel, ReLu	(None, 63, 64)
Max Pooling (p2)	2 kernel	(None, 31, 64)
Convolution (C31)	256 Filter, 4 Kernel, ReLu	(None, 16, 256)
Convolution (C32)	256 Filter, 4 Kernel, ReLu	(None, 8, 256)
Max Pooling (p3)	2 kernel	(None, 4, 256)
Convolution (C41)	512 Filter, 2 Kernel, ReLu	(None, 4, 512)
Convolution (C42)	512 Filter, 2 Kernel, ReLu	(None, 4, 512)
Max Pooling (p4)	2 kernel	(None, 2, 512)
Global Average Pooling	_	(None, 512)
Dropout (D)	0.3	(None, 512)
Dense Layer (FC)	SoftMax	(None, 5)

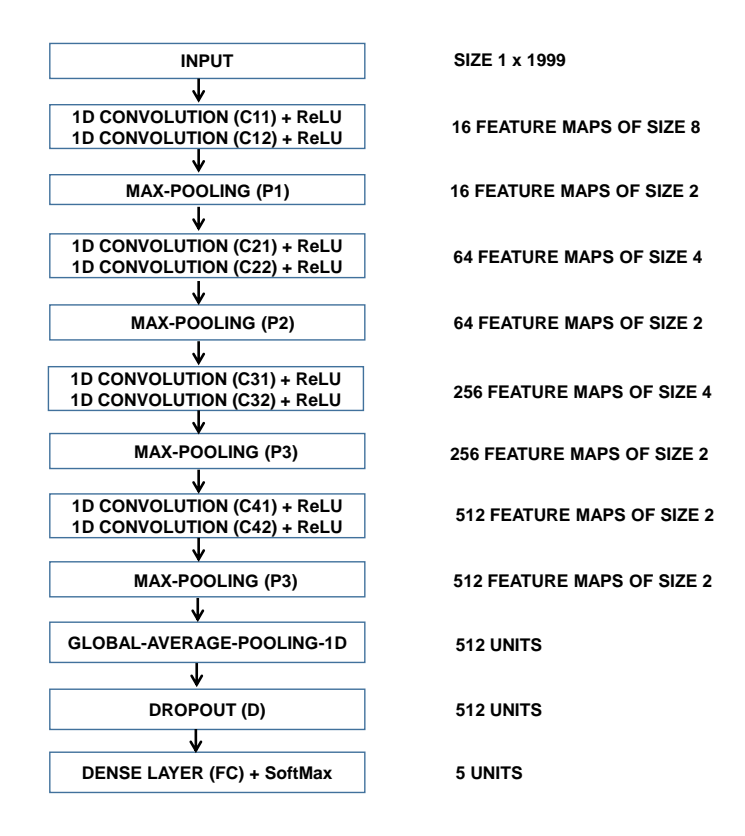


Figure 6.7: Architecture of CNN model

6.4 Experimental setup

We used a 40 kHz ultrasonic sensor for this experiment. The experimental setup consists of an ultrasonic sensor, a micro-controller, and oscilloscope as shown in Figure 6.8. The oscilloscope is used to perform more in-depth investigation of the acquired sensor signal. Moreover, oscilloscope displays and digitizes the interference signals, finally stored on the computer. The sampling rate at which the signal is sampled is 200 MSamples/second which is higher than the nyquist rate of 80 KSamples/second to avoid loss of information. Here, we used five types of materials such as glass, metal plate, wood, cloth, and sponge. The reflected echo signal of the ultrasonic sensor are acquired for all the five materials at different distances. The reflected raw echo signal of the ultrasonic sensor is captured and preprocessed before being used. The final evaluation using an in-house computer program

includes filtering dc-offset removal, classify and display the result.

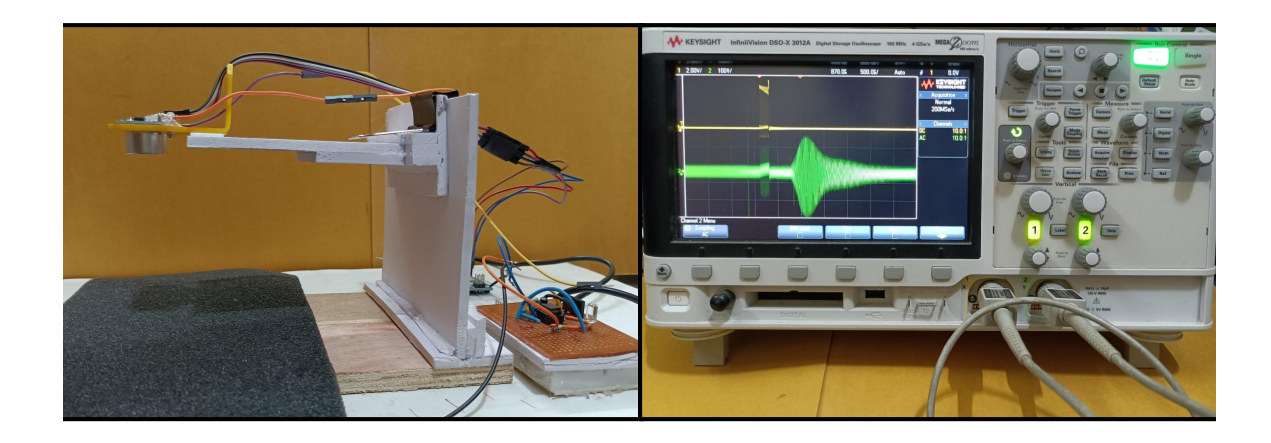


Figure 6.8: Experimental setup

6.5 Results and analysis

The proposed system is trained and validated with 600 data points, we split the dataset into 80-20 and the best model with good accuracy is proposed as shown in the Table 6.2. The model's performance is 98% for training and 95% for validation accuracy. The training and validation loss indicates how the data fit the model. Figure 6.9 (a) shows the progression loss during the training. Figure 6.9 (b) shows how the validation accuracy approaches the intended accuracy after a few epochs.

Here, we use 130 frames for testing purposes. The model can classify this testing data successfully, and out of 130 frames system can classify 126 accurately. We draw a confusion matrix using these test data. From the Confusion matrix, we calculate the accuracy as 96%.

In Figure 6.10 shows the confusion matrix. The number of test instances in each class is 23 (class-1), 21 (class-2), 41 (class-3), 23 (class-4), and 22 (class-5) respectively. The matrix shows few classification errors.

It is observed that in very few cases the data may be misclassified. This is due to the

similar envelope structure of the material class-1 (cloth) and class-4 (sponge). Similarly for material class-2 (glass) and class-3 (metal plate).

Table 6.2: Performance accuracy of training, validation and test

	Size	Accuracy
Training	480	98%
Validation	120	95%
Test	130	96%

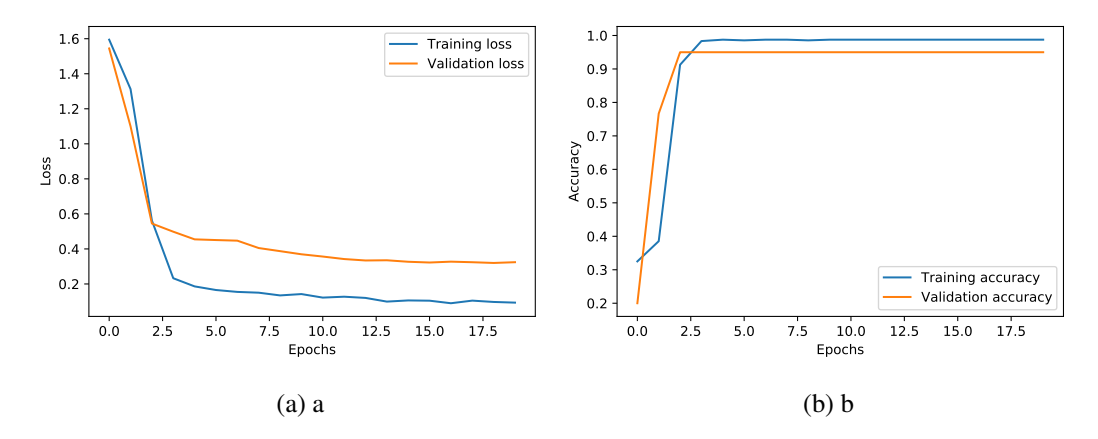


Figure 6.9: (a) Training loss and validation loss of the convolutional neural network versus the number of epochs, (b) Training and validation accuracy of CNN versus number of epochs

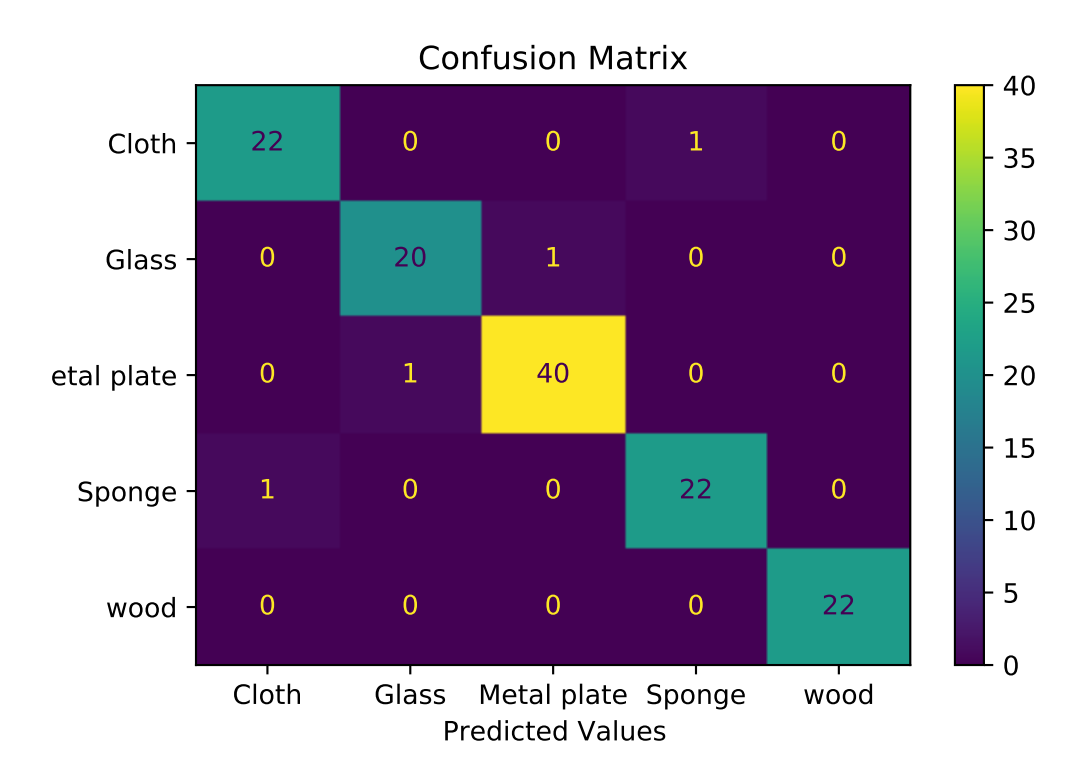


Figure 6.10: Confusion matrix for CNN based material classification using ultrasonic echo envelope signal

6.6 Conclusions

The purpose of this work is to accurately classify the materials using raw ultrasonic echo signal for autonomous mobile robotic applications. The results of this work show that ultrasonic sensors in combination with CNN has a great potential to classify and recognize different materials and objects. In this experiment we consider five different materials for classification. The simple 1-D CNN provides good result for the classification tasks. However, more samples per measurement tends to produce more better result. The proposed CNN based intelligent ultrasonic model can be used for mobile robot navigation. In future work, we will collect as much as material data to train the proposed CNN model to make a more robust classification model. We will also investigate the frequency domain signal in addition to the time domain signal using the proposed method for gesture recognition,

object shape determination, object identification, and various material classification tasks. The combination of ultrasonic sensor data and camera can be fused to detect, recognize, and classify materials in complex scenarios.

REFERENCES

- [1] A. Sharma, V. Sharma, M. Jaiswal, H.-C. Wang, D. N. K. Jayakody, C. M. W. Basnayaka, and A. Muthanna, "Recent Trends in AI-Based Intelligent Sensing," *Electronics*, vol. 11, no. 10, p. 1661, 2022.
- [2] M. Parrilla, J. Anaya, and C. Fritsch, "Digital signal processing techniques for high accuracy ultrasonic range measurements," *IEEE Transactions on Instrumentation and Measurement*, vol. 40, no. 4, pp. 759–763, 1991.
- [3] K. Mizutani, N. Wakatsuki, and T. Ebihara, "Introduction of measurement techniques in ultrasonic electronics: Basic principles and recent trends," *Japanese Journal of Applied Physics*, vol. 55, no. 7S1, p. 07KA02, 2016.
- [4] A. Rocchi, E. Santecchia, F. Ciciulla, P. Mengucci, and G. Barucca, "Characterization and optimization of level measurement by an ultrasonic sensor system," *IEEE Sensors Journal*, vol. 19, no. 8, pp. 3077–3084, 2019.
- [5] A. Egana, F. Seco, and R. Ceres, "Processing of ultrasonic echo envelopes for object location with nearby receivers," *IEEE Transactions on Instrumentation and Measurement*, vol. 57, no. 12, pp. 2751–2755, 2008.
- [6] A. L. Bowler, M. P. Pound, and N. J. Watson, "A review of ultrasonic sensing and machine learning methods to monitor industrial processes," *Ultrasonics*, p. 106776, 2022.
- [7] Z. Qiu, Y. Lu, and Z. Qiu, "Review of ultrasonic ranging methods and their current challenges," *Micromachines*, vol. 13, no. 4, p. 520, 2022.
- [8] P. Mohindru, "Development of liquid level measurement technology: A review," *Flow Measurement and Instrumentation*, p. 102295, 2022.
- [9] K. Santhosh, B. Joy, and S. Rao, "Design of an instrument for liquid level measurement and concentration analysis using multisensor data fusion," *Journal of Sensors*, 2020.
- [10] D. A. Bohn, "Environmental effects on the speed of sound," *Journal of the Audio Engineering Society*, vol. 36, no. 4, pp. 223–231, 1988.
- [11] Y. Huang, Y. Huang, K. Huang, and M.-S. Young, "An accurate air temperature measurement system based on an envelope pulsed ultrasonic time-of-flight technique," *Review of Scientific Instruments*, vol. 78, no. 11, p. 115102, 2007.
- [12] T. Motegi, K. Mizutani, and N. Wakatsuki, "Simultaneous measurement of air temperature and humidity based on sound velocity and attenuation using ultrasonic probe," *Japanese Journal of Applied Physics*, vol. 52, no. 7S, p. 07HC05, 2013.

- [13] D.-H. Kim, S.-R. Lee, and C.-Y. Lee, "Material classification using reflected signal of ultrasonic sensor," *Journal of Institute of Control, Robotics and Systems*, vol. 12, no. 6, pp. 580–584, 2006.
- [14] E. Powner and F. Yalcinkaya, "Intelligent sensors: structure and system," *Sensor Review*, 1995.
- [15] G. Kang and S.-C. Kim, "Deepecho: Echoacoustic recognition of materials using returning echoes with deep neural networks," *IEEE Transactions on Emerging Topics in Computing*, 2020.
- [16] M. J. McGrath and C. N. Scanaill, *Sensing and Sensor Fundamentals*. Berkeley: Apress, 2013.
- [17] C. M. Bishop and N. M. Nasrabadi, *Pattern recognition and machine learning*. Springer, 2006.
- [18] J. Han, M. Kamber, and J. Pei, "Data mining: Concepts and and techniques," *Techniques (3rd ed), Morgan Kauffman*, 2012.
- [19] K. Hornik, "Approximation capabilities of multilayer feedforward networks," *Neural networks*, vol. 4, no. 2, pp. 251–257, 1991.
- [20] K. Hornik, M. Stinchcombe, and H. White, "Multilayer feedforward networks are universal approximators," *Neural networks*, vol. 2, no. 5, pp. 359–366, 1989.
- [21] V. Vapnik, S. E. Golowich, A. Smola, *et al.*, "Support vector method for function approximation, regression estimation, and signal processing," *Advances in neural information processing systems*, pp. 281–287, 1997.
- [22] L. Breiman, "Random forests," *Machine Learning*, vol. 45(1), pp. 5 32, 2001.
- [23] N. Buduma, N. Buduma, and J. Papa, *Fundamentals of deep learning*. "O'Reilly Media, Inc.", 2022.
- [24] K. S. Ojha, T. J. Mason, C. P. O'Donnell, J. P. Kerry, and B. K. Tiwari, "Ultrasound technology for food fermentation applications," *Ultrasonics sonochemistry*, vol. 34, pp. 410–417, 2017.
- [25] K. Nakamura et al., Ultrasonic transducers. Woodhead publishing Oxford, UK:, 2012.
- [26] K. Attenborough, "Sound propagation in the atmosphere," *Handbook of noise and vibration control*, pp. 67–78, 2008.
- [27] C. M. Harris, "Absorption of sound in air versus humidity and temperature," *The Journal of the Acoustical Society of America*, vol. 40, no. 1, pp. 148–159, 1966.

- [28] G. S. Wong and T. F. Embleton, "Variation of the speed of sound in air with humidity and temperature," *The Journal of the Acoustical Society of America*, vol. 77, no. 5, pp. 1710–1712, 1985.
- [29] L. C. Lynnworth, *Ultrasonic measurements for process control: theory, techniques, applications*. Academic press, 2013.
- [30] D. P. Massa, "Choosing an ultrasonic sensor for proximity or distance measurement part 1: Acoustic considerations," *SENSORS-PETERBOROUGH*, vol. 16, pp. 34–37, 1999.
- [31] K. Attenborough, "Sound propagation in the atmosphere," in *Springer handbook of acoustics*, pp. 117–155, Springer, 2014.
- [32] H. E. Bass, L. C. Sutherland, A. J. Zuckerwar, D. T. Blackstock, and D. Hester, "Atmospheric absorption of sound: Further developments," *The Journal of the Acoustical Society of America*, vol. 97, no. 1, pp. 680–683, 1995.
- [33] A. K. Sahoo and S. K. Udgata, "A Novel ANN-Based Adaptive Ultrasonic Measurement System for Accurate Water Level Monitoring," *IEEE Transactions on Instrumentation and Measurement*, vol. 69, no. 6, pp. 3359–3369, 2020.
- [34] A. Carullo and M. Parvis, "An ultrasonic sensor for distance measurement in automotive applications," *IEEE Sensors Journal*, vol. 1, no. 2, pp. 143–147, 2001.
- [35] S. Milligan, H. Vandelinde, and M. Cavanagh, *Understanding Ultrasonic Level Measurement*. Momentum Press, 2013.
- [36] J. Schnake, "Liquid Level Measurement-Basics 101 part-2," *Endress+Hauser White Paper*, 2006.
- [37] U. Grimaldi and M. Parvis, "Noise-tolerant ultrasonic distance sensor based on a multiple driving approach," *Measurement*, vol. 15, no. 1, pp. 33–41, 1995.
- [38] D. Marioli, C. Narduzzi, C. Offelli, D. Petri, E. Sardini, and A. Taroni, "Digital time-of-flight measurement for ultrasonic sensors," *IEEE Transactions on Instrumentation and Measurement*, vol. 41, no. 1, pp. 93–97, 1992.
- [39] M. Greenspan, "Comments on "speed of sound in standard air" [j. acoust. soc. am. 7 9, 1359–1366 (1986)]," *The Journal of the Acoustical Society of America*, vol. 82, no. 1, pp. 370–372, 1987.
- [40] W. Van Schaik, M. Grooten, T. Wernaart, and C. Van Der Geld, "High accuracy acoustic relative humidity measurement induct flow with air," *Sensors*, vol. 10, no. 8, pp. 7421–7433, 2010.
- [41] C. Canali, G. De Cicco, B. Morten, M. Prudenziati, and A. Taroni, "A temperature compensated ultrasonic sensor operating in air for distance and proximity measurements," *IEEE Transactions on Industrial Electronics*, vol. IE-29, no. 4, pp. 336–341, 1982.

- [42] J. Terzic, C. Nagarajah, and M. Alamgir, "Fluid level measurement in dynamic environments using a single ultrasonic sensor and Support Vector Machine (SVM)," *Sensors and Actuators A: Physical*, vol. 161, no. 1, pp. 278–287, 2010.
- [43] M. Mousa, X. Zhang, and C. Claudel, "Flash flood detection in urban cities using ultrasonic and infrared sensors," *IEEE Sensors Journal*, vol. 16, no. 19, pp. 7204–7216, 2016.
- [44] C. Bengtsson, "The engineer's guide to level measurement," *Handbook published by Emerson Process Management*, pp. 30–38, 2013.
- [45] E. Terzic, J. Terzic, R. Nagarajah, and M. Alamgir, "Capacitive sensing technology," in *A Neural Network Approach to Fluid Quantity Measurement in Dynamic Environments*, pp. 11–37, Springer, 2012.
- [46] S. Pal and R. Barik, "Design, development and testing of a semi cylindrical capacitive sensor for liquid level measurement," *Sensors & Transducers*, vol. 116, no. 5, p. 13, 2010.
- [47] M. Z. Aslam and T. B. Tang, "A high resolution capacitive sensing system for the measurement of water content in crude oil," *Sensors*, vol. 14, no. 7, pp. 11351–11361, 2014.
- [48] B. Jin, Z. Zhang, and H. Zhang, "Structure design and performance analysis of a coaxial cylindrical capacitive sensor for liquid-level measurement," *Sensors and Actuators A: Physical*, vol. 223, pp. 84–90, 2015.
- [49] B. Kumar, G. Rajita, and N. Mandal, "A review on capacitive-type sensor for measurement of height of liquid level," *Measurement and Control*, vol. 47, no. 7, pp. 219–224, 2014.
- [50] K. Loizou and E. Koutroulis, "Water level sensing: State of the art review and performance evaluation of a low-cost measurement system," *Measurement*, vol. 89, pp. 204–214, 2016.
- [51] A. Al-Ali, A. Al Nabulsi, S. Mukhopadhyay, M. S. Awal, S. Fernandes, and K. Ailabouni, "Iot-solar energy powered smart farm irrigation system," *Journal of Electronic Science and Technology*, vol. 17, no. 4, p. 100017, 2019.
- [52] S. Marick, S. K. Bera, and S. C. Bera, "A float type liquid level measuring system using a modified inductive transducer," *Sensors & Transducers*, vol. 182, no. 11, p. 111, 2014.
- [53] L. Kučera, B. Patin, T. Gajdošík, R. Palenčár, J. Palenčár, and M. Ujlaky, "Application of metrological approaches in the design of calibration equipment for verification of float level gauges," *Measurement Science Review*, vol. 20, no. 5, pp. 230–235, 2020.
- [54] B. G. Khusainov, "Float method for measuring liquid levels," *Measurement Techniques*, vol. 21, pp. 652–654, May 1978.

- [55] Indumart, Various Techniques of Liquids and Solids Level Measurements, Nov. 2009.
- [56] D. Sengupta, M. Sai Shankar, P. Saidi Reddy, R. Sai Prasad, and K. Srimannarayana, "Sensing of hydrostatic pressure using fbg sensor for liquid level measurement," *Microwave and optical technology letters*, vol. 54, no. 7, pp. 1679–1683, 2012.
- [57] D. Sengupta, M. S. Shankar, P. S. Reddy, R. S. Prasad, and K. Srimannarayana, "An fbg based hydrostatic pressure sensor for liquid level measurements," in *Microstructured and Specialty Optical Fibres*, vol. 8426, pp. 80–84, SPIE, 2012.
- [58] F. D. Maria de Fátima, T. de Brito Paixão, E. F. T. Mesquita, N. Alberto, A. R. Frias, R. A. Ferreira, H. Varum, P. F. da Costa Antunes, and P. S. de Brito Andre, "Liquid hydrostatic pressure optical sensor based on micro-cavity produced by the catastrophic fuse effect," *IEEE Sensors Journal*, vol. 15, no. 10, pp. 5654–5658, 2015.
- [59] L. Schenato, R. Aneesh, L. Palmieri, A. Galtarossa, and A. Pasuto, "Fiber optic sensor for hydrostatic pressure and temperature measurement in riverbanks monitoring," *Optics & Laser Technology*, vol. 82, pp. 57–62, 2016.
- [60] Y. Singh, S. K. Raghuwanshi, and S. Kumar, "Review on liquid-level measurement and level transmitter using conventional and optical techniques," *IETE Technical Review*, vol. 36, no. 4, pp. 329–340, 2019.
- [61] A. G. Leal-Junior, C. Marques, A. Frizera, and M. J. Pontes, "Multi-interface level in oil tanks and applications of optical fiber sensors," *Optical Fiber Technology*, vol. 40, pp. 82–92, 2018.
- [62] C. A. Diaz, A. Leal-Junior, C. Marques, A. Frizera, M. J. Pontes, P. F. Antunes, P. S. Andre, and M. R. Ribeiro, "Optical fiber sensing for sub-millimeter liquid-level monitoring: A review," *IEEE Sensors Journal*, vol. 19, no. 17, pp. 7179–7191, 2019.
- [63] T. Nakagawa, A. Hyodo, K. Kogo, H. Kurata, K. Osada, and S. Oho, "Contactless liquid-level measurement with frequency-modulated millimeter wave through opaque container," *IEEE Sensors Journal*, vol. 13, no. 3, pp. 926–933, 2012.
- [64] X. Lin, L. Ren, Y. Xu, N. Chen, H. Ju, J. Liang, Z. He, E. Qu, B. Hu, and Y. Li, "Low-cost multipoint liquid-level sensor with plastic optical fiber," *IEEE Photonics Technology Letters*, vol. 26, no. 16, pp. 1613–1616, 2014.
- [65] C. Teng, H. Liu, H. Deng, S. Deng, H. Yang, R. Xu, M. Chen, L. Yuan, and J. Zheng, "Liquid level sensor based on a v-groove structure plastic optical fiber," *Sensors*, vol. 18, no. 9, 2018.
- [66] J. Gehring, A. Ferrone, A.-C. Billault-Roux, N. Besic, K. D. Ahn, G. Lee, and A. Berne, "Radar and ground-level measurements of precipitation collected by epfl during the ice-pop 2018 campaign in south-korea," *Earth System Science Data Discussions, in review*, 2020.

- [67] P. Mikuš and R. Hart'anskỳ, "The errors in radar level gauge calibration," *Measurement*, pp. 27–30, 2013.
- [68] M. Vogt, T. Neumann, and M. Gerding, "Frequency-diversity technique for reliable radar level measurement of bulk solids in silos," in *2013 European Radar Conference*, pp. 129–132, IEEE, 2013.
- [69] S. Guan, J. A. Bridge, J. R. Davis, and C. Li, "Compact continuous wave radar for water level monitoring," *Journal of Atmospheric and Oceanic Technology*, 2022.
- [70] P. Devine, *Radar Level Measurement: The User's Guide*. U.K., Burgess Hill: VEGA Controls Ltd, 2000.
- [71] W. Zhang, Z. Ying, S. Yuan, and Z. Tong, "A fiber laser sensor for liquid level and temperature based on two taper structures and fiber bragg grating," *Optics Communications*, vol. 342, pp. 243–246, 2015.
- [72] C. Yuan, P. Gong, and Y. Bai, "Performance assessment of icesat-2 laser altimeter data for water-level measurement over lakes and reservoirs in china," *Remote Sensing*, vol. 12, no. 5, p. 770, 2020.
- [73] S. Xiang, F. Pan, K. Xiang, and X. Wang, "Melt level measurement for the cz crystal growth using an improved laser triangulation system," *Measurement*, vol. 103, pp. 27–35, 2017.
- [74] X. Zhang, D. Liu, S. Wang, X. Zhao, and L. Jiang, "Silicon melt liquid level detection based on improved laser trigonometry," in 2018 37th Chinese Control Conference (CCC), pp. 4169–4173, IEEE, 2018.
- [75] P. Hauptmann, N. Hoppe, and A. Püttmer, "Application of ultrasonic sensors in the process industry," *Measurement Science and Technology*, vol. 13, no. 8, pp. R73–R83, 2002.
- [76] G. Bucci and C. Landi, "Numerical method for transit time measurement in ultrasonic sensor applications," *IEEE Transactions on Instrumentation and Measurement*, vol. 46, no. 6, pp. 1241–1246, 1997.
- [77] J. Terzic, R. Nagarajah, and M. Alamgir, "Accurate fluid level measurement in dynamic environment using ultrasonic sensor and v-svm," *Sensors & Transducers*, vol. 109, no. 10, p. 76, 2009.
- [78] I. Matsuya, Y. Honma, M. Mori, and I. Ihara, "Measuring liquid-level utilizing wedge wave," *Sensors*, vol. 18, no. 1, 2018.
- [79] B. Zhang, Y.-J. Wei, W.-Y. Liu, Y.-J. Zhang, Z. Yao, L. Zhang, and J.-J. Xiong, "A novel ultrasonic method for liquid level measurement based on the balance of echo energy," *Sensors*, vol. 17, no. 4, p. 706, 2017.

- [80] A. Carullo, F. Ferraris, S. Graziani, U. Grimaldi, and M. Parvis, "Ultrasonic distance sensor improvement using a two-level neural-network," *IEEE Transactions on Instrumentation and Measurement*, vol. 45, no. 2, pp. 677–682, 1996.
- [81] E. Terzic, J. Terzic, R. Nagarajah, and M. Alamgir, A neural network approach to fluid quantity measurement in dynamic environments. Springer, 2012.
- [82] V. Magori, "Ultrasonic sensors in air," in 1994 Proceedings of IEEE Ultrasonics Symposium, vol. 1, pp. 471–481 vol.1, 1994.
- [83] M. Brudka and A. Pacut, "Intelligent robot control using ultrasonic measurements," *IEEE Transactions on Instrumentation and Measurement*, vol. 51, no. 3, pp. 454–459, 2002.
- [84] S. Shin, M.-H. Kim, and S. B. Choi, "Ultrasonic distance measurement method with crosstalk rejection at high measurement rate," *IEEE Transactions on Instrumentation and Measurement*, vol. 68, no. 4, pp. 972–979, 2019.
- [85] M. Shen, Y. Wang, Y. Jiang, H. Ji, B. Wang, and Z. Huang, "A new positioning method based on multiple ultrasonic sensors for autonomous mobile robot," *Sensors*, vol. 20, no. 1, p. 17, 2019.
- [86] J. Majchrzak, M. Michalski, and G. Wiczynski, "Distance estimation with a long-range ultrasonic sensor system," *IEEE Sensors Journal*, vol. 9, no. 7, pp. 767–773, 2009.
- [87] X. Zhao, P. Qian, N. Lu, and Y. Li, "Design and experimental study of high precision ultrasonic ranging system," in 2020 5th International Conference on Intelligent Informatics and Biomedical Sciences (ICIIBMS), pp. 8–12, 2020.
- [88] M. Krenik, X. Li, and B. Akin, "Improved tof determination algorithms for robust ultrasonic positioning of smart tools," in *IECON 2014 40th Annual Conference of the IEEE Industrial Electronics Society*, pp. 2351–2356, 2014.
- [89] R. Queirós, F. C. Alegria, P. S. Girao, and A. C. Serra, "A multi-frequency method for ultrasonic ranging," *Ultrasonics*, vol. 63, pp. 86–93, 2015.
- [90] R. Xiang and Z. Shi, "Design of millimeter range high precision ultrasonic distance measurement system," in 2017 International Conference on Computer Systems, Electronics and Control (ICCSEC), pp. 1052–1057, 2017.
- [91] O. Cramer, "The variation of the specific heat ratio and the speed of sound in air with temperature, pressure, humidity, and co2 concentration," *The Journal of the Acoustical Society of America*, vol. 93, no. 5, pp. 2510–2516, 1993.
- [92] F. Ferraris, U. Grimaldi, M. Parvis, and S. Graziani, "A neural network for fast-response ultrasonic distance sensors," in *1993 IEEE Instrumentation and Measure-ment Technology Conference*, pp. 631–635, 1993.

- [93] J. C. for Guides in Metrology, "JCGM 100: Evaluation of Measurement Data Guide to the Expression of Uncertainty in Measurement (GUM)," tech. rep., JCGM, France, 2008.
- [94] H. Coleman and W. Steele, *Experimentation and Uncertainty Analysis for Engineers*. A Wiley Interscience publication, Wiley, 1999.
- [95] S. Haykin, *Neural Networks: A Comprehensive Foundation*. Upper Saddle River, NJ, USA: Prentice Hall PTR, 1st ed., 1994.
- [96] J. J. Moré, "The levenberg-marquardt algorithm: implementation and theory," in *Numerical analysis*, pp. 105–116, Springer, 1978.
- [97] C. Yuan and H. Yang, "Research on k-value selection method of k-means clustering algorithm," *J*, vol. 2, no. 2, pp. 226–235, 2019.
- [98] X. Song, W. Li, D. Ma, Y. Wu, and D. Ji, "An enhanced clustering-based method for determining time-of-day breakpoints through process optimization," *IEEE Access*, vol. 6, pp. 29241–29253, 2018.
- [99] MATLAB, version 9.2.0 (R2017a). Natick, Massachusetts: The MathWorks Inc., 2017.
- [100] W.-Y. Tsai, H.-C. Chen, and T.-L. Liao, "An ultrasonic air temperature measurement system with self-correction function for humidity," *Measurement science and technology*, vol. 16, no. 2, p. 548, 2005.
- [101] M. Dobosz and M. Ściuba, "Ultrasonic measurement of air temperature along the axis of a laser beam during interferometric measurement of length," *Measurement Science and Technology*, vol. 31, no. 4, p. 045202, 2020.
- [102] R. Jia, Q. Xiong, L. Wang, K. Wang, X. Shen, S. Liang, and X. Shi, "Study of ultrasonic thermometry based on ultrasonic time-of-flight measurement," *Aip Advances*, vol. 6, no. 3, p. 035006, 2016.
- [103] M. Guo, Y. Yan, Y. Hu, G. Lu, and J. Zhang, "Temperature measurement of stored biomass using low-frequency acoustic waves and correlation signal processing techniques," *Fuel*, vol. 227, pp. 89 98, 2018.
- [104] T.-L. Liao, W.-Y. Tsai, and C.-F. Huang, "A new ultrasonic temperature measurement system for air conditioners in automobiles," *Measurement Science and Technology*, vol. 15, no. 2, p. 413, 2003.
- [105] A. K. Sahoo and S. K. Udgata, "A novel ann-based adaptive ultrasonic measurement system for accurate water level monitoring," *IEEE Transactions on Instrumentation and Measurement*, vol. 69, no. 6, pp. 3359–3369, 2020.
- [106] D. Meyer, F. Leisch, and K. Hornik, "The support vector machine under test," *Neuro-computing*, vol. 55, no. 1, pp. 169–186, 2003.

- [107] A. Kon, K. Mizutani, and N. Wakatsuki, "Noncontact measurement of humidity and temperature using airborne ultrasound," *Japanese journal of applied physics*, vol. 49, no. 4R, p. 046601, 2010.
- [108] G. Andria, F. Attivissimo, and N. Giaquinto, "Digital signal processing techniques for accurate ultrasonic sensor measurement," *Measurement*, vol. 30, no. 2, pp. 105–114, 2001.
- [109] A. K. Sahoo and S. K. Udgata, "Machine learning-based ambient temperature estimation using ultrasonic sensor," in *Next Generation of Internet of Things*, (Singapore), pp. 657–668, Springer Singapore, 2021.
- [110] C. Zhou, Y. Wang, C. Qiao, S. Zhao, and Z. Huang, "High-accuracy ultrasonic temperature measurement based on MLS-modulated continuous wave," *Measurement*, vol. 88, pp. 1–8, 2016.
- [111] Y. S. Huang and M. S. Young, "An accurate ultrasonic distance measurement system with self temperature compensation," *Instrumentation Science & Technology*, vol. 37, no. 1, pp. 124–133, 2009.
- [112] A. Hayashida, Y. Mizuno, and K. Nakamura, "Estimation of room temperature based on acoustic frequency response," *Acoustical Science and Technology*, vol. 41, no. 4, pp. 693–696, 2020.
- [113] Y. Hu, M. Guo, Y. Yan, G. Lu, and X. Cheng, "Temperature measurement of stored biomass of different types and bulk densities using acoustic techniques," *Fuel*, vol. 257, p. 115986, 2019.
- [114] K. Sampath, M. Perera, P. Ranjith, S. Matthai, X. Tao, and B. Wu, "Application of neural networks and fuzzy systems for the intelligent prediction of co2-induced strength alteration of coal," *Measurement*, vol. 135, pp. 47–60, 2019.
- [115] B. Freisleben and T. Kunkelmann, "Combining fuzzy logic and neural networks to control an autonomous vehicle," in [Proceedings 1993] Second IEEE International Conference on Fuzzy Systems, pp. 321–326 vol.1, 1993.
- [116] S.-J. Huang and R.-J. Lian, "A hybrid fuzzy logic and neural network algorithm for robot motion control," *IEEE Transactions on Industrial Electronics*, vol. 44, no. 3, pp. 408–417, 1997.
- [117] C.-T. Lin and C. Lee, "Neural-network-based fuzzy logic control and decision system," *IEEE Transactions on Computers*, vol. 40, no. 12, pp. 1320–1336, 1991.
- [118] T. J. Ross, Fuzzy logic with engineering applications. John Wiley & Sons, 2005.
- [119] L. Zadeh, "Fuzzy logic," *Computer*, vol. 21, no. 4, pp. 83–93, 1988.
- [120] C.-C. Lee, "Fuzzy logic in control systems: fuzzy logic controller. i," *IEEE Transactions on systems, man, and cybernetics*, vol. 20, no. 2, pp. 404–418, 1990.

- [121] S. Uddin, A. Khan, M. E. Hossain, and M. A. Moni, "Comparing different supervised machine learning algorithms for disease prediction.," *BMC Medical Informatics and Decision Making*, vol. 19, p. 281, 2019.
- [122] C. Cortes and V. Vapnik, "Support-vector networks," *Machine Learning*, vol. 20, pp. 273 297, 1995.
- [123] I. A. Basheer and M. Hajmeer, "Artificial neural networks: fundamentals, computing, design, and application," *Journal of microbiological methods*, vol. 43, no. 1, pp. 3–31, 2000.
- [124] V. Martínez-Martínez, C. Baladrón, J. Gomez-Gil, G. Ruiz-Ruiz, L. M. Navas-Gracia, J. M. Aguiar, and B. Carro, "Temperature and relative humidity estimation and prediction in the tobacco drying process using artificial neural networks," *Sensors*, vol. 12, no. 10, pp. 14004–14021, 2012.
- [125] A. Lady, "Dht11, dht22, and am2302 sensors," 2012.
- [126] J. P. Brown, "Hygrometric measurement in museums: calibration, accuracy, and the specification of relative humidity," *Studies in Conservation*, vol. 39, no. sup2, pp. 39–43, 1994.
- [127] S. Kiranyaz, T. Ince, O. Abdeljaber, O. Avci, and M. Gabbouj, "1-D convolutional neural networks for signal processing applications," in *ICASSP 2019-2019 IEEE International Conference on Acoustics, Speech and Signal Processing (ICASSP)*, pp. 8360–8364, IEEE, 2019.
- [128] C. Barat and N. Ait Oufroukh, "Classification of indoor environment using only one ultrasonic sensor," in *IMTC 2001. Proceedings of the 18th IEEE Instrumentation and Measurement Technology Conference. Rediscovering Measurement in the Age of Informatics (Cat. No.01CH 37188)*, vol. 3, pp. 1750–1755 vol.3, 2001.
- [129] B. Barshan and R. Kuc, "Differentiating sonar reflections from corners and planes by employing an intelligent sensor," *IEEE Transactions on Pattern Analysis and Machine Intelligence*, vol. 12, no. 6, pp. 560–569, 1990.
- [130] S. Barua, A. Saha, A. A. S. Khan, and R. H. Chowdhury, "Comparative study of object shape recognition using ultrasonic sensor arrays with artificial neural network," in 2019 2nd International Conference on Innovation in Engineering and Technology (ICIET), pp. 1–6, IEEE, 2019.
- [131] Y. Ding, H. Kisner, T. Kong, and U. Thomas, "Using machine learning for material detection with capacitive proximity sensors," in 2020 IEEE/RSJ International Conference on Intelligent Robots and Systems (IROS), pp. 10424–10429, IEEE, 2020.
- [132] M. I. Ecemis and P. Gaudiano, "Object recognition with ultrasonic sensors," in *Proceedings 1999 IEEE International Symposium on Computational Intelligence in Robotics and Automation. CIRA'99 (Cat. No. 99EX375)*, pp. 250–255, IEEE, 1999.

- [133] R. Hwasser, *Machine learning classification based on ultrasonic analog data*. PhD thesis, CHALMERS UNIVERSITY OF TECHNOLOGY, 2020.
- [134] L. Kang, A. Feeney, and S. Dixon, "The high frequency flexural ultrasonic transducer for transmitting and receiving ultrasound in air," *IEEE Sensors Journal*, vol. 20, no. 14, pp. 7653–7660, 2020.
- [135] R. Kuc, "Biomimetic sonar locates and recognizes objects," *IEEE Journal of Oceanic Engineering*, vol. 22, no. 4, pp. 616–624, 1997.
- [136] G. Lindstedt and G. Olsson, "Using ultrasonics for sensing in a robotic environment," in [1993] Proceedings IEEE International Conference on Robotics and Automation, pp. 671–676, IEEE, 1993.
- [137] J. Llata, E. Sarabia, and J. Oria, "Pattern recognition with ultrasonic sensors: a neural networks evaluation," *Sensor Review*, 2001.
- [138] K. Ohtani and M. Baba, "A simple identification method for object shapes and materials using an ultrasonic sensor array," in 2006 IEEE Instrumentation and Measurement Technology Conference Proceedings, pp. 2138–2143, 2006.
- [139] J. Perez Oria and A. Gonzalez, "Object recognition using ultrasonic sensors in robotic applications," in *Proceedings of IECON '93 19th Annual Conference of IEEE Industrial Electronics*, pp. 1927–1931 vol.3, 1993.
- [140] P. Smith, D. Bull, and C. Wykes, "Target classification with artificial neural networks using ultrasonic phased arrays," *WIT Transactions on Information and Communication Technologies*, vol. 1, 1970.
- [141] P. L. Worth, *Object detection and classification with a CTFM ultrasonic sensor*. PhD thesis, University of Wollongong, 2011.
- [142] T. Ulrich, "Envelope calculation from the hilbert transform," *Los Alamos Nat. Lab.*, *Los Alamos, NM, USA, Tech. Rep*, 2006.
- [143] W. Xu and F. DU, "A robust qrs complex detection method based on shannon energy envelope and hilbert transform," *Journal of Mechanics in Medicine and Biology*, vol. 22, no. 03, p. 2240013, 2022.
- [144] L. Alzubaidi, J. Zhang, A. J. Humaidi, A. Al-Dujaili, Y. Duan, O. Al-Shamma, J. Santamaría, M. A. Fadhel, M. Al-Amidie, and L. Farhan, "Review of deep learning: Concepts, CNN architectures, challenges, applications, future directions," *Journal of big Data*, vol. 8, no. 1, pp. 1–74, 2021.
- [145] S. Albawi, T. A. Mohammed, and S. Al-Zawi, "Understanding of a convolutional neural network," in *2017 international conference on engineering and technology (ICET)*, pp. 1–6, IEEE, 2017.

[146] F. Mattioli, C. Porcaro, and G. Baldassarre, "A 1-D CNN for high accuracy classification and transfer learning in motor imagery EEG-based brain-computer interface," *Journal of Neural Engineering*, vol. 18, no. 6, p. 066053, 2022.

MACHINE LEARNING BASED INTELLIGENT SENSING USING NON-CONTACT ULTRASONIC SENSOR

by Ajit Kumar Sahoo

Submission date: 30-Dec-2022 10:52AM (UTC+0530)

Submission ID: 1987408338

File name: Ajit-Sahoo-PhD-Thesis-Final-Plagiarism-check.pdf (10.44M)

Word count: 38261

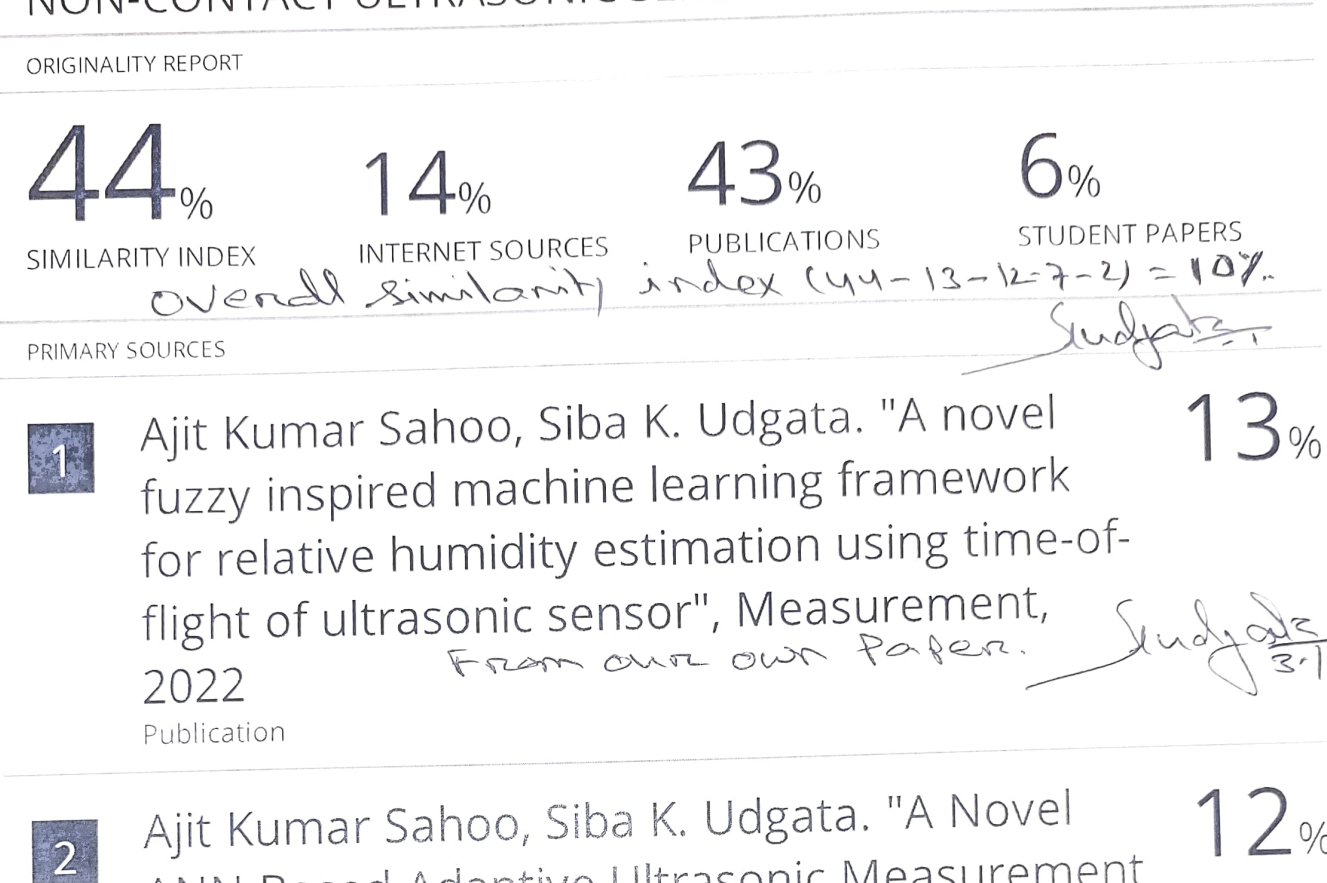
Character count: 200328

Prof. Siba K. Udgata

Professor

School Of Computer & Information Sciences University of Hyderabad

MACHINE LEARNING BASED INTELLIGENT SENSING USING NON-CONTACT ULTRASONIC SENSOR



Ajit Kumar Sahoo, Siba K. Udgata. "A Novel 12% ANN Based Adaptive Ultrasonic Measurement System for Accurate Water Level Monitoring", IEEE Transactions on Instrumentation and Measurement, 2019

Publication Sendyals

"Next Generation of Internet of Things",

Springer Science and Business Media LLC,

From Our own Rapea.

Publication

Ajit Kumar Sahoo, Siba Kumar Udgata. "A Novel ANN-Based Adaptive Ultrasonic Measurement System for Accurate Water 2%

Prof. Siba K. Udgata
Professor
Professor
Professor

Prof. Siba K. Ouga Professor School Of Computer & Information Sciences University of Hyderabad Hyderabad, India.

Level Monitoring", IEEE Transactions on Instrumentation and Measurement, 2020

5	www.researchgate.net Internet Source	1 %
6	"Neural Information Processing", Springer Science and Business Media LLC, 2017 Publication	<1%
7	researchbank.swinburne.edu.au Internet Source	<1%
8	Submitted to Higher Education Commission Pakistan Student Paper	<1%
9	www.mdpi.com Internet Source	<1%
10	Pankaj Mohindru. "Development of liquid level measurement technology: A review", Flow Measurement and Instrumentation, 2022 Publication	<1%
11	doctorpenguin.com Internet Source	<1%
12	Submitted to Xiamen University Student Paper	<1%
13	Lecture Notes in Computer Science, 2006. Publication	<1%

14	Issam Moumene, Nouredine Ouelaa. "Gears and bearings combined faults detection using optimized wavelet packet transform and pattern recognition neural networks", The International Journal of Advanced Manufacturing Technology, 2022 Publication	<1%
15	worldwidescience.org Internet Source	<1%
16	diglib.tugraz.at Internet Source	<1%
17	Charu C. Aggarwal. "Neural Networks and Deep Learning", Springer Science and Business Media LLC, 2018 Publication	<1%
18	Ultrasonic Fluid Quantity Measurement in Dynamic Vehicular Applications, 2013. Publication	<1%
19	www.predig.com Internet Source	<1%
20	www.physicsclassroom.com Internet Source	<1%
21	epdf.pub Internet Source	<1%
22	Rong Xiang, Zhengui Shi. "Design of Millimeter Range High Precision Ultrasonic Distance	<1%

Measurement System", 2017 International Conference on Computer Systems, Electronics and Control (ICCSEC), 2017

23	docplayer.net Internet Source	<1%
24	Oludare Isaac Abiodun, Aman Jantan, Abiodun Esther Omolara, Kemi Victoria Dada, Nachaat AbdElatif Mohamed, Humaira Arshad. "State- of-the-art in artificial neural network applications: A survey", Heliyon, 2018 Publication	<1%
25	tel.archives-ouvertes.fr Internet Source	<1%
26	www.electronicshub.org Internet Source	<1%
27	Abhishek Sharma, Vaidehi Sharma, Mohita Jaiswal, Hwang-Cheng Wang et al. "Recent Trends in Al-Based Intelligent Sensing", Electronics, 2022 Publication	<1%
28	Submitted to K12 Incorporated Student Paper	<1%
29	Submitted to Imperial College of Science, Technology and Medicine Student Paper	<1%

	30	lastminuteengineers.com Internet Source	<1%
_	31	J. Dehghannya. "Simultaneous Aerodynamic and Thermal Analysis during Cooling of Stacked Spheres inside Ventilated Packages", Chemical Engineering & Technology, 11/2008 Publication	<1 %
	32	Submitted to University of Strathclyde Student Paper	<1%
	33	Springer Handbook of Acoustics, 2014. Publication	<1%
	34	ieee-uffc.org Internet Source	<1%
	35	www.ncbi.nlm.nih.gov Internet Source	<1%
	36	Andrea Rocchi, Eleonora Santecchia, Fabrizio Ciciulla, Paolo Mengucci, Gianni Barucca. "Characterization and Optimization of Level Measurement by an Ultrasonic Sensor System", IEEE Sensors Journal, 2019 Publication	<1%
_	37	Seungin Shin, Min-Hyun Kim, Seibum B. Choi. "Ultrasonic Distance Measurement Method With Crosstalk Rejection at High Measurement Rate", IEEE Transactions on Instrumentation and Measurement, 2019	<1%

38	aip.scitation.org Internet Source	<1%
39	Edin Terzic, Jenny Terzic, Romesh Nagarajah, Muhammad Alamgir. "A Neural Network Approach to Fluid Quantity Measurement in Dynamic Environments", Springer Nature, 2012	<1%
40	Submitted to Indian School of Business Student Paper	<1%
41	adatis.co.uk Internet Source	<1%
42	"New Concepts and Applications in Soft Computing", Springer Science and Business Media LLC, 2013 Publication	<1%
43	Jawaher Lafi Aljohani, Eman Salem Alaidarous, Muhammad Asif Zahoor Raja, Muhammad Shoaib, Muhammed Shabab Alhothuali. "Intelligent computing through neural networks for numerical treatment of non-Newtonian wire coating analysis model", Scientific Reports, 2021 Publication	<1%
	m seirn ora	A

45	odr.chalmers.se Internet Source	<1%
46	stax.strath.ac.uk Internet Source	<1%
47	www.scribd.com Internet Source	<1%
48	web.archive.org Internet Source	<1%
49	Submitted to Dr. S. P. Mukherjee International Institute of Information Technology (IIIT-NR) Student Paper	<1%
50	Submitted to University of Wales Institute, Cardiff Student Paper	<1%
51	Submitted to De Montfort University Student Paper	<1%
52	Kelly, Jeffrey J., Katherine A. Kelly, Clyde H. Barlow, and Robert R. Alfano. "", Optical Tomography Photon Migration and Spectroscopy of Tissue and Model Media Theory Human Studies and Instrumentation, 1995. Publication	<1%
53	etd.lib.metu.edu.tr Internet Source	<1%

54	nrl.northumbria.ac.uk Internet Source	<1%
55	Submitted to Berlin School of Business and Innovation Student Paper	<1%
56	Submitted to Southern Illinois University Edwardsville Student Paper	<1%
57	Xin Zhao, Pin Qian, Na Lu, Yaoyao Li. "Design and Experimental Study of High Precision Ultrasonic Ranging System", 2020 5th International Conference on Intelligent Informatics and Biomedical Sciences (ICIIBMS), 2020 Publication	<1%
58	silo.pub Internet Source	<1%
59	Submitted to Madan Mohan Malaviya University of Technology Student Paper	<1%
60	Submitted to University of Wales Swansea Student Paper	<1%
61	Yijun Yan, Jinchang Ren, Julius Tschannerl, Huimin Zhao, Barry Harrison, Frances Jack. "Nondestructive Phenolic Compounds Measurement and Origin Discrimination of	<1%

Peated Barley Malt using Near-infrared Hyperspectral Imagery and Machine Learning", IEEE Transactions on Instrumentation and Measurement, 2021

62	archive.org Internet Source	<1%
63	"MultiMedia Modeling", Springer Nature, 2017	<1%
64	Agarwal, V., N.V. Murali, and C. Chandramouli. "A Cost-Effective Ultrasonic Sensor-Based Driver-Assistance System for Congested Traffic Conditions", IEEE Transactions on Intelligent Transportation Systems, 2009. Publication	<1%
65	Submitted to Hunter College High School Student Paper	<1%
66	Sapana Ranwa, Mahesh Kumar. "Sensing Materials: Ceramics", Elsevier BV, 2021 Publication	<1%
67	Submitted to University of Birmingham Student Paper	<1%
68	Hager Ahmed, Eman M.G. Younis, Abdeltawab Hendawi, Abdelmgeid A. Ali. "Heart disease identification from patients' social posts, machine learning solution on Spark", Future Generation Computer Systems, 2019	<1%

69	Lecture Notes in Computer Science, 2012. Publication	<1%
70	Lecture Notes in Computer Science, 2015. Publication	<1%
71	Santanu Pattanayak. "Pro Deep Learning with TensorFlow", Springer Science and Business Media LLC, 2017 Publication	<1%
72	Submitted to Universiti Teknologi Petronas Student Paper	<1%
73	Submitted to University of the West Indies Student Paper	<1%
74	catalog.lib.kyushu-u.ac.jp Internet Source	<1%
75	downloads.hindawi.com Internet Source	<1%
76	ebin.pub Internet Source	<1%
77	hdl.handle.net Internet Source	<1%
78	ipfs.io Internet Source	<1%
79	uni-das.de Internet Source	<1%

80	www.concepts-of-physics.com Internet Source	<1%
81	Submitted to Charotar University of Science And Technology Student Paper	<1%
82	Submitted to University of Bristol Student Paper	<1%
83	Submitted to University of Edinburgh Student Paper	<1%
84	dokumen.pub Internet Source	<1%
85	espace.curtin.edu.au Internet Source	<1%
86	kar.kent.ac.uk Internet Source	<1%
87	moam.info Internet Source	<1%
88	pianalytix.com Internet Source	<1%
89	"Computer Vision – ACCV 2018 Workshops", Springer Science and Business Media LLC, 2019 Publication	<1%
90	Gao, Yan, Li Na Jia, Bo Wang, Li Hua Liu, and Li Ming Huang. "High Precision Ultrasonic	<1%

Ranging System for Mobile Robot Navigation", Applied Mechanics and Materials, 2012.

91	Submitted to Mar Baselios Engineering College Student Paper	<1%
92	Mohammed Azher Therib, Ibrahim H. Al- Kharsan, Ahmed Fahem Al-Baghdadi. "Design a Suitable Optimized Low Pass FIR Filter for Ultrasonic Signal", IOP Conference Series: Materials Science and Engineering, 2020 Publication	<1%
93	arxiv.org Internet Source	<1%
94	opus.bath.ac.uk Internet Source	<1%
95	patents.justia.com Internet Source	<1%
96	www.frontiersin.org Internet Source	<1%
97	www.ijnrd.org Internet Source	<1%
98	www.spiedigitallibrary.org Internet Source	<1%
99	Submitted to Institute of Technology Carlow Student Paper	<1%

100	K. Takahashi. "Advanced intelligent sensing system using sensor fusion", Proceedings of the 1992 International Conference on Industrial Electronics Control Instrumentation and Automation, 1992 Publication	<1%
101	Submitted to Roskilde University Student Paper	<1%
102	docksci.com Internet Source	<1%
103	riuma.uma.es Internet Source	<1%
104	unsworks.unsw.edu.au Internet Source	<1 %
105	Submitted to Academic Library Consortium Student Paper	<1%
106	Submitted to Curtin University of Technology Student Paper	<1 %
107	Submitted to Loughborough College Student Paper	<1%
108	Ramazan Ekinci. "Chapter 6 The Impact on Digitalization on Financial Sector Performance", Springer Science and Business Media LLC, 2021 Publication	<1%

109	Submitted to SHAPE (VTC college) Student Paper	<1%
110	Submitted to University of Bath Student Paper	<1%
111	Submitted to University of Sheffield Student Paper	<1%
112	coek.info Internet Source	<1%
113	cyberleninka.org Internet Source	<1%
114	philpapers.org Internet Source	<1%
115	www.gta.ufrj.br Internet Source	<1%

Exclude quotes On Exclude bibliography On Exclude matches < 14 words